Electronic Supplementary Material (ESI) for Inorganic Chemistry Frontiers.

Supplementary Information

Reversible Hydrosilanes Addition to Pyridines Enabled by Low-coordinate Ca(II) and Yb(II) Hydrides

Alexander N. Selikhov,[a,b] Mikhail A. Bogachev,[a] Yulia V. Nelyubina,[b] Grigory Yu. Zhigulin,[a] Sergey Yu. Ketkov [a] and Alexander A. Trifonov*[b,a]

[a]G.A. Razuvaev Institute of Organometallic Chemistry of Russian Academy of Sciences, Tropinina 49, GSP-445, 603950, Nizhny Novgorod, Russia

[b]A.N. Nesmeyanov Institute of Organoelement Compounds of Russian Academy of Sciences, Vavilova Str. 28, bld. 1, 119334, Moscow, Russia

Table of Contents

General Experimental Details.

Reagents, solvents and techniques: All operations were carried out in vacuum or under an atmosphere of argon, using Schlenk techniques or in an argon filled glovebox. After drying over KOH, THF, toluene and benzene were purified by distillation from sodium/benzophenone ketyl. Hexane, C_6D_6, and THF-d_8 were dried over Na/K alloy, transferred under vacuum, and stored over 4 Å molecular sieves in an argon-filled glovebox. 3,6-di-*tert*-butyl-1,8-bis-(3,5-di-*tert*-butylphenyl)-9H-carbazole (tBu$_2$CarbAr$_2$H),[1] M[N(SiMe$_3$)$_2$]$_2$(THF)$_2$ (M = Ca,[2] Yb [3]) and {[(Me$_3$Si)$_2$N]$_2$M}$_2$ (M = Ca,[4] Yb [5]), were prepared according to literature procedures. Pyridine-d_5 was dried over CaH_2 and kept in an Ar-filled glovebox. Pyridine, 2-methylpyridine, 3-methylpyridine, 4-methylpyridine, 3,4-dimethylpyridine, quinoline, 4-methylquinoline, 6-methylquinoline, 4-methyl-7-bromoquinoline, isoquinoline, $PhSiH_3$ and Ph_2SiH_2 were purchased from Aldrich, dried over CaH_2, vacuum-transferred, degassed by two freeze-pump-thaw cycles and kept in a glovebox. p-tBuC$_6$H$_4$SiH$_3$,[6] p-MeOC$_6$H$_4$SiH$_3$,[7] α-C$_{10}$H$_7$SiH$_3$,[7] o-MeOC$_6$H$_4$SiH$_3$[7] were prepared according to literature procedures, vacuum-distilled and kept in a glovebox. 1-bromo-2,4-diisopropylbenzene were prepared according to literature procedure from commercial 1,3-diisopropylbenzene.[8] (EtO)$_4$Si and $LiAlH_4$ were purchased from Aldrich and used without additional purification.

NMR Spectroscopy: ^{1}H and ^{13}C NMR spectra were recorded on a Bruker Avance 400 (400 and 100 MHz) and Bruker DPX 300 (300 and 75 MHz) instruments, and are internally referenced to residual solvent signals, $CDCl_3$ referenced at δ 7.26 and 77.0 ppm, C_6D_6 referenced at δ 7.16 and 128.06 ppm. Where required COSY and HSQC spectra were used to assign NMR spectra. Data for ^{1}H NMR are reported as follows: chemical shift (δ ppm), integration, multiplicity (s = singlet, d = doublet, t = triplet, q = quartet, p = pentad, sext = sextet, hept = septet, m = multiplet, br s = broad singlet, compl m = complex multiplet), coupling constant (Hz) and assignment. Data for ^{13}C NMR are reported in terms of chemical shift, multiplicity (s = singlet, d = doublet, t = triplet, q = quartet, p = pentet, sext = sextet, hept = heptet, m = multiplet. br. s = broad singlet), coupling constant (Hz) and no special nomenclature is used for equivalent carbons.

Mass and IR Spectroscopy: IR spectra were recorded as Nujol mulls or KBr plates on FSM 1201 and Bruker Vertex 70 instruments and are reported in terms of frequency of absorption (cm^{-1}). A "Polaris Q GC/MS" spectrometer was used for GS/MS analysis. The N, C, H elemental analyses were carried out in the microanalytical laboratory of the IOMC by means of a Carlo Erba Model 1106 elemental analyzer with an accepted tolerance of 0.4 unit on carbon (C), hydrogen (H), and nitrogen (N). Lanthanide metal analysis was carried out by complexonometric titration.[9]

X-ray Crystallography: X-ray diffraction data for **7-9**, **11** and **12** were collected at 100 K with a Bruker Quest D8 CMOS diffractometer; those for **6** and **10+12**, at 120 K with a Bruker APEXII DUO CCD diffractometer, both using graphite monochromated Mo-Kα radiation (λ = 0.71073 Å, ω-scans). Structures were solved using Intrinsic Phasing with the ShelXT [10] structure solution program in Olex2 [11] and then refined with the XL [12] refinement package using Least-Squares minimization against F^2 in the anisotropic approximation for non-hydrogen atoms. Hydrogen atoms at the calcium ions in **9** and **11** were located from difference Fourier synthesis; those at the ytterbium ions in **10+12** and **12** were not located owing to a severe disorder of the complexes. Positions of other hydrogen atoms were calculated, and they all were refined in the isotropic approximation within the riding model. Crystal data and structure refinement parameters are given in Tables S1 and S2. CCDC 2338913 (**6**), 2338914 (**7**), 2338918 (**8**), 2338915 (**9**), 2338916

(**10+12**), 2338912 (**11**) and 2338917 (**12**) contain the supplementary crystallographic data for this paper.

Computational details: Catalytic activity of the calcium hydride complex **11** in the hydrosilylation reaction of pyridine was investigated within the framework of the density functional theory (DFT) using the Gaussian 09 package [13]. All the molecular structures presented here were fully optimized employing the M062X functional[14] and the DGDZVP basis set.[15, 16] The polarizable continuum model (PCM) [17] was used to take into account the non-specific solvation effects in the aromatic solvent (toluene). All structures were treated as closed-shell singlet systems. Cartesian coordinates of atoms for geometry optimization of the dimeric complex **11** were adopted from the corresponding X-ray data. Structures of the intermediates participating in the elementary reactions were obtained further by consecutive modifications of the optimized geometry of **11**. The transition state structures were localized by the quadratic synchronous transit (QST3) procedure[18, 19]. All the optimized geometries correspond to the local minima (intermediates, initial and final products of the reactions) or first-order saddle points (transition states) on the potential energy surface (PES) as indicated by the calculated harmonic vibrational frequencies. Enthalpy changes for the catalytic reactions ($\Delta H°_{sol}$) were computed on the basis of the $H°_{sol}$ values taken directly from the frequency analyses of the PCM optimized structures at 1 atm and 298.15 K. Similarly, the $G°_{sol}$ values were obtained but the Gibbs free energy variations (ΔG_{sol}) were corrected for the solution phase with the 1 M standard state. Additionally, we estimated the temperature dependence of the enthalpy and Gibbs free energy changes for the brutto-reactions of the hydrosilylation of pyridine at the higher M062X/def2-TZVPP[20] level of DFT. The ΔG_{sol} values were computed at T = 298, 333, and 363 K.

Table S1. Crystal data and structure refinement parameters for **6**, **7**, **8** and **9**.

	6	**7**	**8**	**9**
Empirical formula	$C_{58}H_{90}N_2OSi_2Yb$	$C_{54}H_{82}CaN_2Si_2$	$C_{54}H_{82}N_2Si_2Yb$	$C_{104}H_{146}Ca_2N_2O_2$
Formula weight	1060.53	855.47	988.43	1536.38
T, K	120	100	100	100
Crystal system	Monoclinic	Monoclinic	Monoclinic	Triclinic
Space group	*P2₁/n*	*P2₁/n*	*P2₁/n*	*P-1*
Z	4	4	4	1
a, Å	16.0441(16)	16.3814(2)	16.2849(3)	13.084(4)
b, Å	18.2621(19)	16.1669(2)	16.1044(3)	13.602(4)
c, Å	19.510(2)	20.0917(3)	20.2204(4)	14.178(4)
α, °	90	90	90	74.332(6)
β, °	97.780(2)	91.5050(10)	91.6240(10)	86.407(7)
γ, °	90	90	90	76.759(6)
V, Å^3	5663.8(10)	5319.18(12)	5300.84(17)	2364.9(11)
D_{calc} (g cm^{-1})	1.244	1.068	1.239	1.079
Linear absorption, μ (cm^{-1})	17.31	1.97	18.44	1.68
F(000)	2232	1872	2072	840
$2\theta_{max}$, °	50	52	52	50
Reflections measured	49853	55268	54745	28201
Independent reflections	9956	10442	10408	8309
Observed reflections [$I > 2\sigma(I)$]	7289	8345	8738	4312
Parameters	614	639	599	544
R1	0.0530	0.0587	0.0343	0.0717
wR2	0.1660	0.1460	0.0775	0.2225
GOF	1.131	1.030	1.023	0.974
$\Delta\rho_{max}$/ $\Delta\rho_{min}$ (e Å^{-3})	3.119/-1.989	0.819/-0.484	0.914/-0.762	0.538/-0.550

Table S1. Crystal data and structure refinement parameters for **10+12**, **11** and **12**.

	10+12	**11**	**12**
Empirical formula	$C_{107}H_{144}N_2OYb_2$	$C_{110}H_{146}Ca_2N_2$	$C_{110}H_{144}N_2Yb_2$
Formula weight	1820.31	1576.44	1840.34
T, K	120	100	100
Crystal system	Triclinic	Triclinic	Triclinic
Space group	*P-1*	*P-1*	*P-1*
Z	2	2	2
a, Å	14.287(4)	15.826(3)	15.7873(8)
b, Å	15.583(4)	16.462(3)	16.3820(8)
c, Å	24.302(6)	21.841(4)	21.7459(11)
α, °	87.079(5)	84.70(3)	84.709(3)
β, °	85.262(5)	75.62(3)	75.878(3)
γ, °	65.519(5)	84.29(3)	84.718(3)
V, Å^3	4906(2)	5471(2)	5416.8(5)
D_{calc} (g cm^{-1})	1.232	0.957	1.128
Linear absorption, μ (cm^{-1})	19.4	1.45	17.57
F(000)	1896	1720	1916
$2\theta_{max}$, °	50	50	50
Reflections measured	67789	42160	49818
Independent reflections	17261	18045	18999
Observed reflections [$I > 2\sigma(I)$]	8345	7482	12871
Parameters	1120	1130	1142
R1	0.0830	0.1386	0.0559
wR2	0.2432	0.3826	0.1548
GOF	1.004	1.028	1.034
$\Delta\rho_{max}$/ $\Delta\rho_{min}$ (e Å^{-3})	1.515/-1.659	0.711/-0.448	2.405/-1.816

Experimental Procedures and Data

Synthesis of [*t*Bu$_2$CarbAr$_2$]CaN(SiMe$_3$)$_2$(THF) (5). 3,6-di-*tert*-butyl-1,8-bis-(3,5-di-*tert*-butylphenyl)-9H-carbazole (0.75 g, 1.15 mmol) was added to a solution of [(Me$_3$Si)$_2$N]$_2$Ca(THF)$_2$ (0.64 g, 1.26 mmol) in toluene (10 mL) at room temperature. The reaction mixture was heated at 90 °C for 20 h. The resulting luminescent yellow solution was brought to ambient temperature, and the volatiles were removed in vacuum. The yellow oily residue was dissolved in fresh hexane (13 mL), and centrifuged, the mother liquor was decanted. Large yellow crystals were obtained by slow concentration of the mother liqueur of **5**. The yield of **5** is 0.90 g (90%). ^{1}H NMR (400 MHz, C$_6$D$_6$, 298 K): δ 8.53 (d, 2H, 4,5-CH-carbazolyl, $^4J_{HH}$= 2.0 Hz), 8.11 (d, 4H, 2,6-CH-aryl, $^4J_{HH}$= 1.8 Hz), 7.65 (d, 2H, 2,7-CH-carbazolyl, $^4J_{HH}$= 2.0 Hz), 7.62 (t, 2H, 4-CH-aryl, $^4J_{HH}$= 1.8 Hz), 2.81 (t, 4H, α-CH$_2$-THF, $^3J_{HH}$ = 6.0 Hz), 1.52 (s, 18H, *t*Bu-carbazolyl), 1.43 (s, 36H, *t*Bu-aryl), 1.05-0.93 (m, 4H, β-CH$_2$-THF), -0.16 (s, 18H, SiMe$_3$). ^{13}C{^{1}H} NMR (100 MHz, C$_6$D$_6$, 298 K): δ 152.11 (s, *ipso*-C-aryl), 146.94 (s, C-carbazolyl), 142.10 (s, C-carbazolyl), 139.06 (s, C-carbazolyl), 127.55 (s, C-carbazolyl), 126.86 (s, *ipso*-C-aryl), 125.20 (s, CH-carbazolyl), 123.51 (s, 2,6-CH-aryl), 122.84 (s, 4-CH-aryl), 115.72 (s, CH-carbazolyl), 69.01 (s, α-CH$_2$-THF), 34.92 (s, *C*(CH$_3$)$_3$-aryl), 34.37 (s, *C*(CH$_3$)$_3$-carbazolyl), 32.08 (s, C(*C*H$_3$)$_3$-carbazolyl), 31.60 (s, C(*C*H$_3$)$_3$-aryl), 24.41 (s, β-CH$_2$-THF), 4.91 (s, SiMe$_3$). ^{29}Si NMR (79.5 MHz, C$_6$D$_6$, 298 K): δ -15.53. IR (KBr): 1588 (s), 1335 (s), 1287 (m), 1265 (m), 1248 (s), 1225 (m), 1188 (s), 1125 (w), 1067 (w), 1022 (s), 957 (m), 866 (s), 837 (s), 810 (s), 694 (m), 642 (m). Anal. Calcd for C$_{58}$H$_{88}$CaN$_2$OSi$_2$ (925.60 g mol^{-1}) C, 75.26; H, 9.58; N 3.03. Found C, 74.85; H, 9.26; N 3.10.

Synthesis of [*t*Bu$_2$CarbAr$_2$]YbN(SiMe$_3$)$_2$(THF) (6). The synthetic protocol analogous to that for **5** was applied. 3,6-di-*tert*-butyl-1,8-bis-(3,5-di-*tert*-butylphenyl)-9H-carbazole (0.97 g, 1.50 mmol) and [(Me$_3$Si)$_2$N]$_2$Yb(THF)$_2$ (1.00 g, 1.56 mmol) were used in the synthesis. The reaction was carried out in toluene (10 mL) at 90 °C within 20 h. The volatiles were removed in vacuum, the solid red residue was redissolved in hexane (13 mL), and centrifuged from a small amount of brown turbidity. Large deep-red crystals suitable for X-ray diffraction were obtained by slow concentration of the mother liqueur of **5**. The yield of **5** is 1.22 g (84%). ^{1}H NMR (400 MHz, C$_6$D$_6$, 298 K): δ 8.57 (d, 2H, 4,5-CH-carbazolyl, $^4J_{HH}$= 2.0 Hz), 8.09 (d, 4H, 2,6-CH-aryl, $^4J_{HH}$= 1.8 Hz), 7.69 (d, 2H, 2,7-CH-carbazolyl, $^4J_{HH}$= 2.0 Hz), 7.60 (t, 2H, 4-CH-aryl, $^4J_{HH}$= 1.8 Hz), 2.95 (br s, 4H, α-CH$_2$-THF), 1.53 (s, 18H, *t*Bu-carbazolyl), 1.40 (s, 36H, *t*Bu-aryl), 1.07 (br s, 4H, β-CH$_2$-THF), -0.16 (s, 18H, SiMe$_3$). ^{13}C{^{1}H} NMR (100 MHz, C$_6$D$_6$, 298 K): δ 152.36 (s, *ipso*-C-aryl), 147.02 (s, C-carbazolyl), 142.80 (s, C-carbazolyl), 139.00 (s, C-carbazolyl), 127.84 (s, C-carbazolyl), 126.47 (s, *ipso*-C-aryl), 124.51 (s, CH-carbazolyl), 123.27 (s, 2,6-CH-aryl), 122.59 (s, 4-CH-aryl), 115.92 (s, CH-carbazolyl), 68.81 (s, α-CH$_2$-THF), 34.95 (s, *C*(CH$_3$)$_3$-aryl), 34.40 (s, *C*(CH$_3$)$_3$-carbazolyl), 32.11 (s, C(*C*H$_3$)$_3$-carbazolyl), 31.66 (s, C(*C*H$_3$)$_3$-aryl), 24.62 (s, β-CH$_2$-THF), 4.74 (s, SiMe$_3$). ^{29}Si NMR (79.5 MHz, C$_6$D$_6$, 298 K): δ - 16.15. IR (KBr): 1588 (s), 1285 (s), 1233 (s), 1179 (s), 1152 (m), 1067 (s), 1026 (s), 928 (m), 866 (s), 816 (s), 762 (s), 746 (m), 696 (m), 669 (s), 644 (s), 582 (s). Anal. Calcd for C$_{58}$H$_{88}$YbN$_2$OSi$_2$ (1058.58 g mol^{-1}) C, 65.81; H, 8.38; N 2.65; Yb, 16.35. Found C, 65.50; H, 8.12; N 2.50; Yb, 16.20.

Synthesis of [*t*Bu$_2$CarbAr$_2$]CaN(SiMe$_3$)$_2$ (7). 3,6-di-*tert*-butyl-1,8-bis-(3,5-di-*tert*-butylphenyl)-9H-carbazole (1.15 g, 1.78 mmol) was added to a solution of {[(Me$_3$Si)$_2$N]$_2$Ca}$_2$ (0.70 g, 1.95 mmol) in toluene (10 mL) at room temperature. The reaction mixture was heated at

90 °C for 1 h. The resulting luminescent yellow solution was brought to ambient temperature, and the volatiles were removed in vacuum. The yellow oily residue was dissolved in fresh toluene (10 mL) and centrifuged, the mother liquor was decanted and concentrated to 2 mL. Large yellow crystals suitable for X-ray diffraction were obtained by slow diffusion of hexane (10 mL) into the toluene-solution of **7**. The yield of **7** is 1.11 g (74%). ^{1}H NMR (400 MHz, C_6D_6, 298 K): δ 8.62 (d, 2H, 4,5-CH-carbazolyl, $^{4}J_{HH}$= 1.9 Hz), 7.95 (d, 4H, 2,6-CH-aryl, $^{4}J_{HH}$= 1.9 Hz), 7.66 (d, 2H, 2,7-CH-carbazolyl, $^{4}J_{HH}$= 1.9 Hz), 7.58 (t, 2H, 4-CH-aryl, $^{4}J_{HH}$= 1.8 Hz), 1.57 (s, 18H, *t*Bu-carbazolyl), 1.29 (s, 36H, *t*Bu-aryl), -0.28 (s, 18H, $SiMe_3$). $^{13}C\{^{1}H\}$ NMR (100 MHz, C_6D_6, 298 K): δ 154.09 (s, *ipso*-C-aryl), 147.61 (s, C-carbazolyl), 145.24 (s, C-carbazolyl), 138.95 (s, C-carbazolyl), 126.46 (s, C-carbazolyl), 126.01 (s, *ipso*-C-aryl), 123.15 (s, CH-carbazolyl), 122.87 (s, 2,6-CH-aryl), 122.76 (s, 4-CH-aryl), 116.60 (s, CH-carbazolyl), 35.06 (s, $C(CH_3)_3$-aryl), 34.53 (s, $C(CH_3)_3$-carbazolyl), 32.21 (s, $C(CH_3)_3$-carbazolyl), 31.42 (s, $C(CH_3)_3$-aryl), 4.87 (s, $SiMe_3$). ^{29}Si NMR (79.5 MHz, C_6D_6, 298 K): δ - 15.49. IR (KBr): 1580 (s), 1285 (s), 1229 (s), 1180 (m), 1066 (s), 1026 (s), 926 (m), 870 (s), 810 (s), 764 (s), 746 (m), 694 (m), 667 (s), 648 (m), 601 (m), 584 (s). Anal. Calcd for $C_{54}H_{82}CaN_2Si_2$ (855.51 g mol^{-1}) C, 75.81; H, 9.66; N 3.27. Found C, 75.50; H, 9.38; N 3.30.

Synthesis of [*t*Bu$_2$CarbAr$_2$]YbN(SiMe$_3$)$_2$ (8). The synthetic protocol analogous to that for **7** was applied. 3,6-di-*tert*-butyl-1,8-bis-(3,5-di-*tert*-butylphenyl)-9H-carbazole (1.10 g, 1.70 mmol) and $\{[(Me_3Si)_2N]_2Yb\}_2$ (1.00 g, 2.00 mmol) were used in the synthesis. The reaction was carried out in toluene at 90 °C within 20 h. The resulting deep-red solution was brought to ambient temperature, and the volatiles were removed in vacuum. The red oily residue was dissolved in fresh toluene (10 mL) and centrifuged, the mother liquor was and concentrated to 2 mL. Large red crystals suitable for X-ray diffraction were obtained by slow diffusion of hexane (10 mL) into the toluene-solution of **8**. The yield of **8** is 1.26 g (76%). ^{1}H NMR (400 MHz, C_6D_6, 298 K): δ 8.60 (s, 2H, 4,5-CH-carbazolyl), 7.97 (s, 4H, 2,6-CH-aryl), 7.70 (s, 2H, 2,7-CH-carbazolyl), 7.55 (s, 2H, 4-CH-aryl), 1.58 (s, 18H, *t*Bu-carbazolyl), 1.28 (s, 36H, *t*Bu-aryl), -0.25 (s, 18H, $SiMe_3$). $^{13}C\{^{1}H\}$ NMR (100 MHz, C_6D_6, 298 K): δ 153.79 (s, *ipso*-C-aryl), 148.27 (s, C-carbazolyl), 145.50 (s, C-carbazolyl), 138.86 (s, C-carbazolyl), 126.53 (s, C-carbazolyl), 125.79 (s, *ipso*-C-aryl), 123.12 (s, CH-carbazolyl), 122.48 (s, 2,6-CH-aryl), 122.34 (s, 4-CH-aryl), 116.63 (s, CH-carbazolyl), 35.07 (s, $C(CH_3)_3$-aryl), 34.55 (s, $C(CH_3)_3$-carbazolyl), 32.24 (s, $C(CH_3)_3$-carbazolyl), 31.38 (s, $C(CH_3)_3$-aryl), 4.75 (s, $SiMe_3$). ^{29}Si NMR (79.5 MHz, C_6D_6, 298 K): δ - 15.52. ^{171}Yb NMR (70.0 MHz, C_6D_6, 298 K): δ 651.60. IR (KBr): 1586 (s), 1285 (s), 1229 (s), 1181 (m), 1152 (w), 1065 (s), 1026 (s), 926 (m), 870 (s), 810 (s), 764 (s), 746 (m), 694 (m), 667 (s), 648 (m), 601 (m), 584 (s). Anal. Calcd for $C_{54}H_{82}YbN_2Si_2$ (988.49 g mol^{-1}) C, 65.61; H, 8.36; N 2.83; Yb, 17.51. Found C, 65.30; H, 8.10; N 2.60; Yb, 17.38.

Synthesis of {[*t*Bu$_2$CarbAr$_2$]Ca(μ^2-H)(THF)}$_2$ (9). $PhSiH_3$ (0.13 g, 1.40 mmol) was added to a solution of **5** (0.85 g, 0.93 mmol) in toluene (15 mL) at room temperature and the reaction mixture was left overnight. After this time, large prism-like yellow luminescent crystals grew on the walls of the flask. The reaction was sustained under these conditions for another 24 h. The mother liquor was separated from yellow crystals by decantation. The crystals of **9** were washed with hexane and dried for 20 min in vacuum. Compound **9** was isolated in 75% yield (0.53 g). ^{1}H NMR (400 MHz, $C_5D_5CD_3$-THF-d_8 (1:1), 298 K): δ 8.12 (br s, 4H, 4,5-CH-carbazolyl), 7.90 (br s, 4H, 4-CH-aryl), 7.43-7.23 (compl m, 12H, 2,6-CH-aryl and 2,7-CH-carbazolyl), 3.50 (br s, 8H, α-CH_2-THF), 1.49 (br s, 8H, β-CH_2-THF), 1.44 (s, 36H, *t*Bu-carbazolyl), 1.32 (s, 72H, *t*Bu-aryl). $^{13}C\{^{1}H\}$ NMR (100 MHz, C_6D_6, 298 K): δ 153.22 (s, *ipso*-C-aryl), 149.70 (s, C-carbazolyl), 142.70 (s, C-carbazolyl), 135.70 (s, C-carbazolyl), 129.52 (s, C-carbazolyl), 128.81 (s, *ipso*-C-aryl), 127.80 (s, CH-carbazolyl), 125.15 (s, 2,6-CH-aryl), 123.55 (s, 4-CH-aryl), 114.43 (s, CH-

carbazolyl), 67.20 (α-*C*H$_2$-THF), 34.66 (s, *C*(CH$_3$)$_3$-aryl), 34.18 (s, *C*(CH$_3$)$_3$-carbazolyl), 32.08 (s, C(*C*H$_3$)$_3$-carbazolyl), 31.55 (s, C(*C*H$_3$)$_3$-aryl), 25.42 (s, β-*C*H$_2$-THF). IR (KBr): 1767 (m), 1590 (s), 1291 (s), 1265 (m), 1248 (m), 1202 (m), 1177 (m), 1155 (m), 1072 (s), 1026 (s), 937 (s), 870 (s), 845 (s), 795 (s), 758 (m), 646 (s), 584 (s). Anal. Calcd for $C_{108}H_{158}Ca_2N_2O_2$ (1596.62 g mol^{-1}) C, 81.25; H, 9.98; N 1.75. Found C, 80.88; H, 9.60; N 1.70.

Synthesis of mixture {[*t*Bu$_2$CarbAr$_2$]Yb(μ^2-H)(THF)}$_2$ (10) and {[*t*Bu$_2$CarbAr$_2$]Yb(μ^2-H) (η^6-C$_7$H$_8$)}$_2$ (12). The synthetic protocol analogous to that for **9** was applied. Complex **6** (1.00 g, 0.95 mmol) and PhSiH$_3$ (0.13 g, 1.23 mmol) were used in the synthesis. The reaction was carried out in toluene at 23 °C within 48h. The mother liquor was separated from black crystals by decantation. The crystals of mixture (1:1) **10** and **12** were washed with hexane and dried for 20 min in vacuum. Yield 80% (0.64 g). IR (KBr): 1767 (m), 1590 (s), 1291 (s), 1265 (m), 1248 (m), 1202 (m), 1177 (m), 1155 (m), 1072 (s), 1026 (s), 937 (s), 870 (s), 845 (s), 795 (s), 758 (m), 646 (s), 584 (s). Anal. Calcd for $C_{214}H_{292}Yb_4N_4O_2$ (3644.93 g mol^{-1}) C, 70.52; H, 8.08; N, 1.54; Yb, 18.99. Found C, 70.17; H, 7.65; N, 1.50; Yb, 18.67.

Synthesis of {[*t*Bu$_2$CarbAr$_2$]Ca(μ^2-H) (η^6-C$_7$H$_8$)}$_2$ (11). PhSiH$_3$ (0.188 g, 1.74 mmol) was added to a solution of **7** (1.00 g, 1.16 mmol) in toluene (15 mL) at room temperature and the reaction mixture was left overnight. Large prism-like yellow luminescent crystals grew on the walls of the flask. The reaction was sustained under these conditions for another 24 h. The mother liquor was separated from yellow crystals by decantation. The crystals of **11** were washed with hexane (2×10 mL) and dried for 20 min in vacuum. **11** was isolated in 75% yield (0.53 g). ^{1}H NMR (400 MHz, C$_5$D$_5$N, 298 K): δ 8.67 (br s, 2H, 4,5-CH-carbazolyl), 8.47 (br s, 4H, 2,6-CH-aryl), 7.74 (br s, 2H, 4-CH-aryl), 7.53 (s, 2H, 2,7-CH-carbazolyl), 7.30-7.07 (compl m, 5H, CH-toluene), 3.83 (s. 1H, C*H*D-DHP), 2.19 (s, 3H, C*H*$_3$Ph), 1.57 (s, 18H, *t*Bu-carbazolyl), 1.37 (s, 36H, *t*Bu-aryl). ^{13}C{^{1}H} NMR (100 MHz, C$_5$D$_5$N, 298 K): δ 152.53 (br s, *ipso*-C-aryl), 145.93 (br s, C-carbazolyl), 143.83 (s, C-carbazolyl), 138.93 (s, *ipso*-C-toluene), 134.75 (br s, C-carbazolyl), 130.32 (s, CH-toluene), 129.75 (s, C-carbazolyl), 129.57 (s, CH-toluene), 127.95 (br s, *ipso*-C-aryl), 126.67 (s, CH-toluene), 126.49 (br s, *C*D-DHP), 125.84 (s, 2,6-CH-aryl), 125.13 (br s, *C*D-DHP), 123.75 (br s, *C*D-DHP), 122.90 (br s, 4-CH-aryl), 120.45 (br s, CH-carbazolyl), 115.81 (br s, CH-carbazolyl), 93.87 (br s, *C*D-DHP), 49.22 (t, *C*HD-DHP, J_{CD} = 20.5 Hz), 35.99 (s, *C*(CH$_3$)$_3$-aryl), 35.67 (s, *C*(CH$_3$)$_3$-carbazolyl), 33.87 (s, C(*C*H$_3$)$_3$-carbazolyl), 32.95 (s, C(*C*H$_3$)$_3$-aryl), 22.25 (s, CH$_3$-toluene). IR (KBr): 1765 (s), 1592 (s), 1291 (s), 1264 (m), 1246 (s), 1200 (m), 1175 (m), 1154 (m), 1071 (s), 1024 (s), 932 (s), 870 (s), 845 (s), 785 (s), 758 (m), 698 (s), 586 (s). Anal. Calcd for $C_{110}H_{146}Ca_2N_2$ (1576.55 g mol^{-1}) C, 83.80; H, 9.33; N, 1.78. Found C, 83.45; H, 9.00; N, 1.45.

Synthesis of {[*t*Bu$_2$CarbAr$_2$]Yb(μ^2-H)(η^6-C$_7$H$_8$)}$_2$ (12). The synthetic protocol analogous to that for **11** was applied. Complex **8** (1.00 g, 1.01 mmol) and PhSiH$_3$ (0.163 g, 1.51 mmol) were used in the synthesis. The reaction was carried out in toluene (15 mL) at 23 °C within 48h. The mother liquor was separated from black crystals by decantation. The crystals of **12** were washed with hexane (2×10 mL) and dried for 20 min in vacuum. Yield 87% (0.80 g). ^{1}H NMR (400 MHz, C$_5$D$_5$N, 298 K): δ 8.70-8.35 (compl m, 6H, 4,5-CH-carbazolyl and 2,6-CH-aryl), 7.75 (br s, 2H, 4-CH-aryl), 7.57 (s, 2H, 2,7-CH-carbazolyl), 7.30-7.07 (compl m, 5H, CH-toluene), 3.65 (s. 1H, C*H*D-DHP), 2.22 (s, 3H, C*H*$_3$Ph), 1.58 (s, 18H, *t*Bu-carbazolyl), 1.38 (s, 36H, *t*Bu-aryl). ^{13}C{^{1}H} NMR (100 MHz, C$_5$D$_5$N, 298 K): δ 150.61 (br s, *ipso*-C-aryl), 144.28 (br s, C-carbazolyl), 137.81 (s, *ipso*-C-toluene), 134.00 (s, C-carbazolyl), 130.10 (br s, C-carbazolyl), 129.21 (s, CH-toluene), 129.08 (s, C-carbazolyl), 128.35 (s, CH-toluene), 127.32 (br s, *ipso*-C-aryl), 125.57 (s, CH-toluene), 125.48 (br s, *C*D-DHP), 124.56 (s, 2,6-CH-aryl), 124.00 (br s, overlapped with py-d$_5$,

*C*D-DHP), 123.56 (br s, overlapped with py-d_5, *C*D-DHP), 122.83 (br s, 4-CH-aryl), 119.86 (br s, CH-carbazolyl), 115.03 (br s, CH-carbazolyl), 92.17 (br s, *C*D-DHP), 47.78 (br s, *C*HD-DHP), 34.89 (s, *C*$(CH_3)_3$-aryl), 34.57 (s, *C*$(CH_3)_3$-carbazolyl), 32.60 (s, C(*C*$H_3)_3$-carbazolyl), 31.82 (s, C(*C*$H_3)_3$-aryl), 21.15 (s, CH_3-toluene). IR (KBr): 1767 (m), 1590 (s), 1291 (s), 1265 (m), 1248 (m), 1202 (m), 1177 (m), 1155 (m), 1072 (s), 1026 (s), 937 (s), 870 (s), 845 (s), 795 (s), 758 (m), 646 (s), 584 (s). Anal. Calcd for $C_{110}H_{146}Yb_2N_2$ (1842.50 g mol^{-1}) C, 71.71; H, 7.99; N, 1.52; Yb, 18.78. Found C, 71.36; H, 7.60; N, 1.46; Yb, 18.54.

Synthesis of 2,4-*i*$Pr_2C_6H_3SiH_3$.

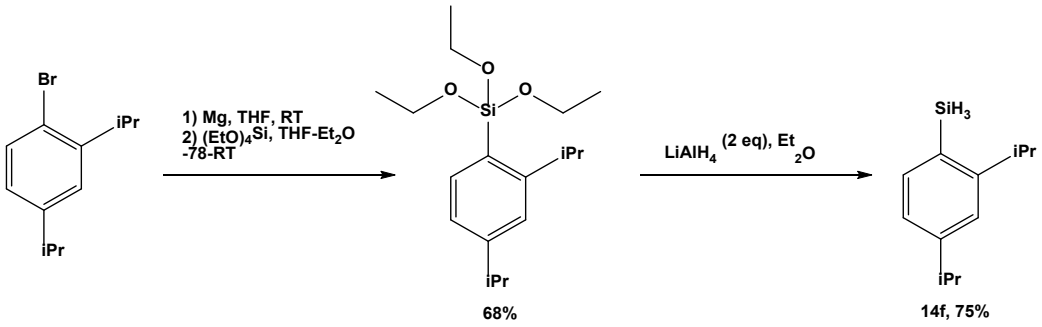

Stage 1. A flame dried 2-neck round bottom flask was purged with Ar, charged with Mg turnings (0.9 g, 37 mmol), THF (50 mL) and 2,4-i$Pr_2C_6H_4Br$ (6.00 g, 25 mmol) was added slowly over the course of 45 in Ar atmosphere. The reaction mixture was refluxed for an additional hour and left overnight under Ar. Then it was cooled to -35 °C and $(EtO)_4Si$ (10 g, 50 mmol in 30 mL of Et_2O) was added dropwise. The mixture was slowly brought to room temperature and left overnight. The volatiles were removed in vacuum and the Kugelrohr distillation of the residue (100 °C, 3×10^{-2} mm Hg) afforded 5.50 g (68%) of $ArSi(OEt)_3$. ^{1}H NMR (300 MHz, $CDCl_3$, 298 K): δ 7.67 (d, 1H, CH-Ar, $^3J_{HH}$ = 7.7 Hz), 7.21 (d, 1H, CH-Ar, $^4J_{HH}$ = 1.2 Hz), 7.07 (dd, 1H, CH-Ar, $^3J_{HH}$ = 7.7 Hz, $^4J_{HH}$ = 1.5 Hz), 3.89 (q, 6H, OCH_2, $^3J_{HH}$ = 7.0 Hz), 3.35 (hept, 1H, C*H*$(CH_3)_2$, $^3J_{HH}$ = 7.7 Hz), 2.91 (hept, 1H, C*H*$(CH_3)_2$, $^3J_{HH}$ = 7.6 Hz), 1.41-1.16 (compl m, 21H, CH(C*H*$_3)_2$ and CH_2CH_3). ^{13}C{^{1}H} NMR (75 MHz, $CDCl_3$, 298 K): δ 156.13 (s, , *ipso*-C-aryl), 151.44 (s, *ipso*-C-aryl), 136.59 (s, CH-Ar), 125.86 (s, C-Si), 123.37 (s, CH-Ar), 123.12 (s, CH-Ar), 58.51 (s, *C*H_2CH_3), 34.30 (s, *C*H$(CH_3)_2$), 33.65 (s, *C*H$(CH_3)_2$), 24.67 (s, CH(*C*$H_3)_2$), 23.84 (s, CH(*C*$H_3)_2$), 18.21 (s, CH_2*C*H_3). Anal. Calcd for $C_{18}H_{32}SiO_3$ (324.54 g mol^{-1}) C, 66.62; H, 9.94. Found C, 66.45; H, 9.80.

Stage 2. The solution of 2,4-*i*$Pr_2C_6H_4Si(OEt)_3$ (5.50 g, 17 mmol) in Et_2O (15 mL) was gradually poured into suspension of $LiAlH_4$ (1.93 g, 51 mmol) in Et_2O (25 mL) at 0 °C. The suspension was brought to room temperature and left for 2 days under an Ar atmosphere. The mixture was filtered to remove excess of $LiAlH_4$, the volatiles were removed in vacuo and the residue was distilled (55 °C, 3×10^{-2} mm Hg) to afford 2.44 g (75%) of 2,4-*i*$Pr_2C_6H_4SiH_3$. ^{1}H NMR (300 MHz, $CDCl_3$, 298 K): δ 7.56 (d, 1H, CH-Ar, $^3J_{HH}$ = 7.6 Hz), 7.19 (s, 1H, CH-Ar), 7.08 (dd, 1H, CH-Ar, $^3J_{HH}$ = 7.6 Hz, $^4J_{HH}$ = 1.3 Hz), 4.25 (s, 3H, SiH_3), 3.14-2.95 (m, 1H, C*H*$(CH_3)_2$), 2.99-2.82 (m, 1H, C*H*$(CH_3)_2$), 1.35-1.23 (m, 12H, CH(C*H*$_3)_2$). ^{13}C{^{1}H} NMR (75 MHz, $CDCl_3$, 298 K): δ 155.54 (s, *ipso*-C-aryl), 151.94 (s, *ipso*-C-aryl), 137.62 (s, CH-Ar), 124.05 (s, C-Si), 123.67 (s, CH-Ar), 123.01 (s, CH-Ar), 35.10 (s, *C*H$(CH_3)_2$), 34.41 (s, *C*H$(CH_3)_2$), 23.98 (s, CH(*C*$H_3)_2$), 23.93 (s, CH(*C*$H_3)_2$). Anal. Calcd for $C_{12}H_{20}Si$ (192.38 g mol^{-1}) C, 74.92; H, 10.48. Found C, 74.70; H, 10.30.

General procedure for catalytic $PhSiH_3$ addition to pyridine-type heterocycles.

In a nitrogen-filled glovebox, **11** (2 mol %), heterocycle **13** (0.2 mmol), $PhSiH_3$ and C_6D_6 were charged into NMR-tube. The NMR-tube was sealed and the mixture was left at 23 °C for the desired reaction time (see Scheme 3). The progress of the reaction was monitored by ^1H NMR spectroscopy. The chemo- and regioselectivity (1,2-silylation vs 1,4-silylation products) and yield were determined by ^1H NMR -spectra.

Preparative catalytic procedure for bis-(1,2-dihydroisoquinoline)-4-*t*-Bu-phenylsilane (**15j**). To a suspension of **11** (0.02 g, 0.025 mmol, 2 mol %) in C_6D_6 (0.5 mL) *i*-quinoline (0.32 g, 2.5 mmol) and 4-*t*-Bu-phenylsilane (0.20 g, 1.26 mmol) were added at 23 °C. In 2 h the solvent was removed in vacuum and the product was obtained as air-sensitive viscous yellow oil in 99% yield (0.50 g). ^1H NMR (300 MHz, $CDCl_3$, 298 K): δ 7.47 (d, 2H, CH-Ar, $^3J_{HH}$ = 8.2 Hz), 7.19 (d, 2H, CH-Ar, $^3J_{HH}$ = 8.2 Hz), 7.01 (td, 2H, CH-DHQ, $^3J_{HH}$ = 7.5 Hz, $^4J_{HH}$ = 3.7 Hz), 6.91 (td, 2H, CH-DHQ, $^3J_{HH}$ = 7.4 Hz, $^4J_{HH}$ = 1.2 Hz), 6.82 (d, 2H, CH-DHQ, $^3J_{HH}$ = 7.4 Hz), 6.61 (d, 2H, CH-DHQ, $^3J_{HH}$ = 7.3 Hz), 6.35 (d, 2H, CH-DHQ, $^3J_{HH}$ = 7.3 Hz), 5.59 (d, 2H, CH-DHQ, $^3J_{HH}$ = 7.3 Hz), 5.12 (s, 1H, SiH), 4.35-4.20 (m, 4H, CH_2-DHQ), 1.13 (s, 9H, *t*Bu). $^{13}C\{^1H\}$ NMR (75 MHz, $CDCl_3$, 298 K): δ 154.17 (s, *ipso*-C), 135.11 (s, CH-Ar), 134.65 (s, CH-DHQ), 133.78 (s, *ipso*-C), 127.76 (s, CH-DHQ), 127.13 (s, *ipso*-C), 126.55 (s, C-Si), 125.74 (s, CH-DHQ), 125.60 (s, CH-Ar), 125.05 (s, CH-DHQ), 122.90 (s, CH-DHQ), 105.19 (s, CH-DHQ), 47.07 (s, CH_2N), 34.57 (s, $C(CH_3)_3$), 30.96 (s, $C(CH_3)_3$). Anal. Calcd for $C_{28}H_{30}N_2Si$ (422.65 g mol^{-1}) C, 79.57; H, 7.15; N, 6.63. Found C, 79.76; H, 7.30; N, 6.59.

Preparative catalytic procedure for bis-(1,2-dihydroisoquinoline)-4-*p*-MeO-phenylsilane (**15k**). To a suspension of **11** (0.02 g, 0.025 mmol, 2 mol %) in C_6D_6 (0.5 mL) *i*-quinoline (0.32 g, 2.5 mmol) and 4-*p*-MeO-phenylsilane (0.17 g, 1.26 mmol) were added at 23 °C. In 24 h the volatiles were removed in vacuum and the product was obtained as air-sensitive viscous yellow oil in 97% yield (0.48 g). ^1H NMR (300 MHz, $CDCl_3$, 298 K): δ 7.38 (d, 2H, CH-Ar, $^3J_{HH}$ = 8.6 Hz), 7.01 (td, 2H, CH-DHQ, $^3J_{HH}$ = 7.4 Hz, $^4J_{HH}$ = 1.1 Hz), 6.91 (td, 2H, CH-DHQ, $^3J_{HH}$ = 7.4 Hz, $^4J_{HH}$ = 1.3 Hz), 6.82 (d, 2H, CH-DHQ, $^3J_{HH}$ = 7.4 Hz), 6.71-6.59 (compl m, 4H, CH-DHQ), 6.36 (d, 2H, CH-Ar, $^3J_{HH}$ = 7.3 Hz),), 5.63 (d, 2H, CH-DHQ, $^3J_{HH}$ = 7.3 Hz), 5.10 (s, 1H, SiH), 4.26 (s, 4H, CH_2-DHQ), 3.22 (s, 3H, OMe). $^{13}C\{^1H\}$ NMR (75 MHz, $CDCl_3$, 298 K): δ 162.25 (s, *ipso*-*C*OMe), 136.72 (s, CH-Ar), 134.72 (s, CH-DHQ), 133.84 (s, *ipso*-C), 127.59 (s, CH-DHQ), 127.15 (s, *ipso*-C), 125.72 (s, CH-Ar), 125.03 (s, CH-DHQ), 122.87 (s, CH-DHQ), 120.48 (s, C-Si), 114.42 (s, CH-DHQ), 105.19 (s, CH-DHQ), 54.38 (s, OMe), 47.02 (s, CH_2N). Anal. Calcd for $C_{25}H_{24}N_2SiO$ (396.57 g mol^{-1}) C, 75.72; H, 6.10; N, 7.06. Found C, 75.90; H, 6.31; N, 6.90.

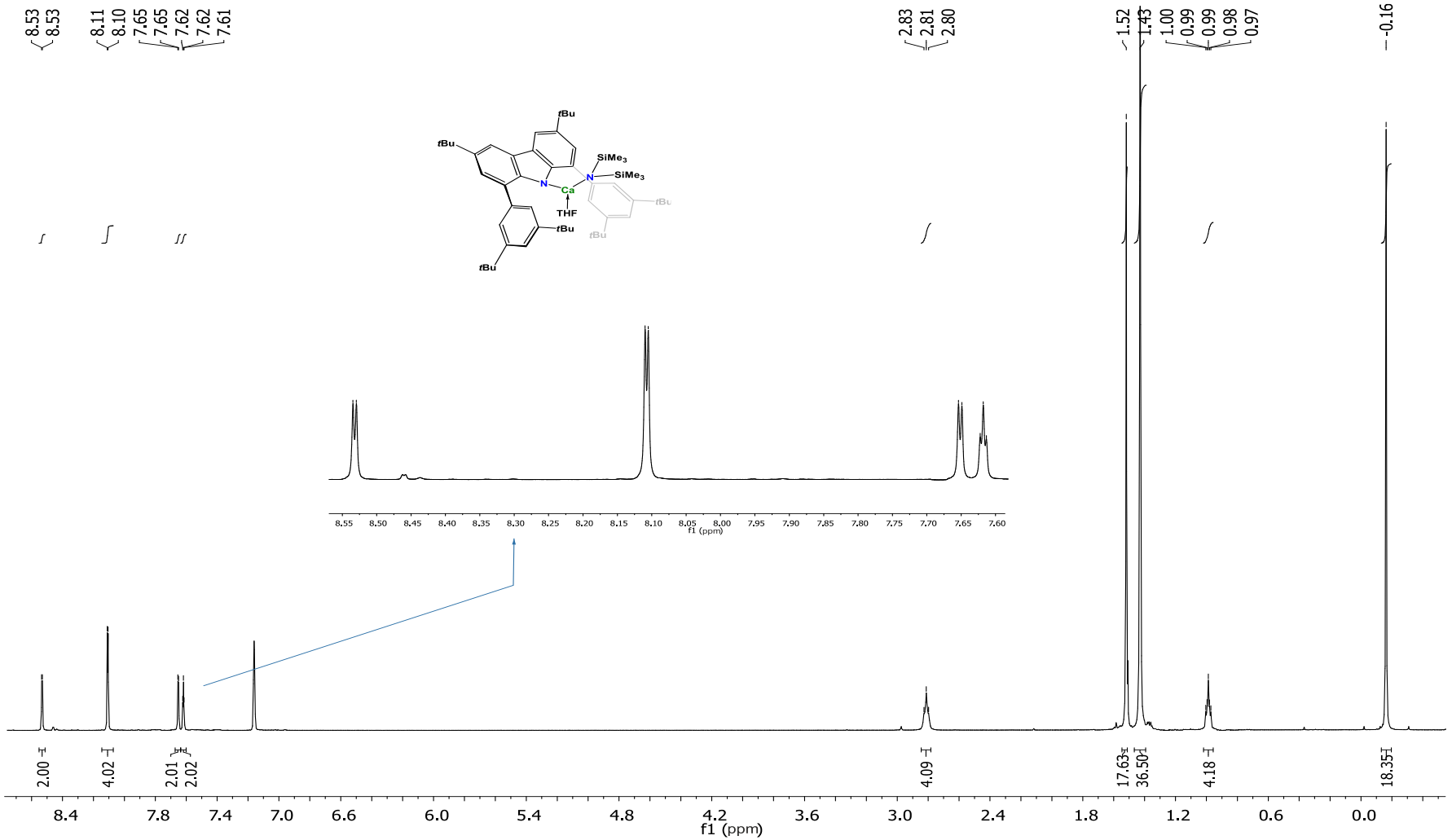

Figure S1. ^{1}H NMR spectrum of **5** (400 MHz, C_6D_6, 293 K).

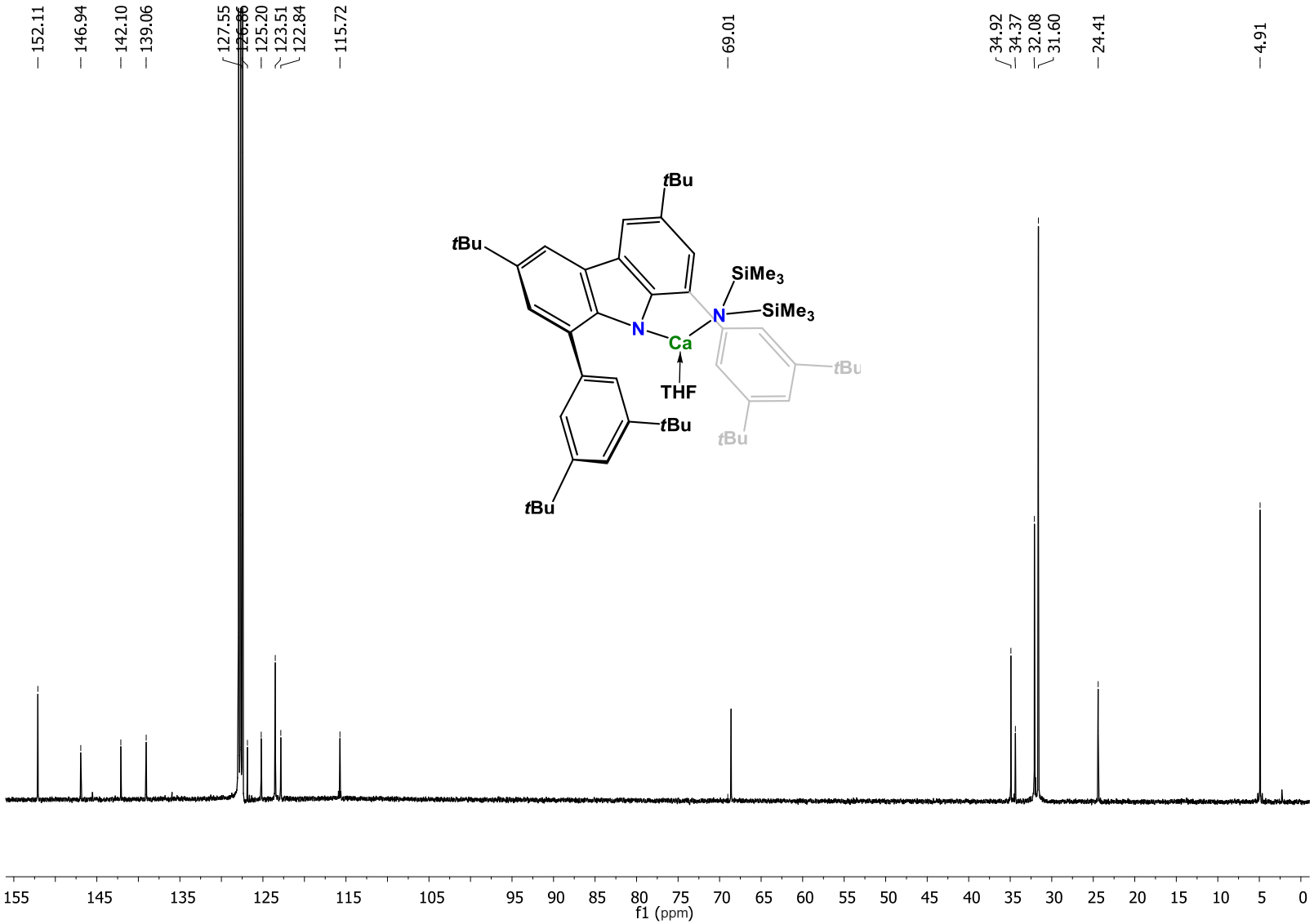

Figure S2. $^{13}C\{^{1}H\}$ NMR spectrum of **5** (100 MHz, C_6D_6, 293 K).

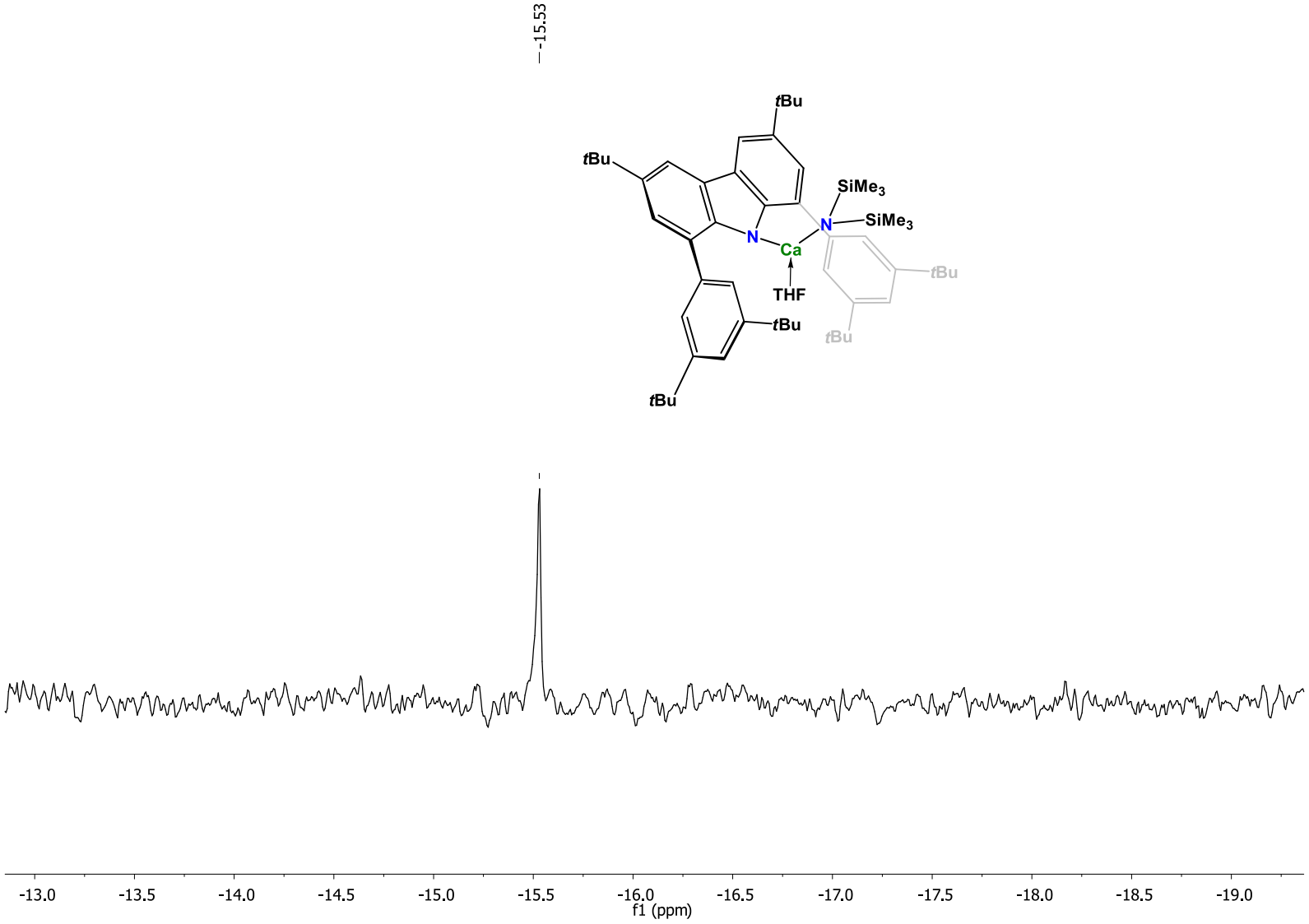

Figure S3. ^{29}Si NMR spectrum of **5** (79.5 MHz, C_6D_6, 293 K).

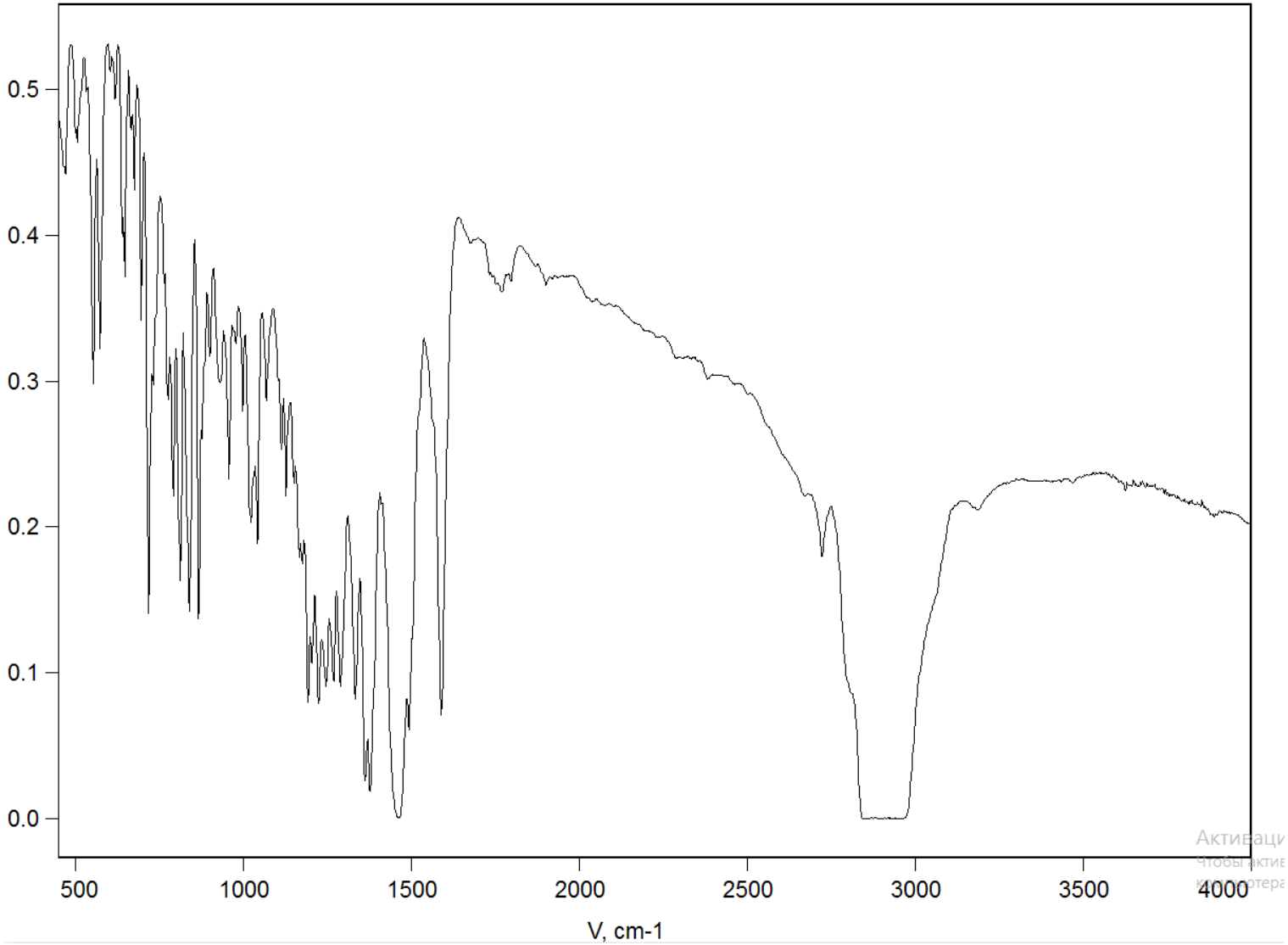

Figure S4. IR (KBr, Nujol) spectrum of complex **5**.

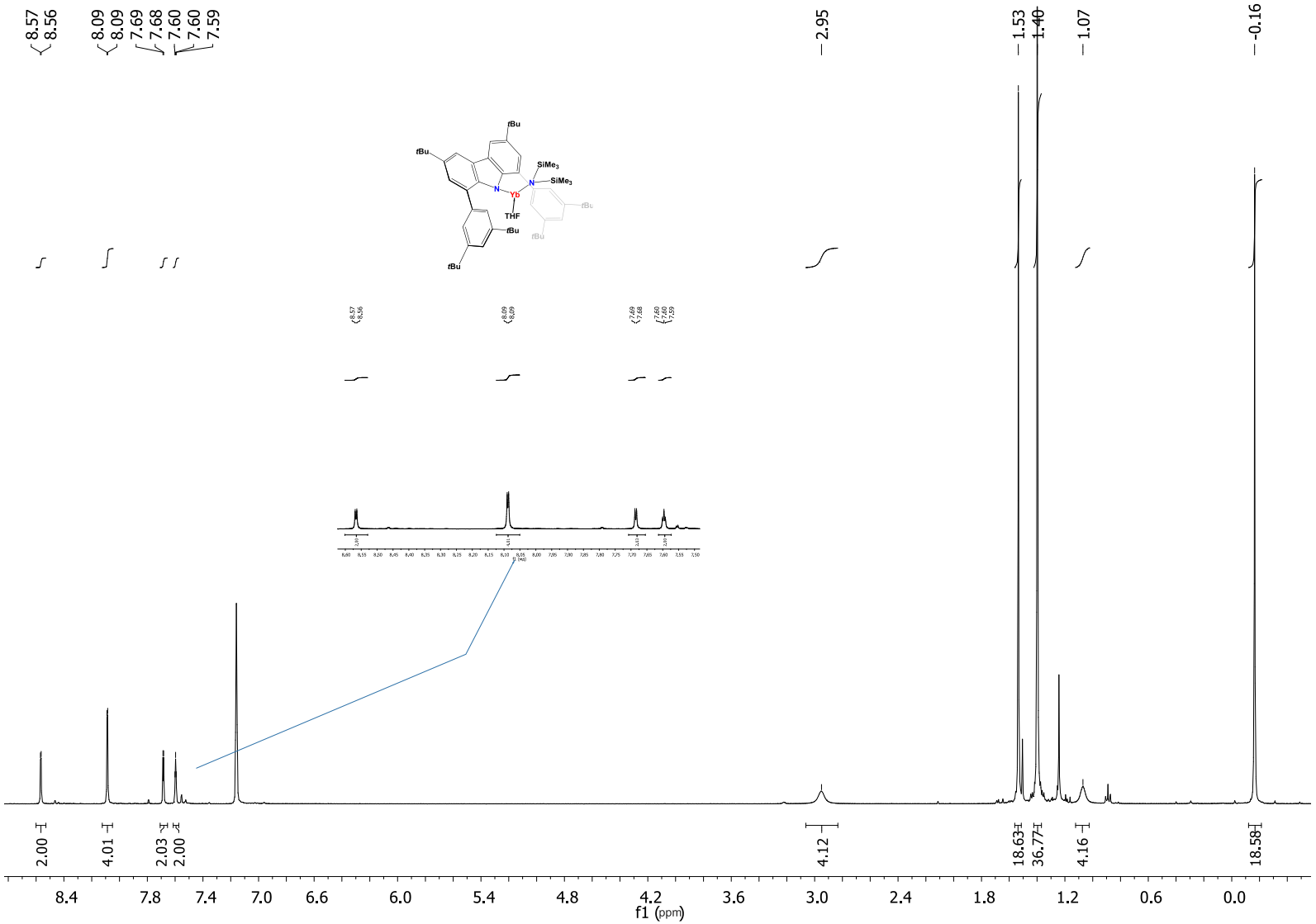

Figure S5. ^{1}H NMR spectrum of **6** (400 MHz, C_6D_6, 293 K).

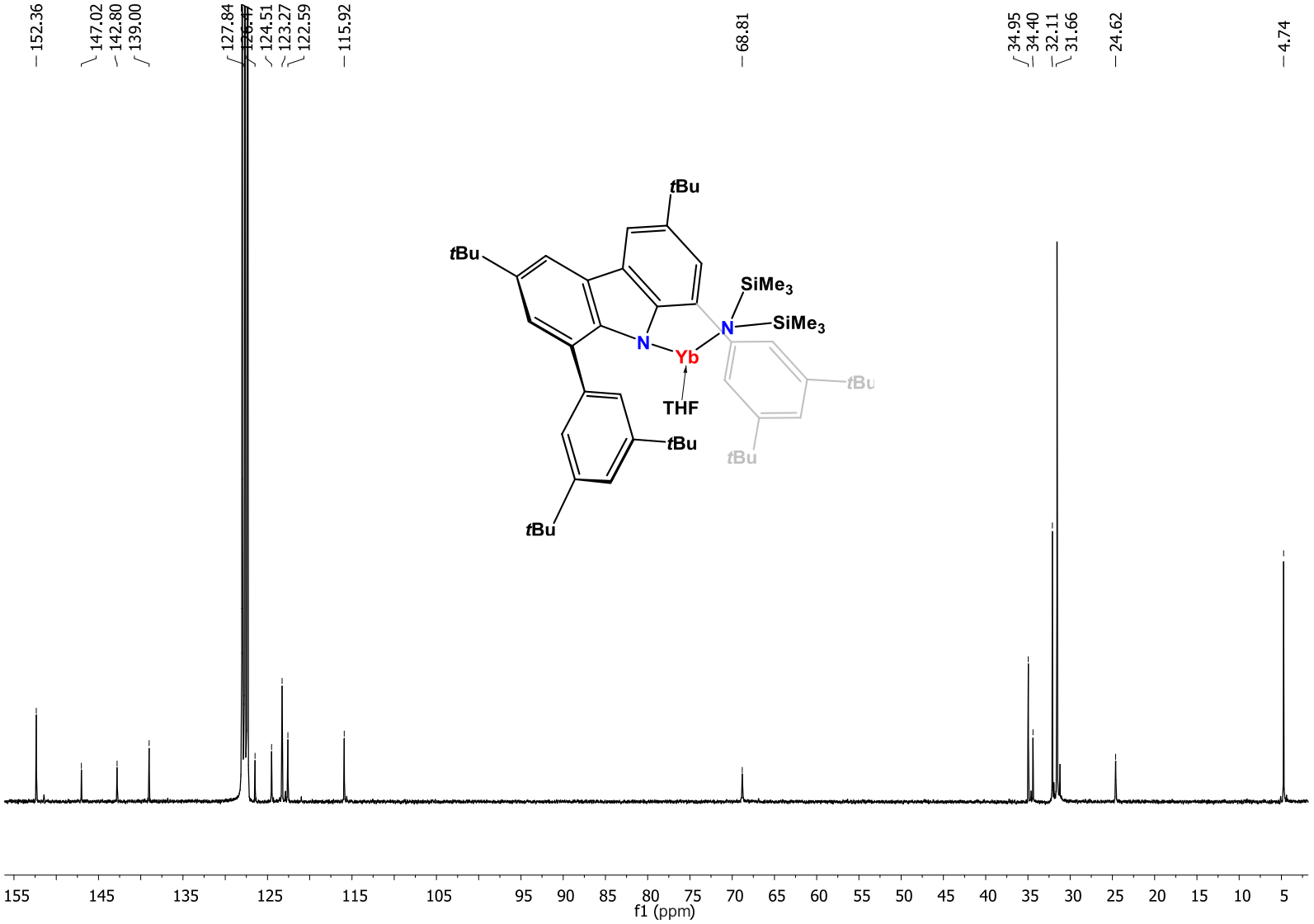

Figure S6. $^{13}C\{^{1}H\}$ NMR spectrum of **6** (100 MHz, C_6D_6, 293 K).

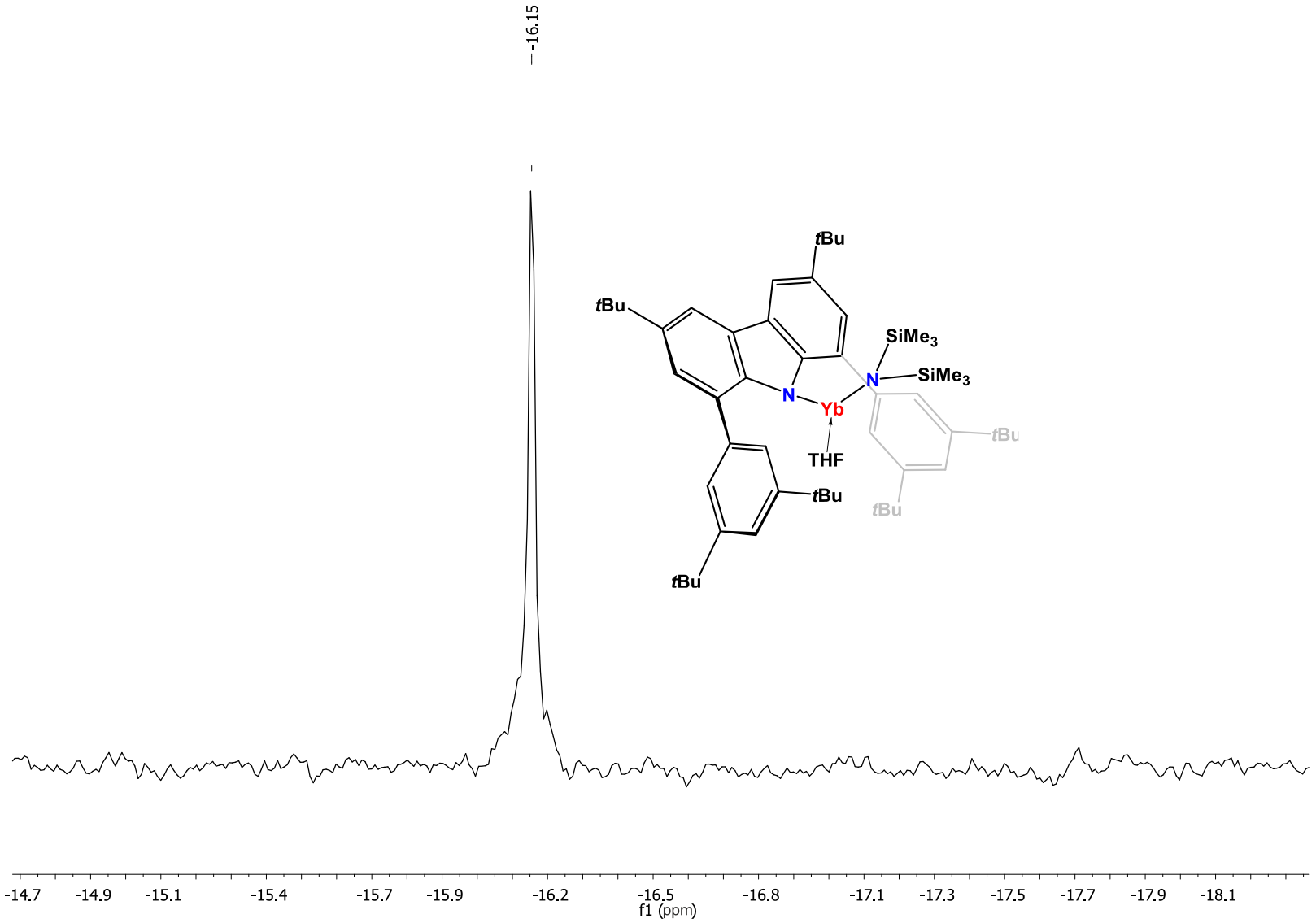

Figure S7. ^{29}Si NMR spectrum of **6** (79.5 MHz, C_6D_6, 293 K).

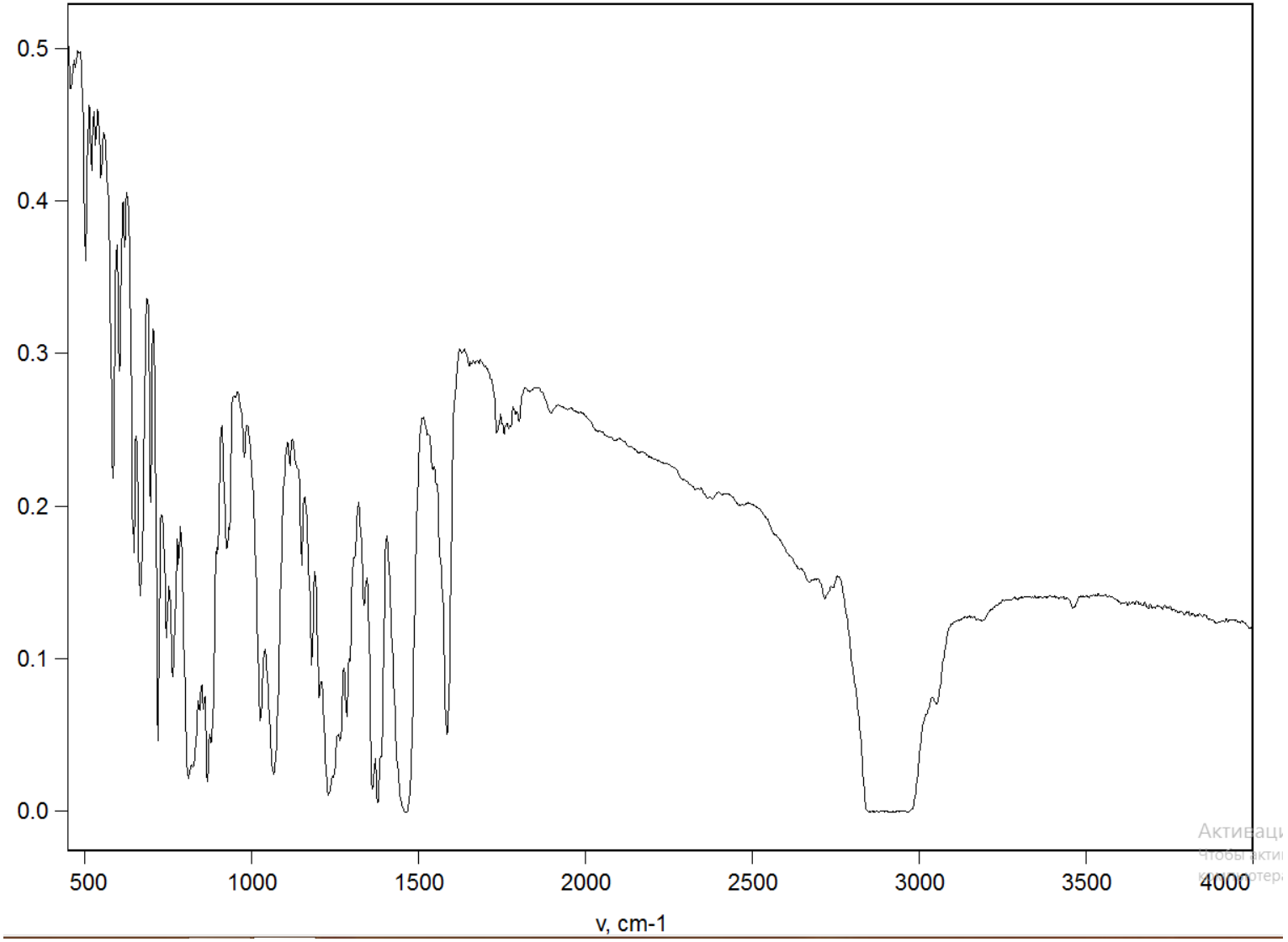

Figure S8. IR (KBr, Nujol) spectrum of complex **6**.

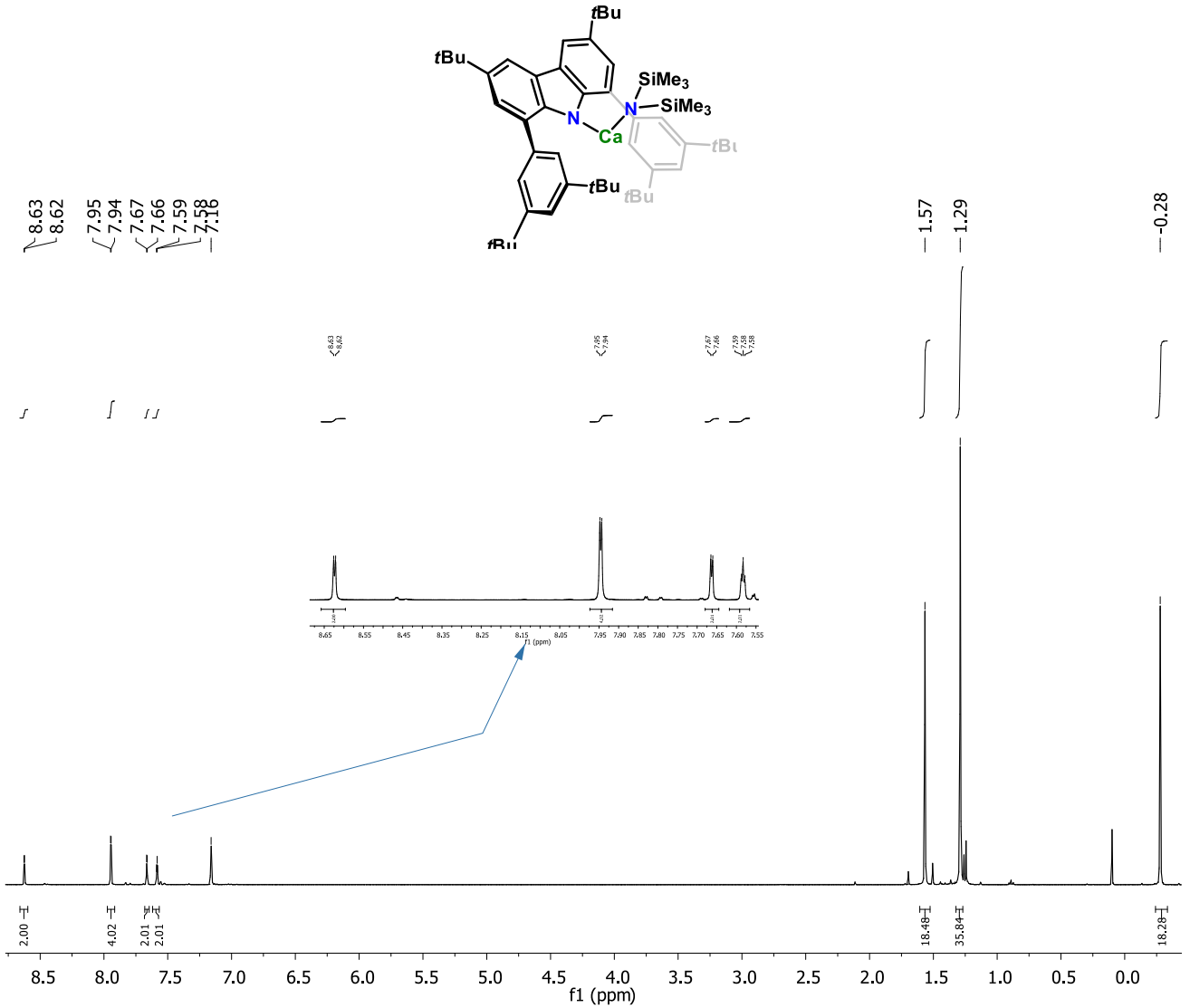

Figure S9. ^{1}H NMR spectrum of **7** (400 MHz, C_6D_6, 293 K).

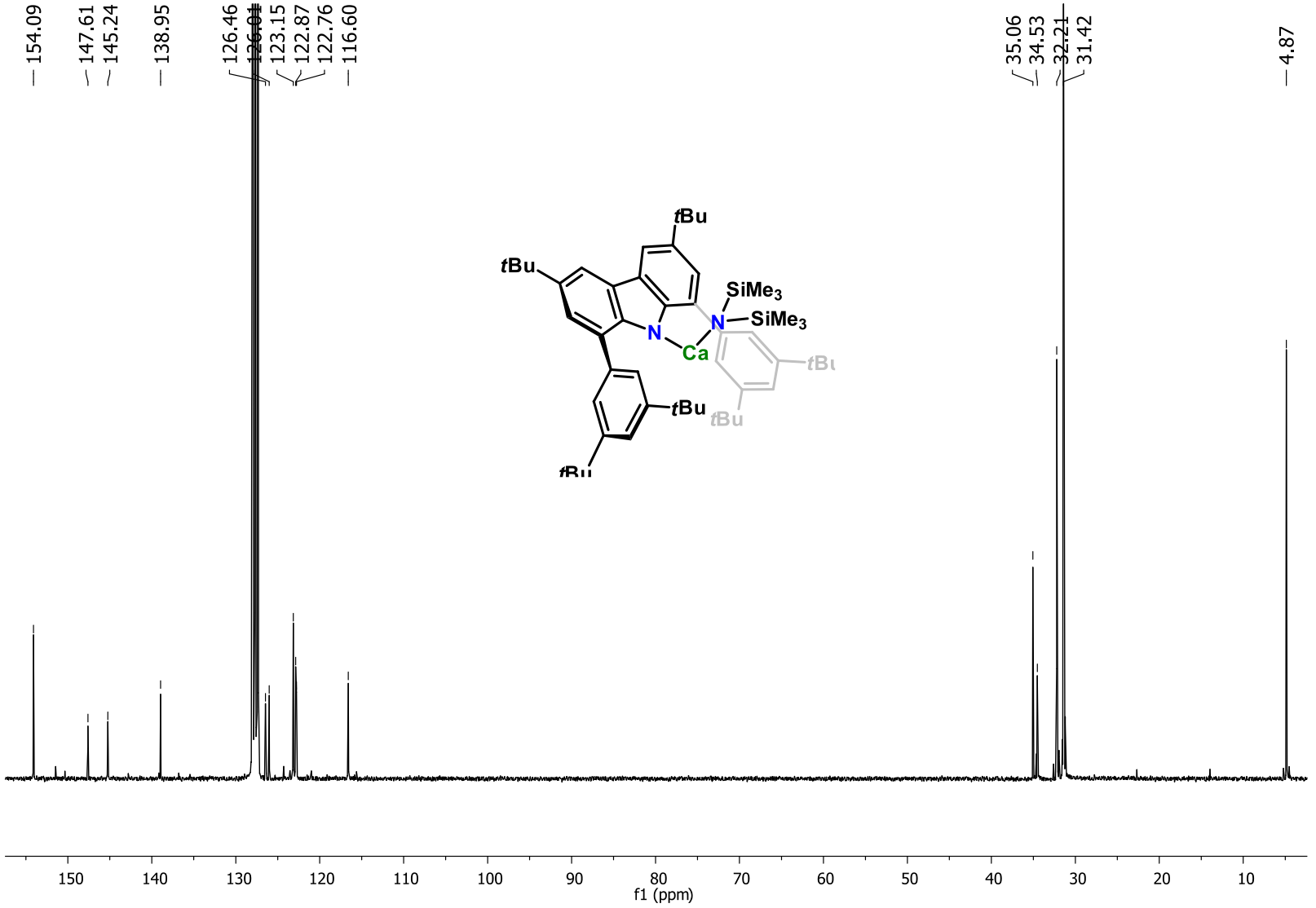

Figure S10. $^{13}C\{^{1}H\}$ NMR spectrum of **7** (100 MHz, C_6D_6, 293 K).

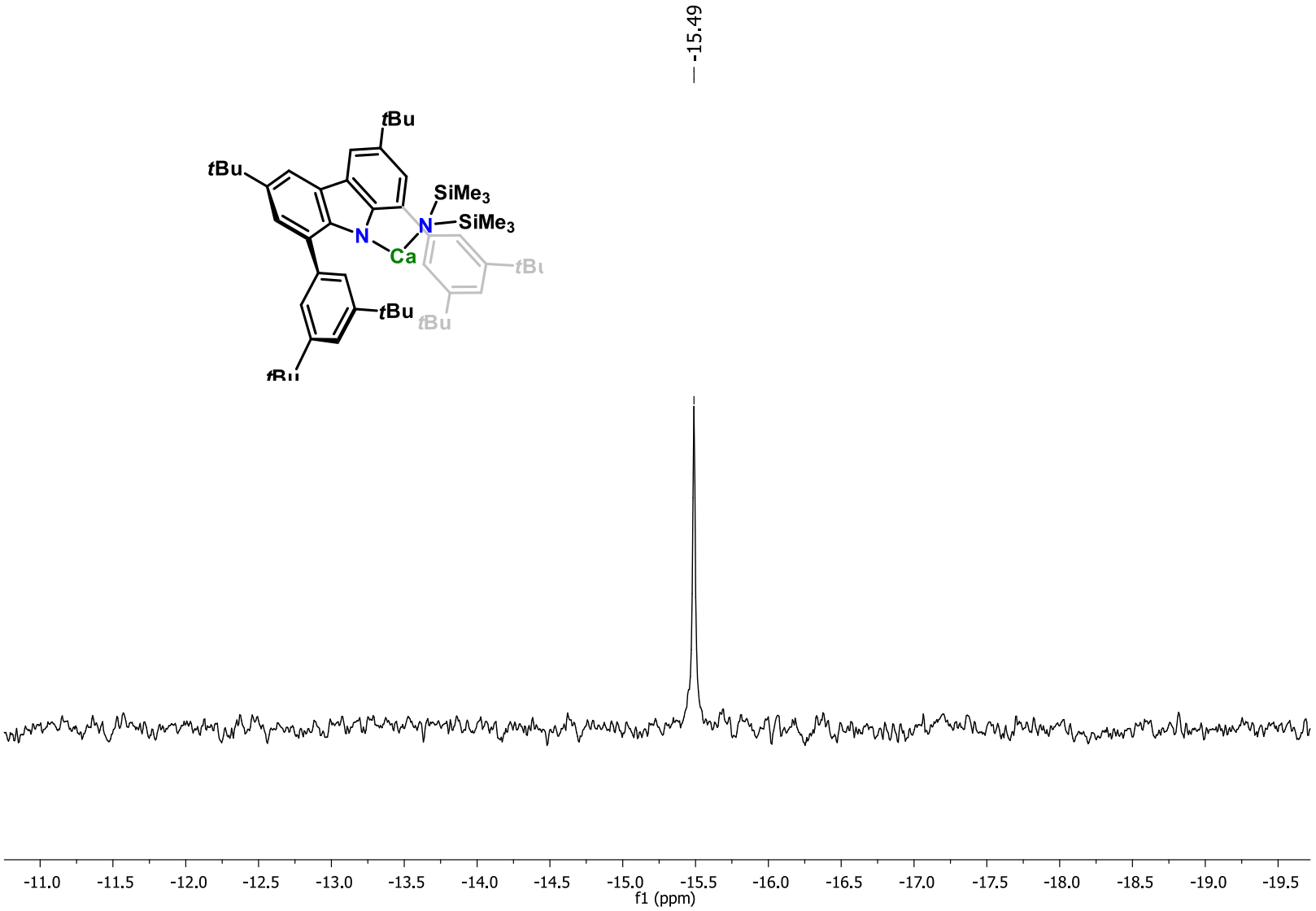

Figure S11. ^{29}Si NMR spectrum of **7** (79.5 MHz, C_6D_6, 293 K).

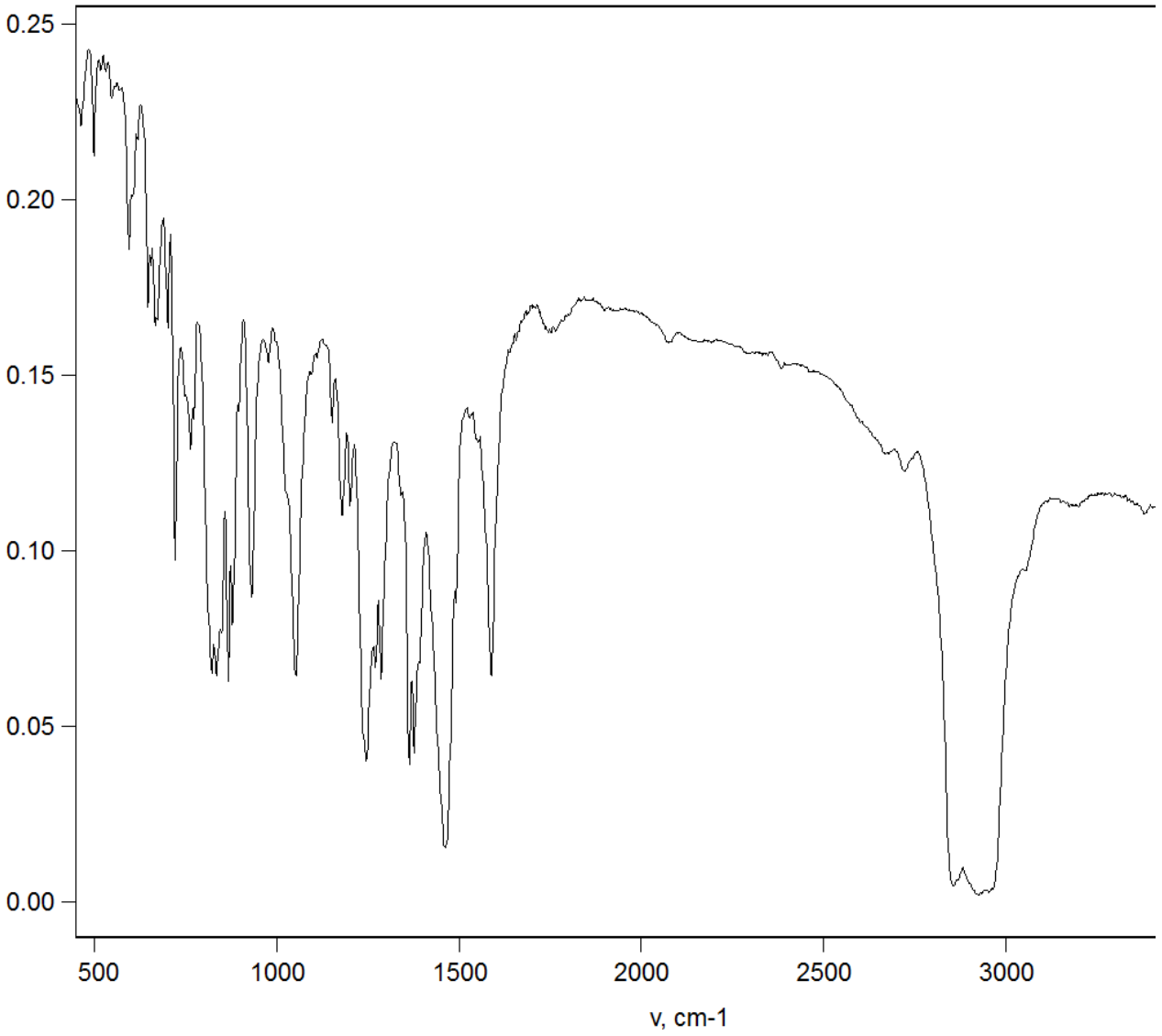

Figure S12. IR (KBr, Nujol) spectrum of complex **7**.

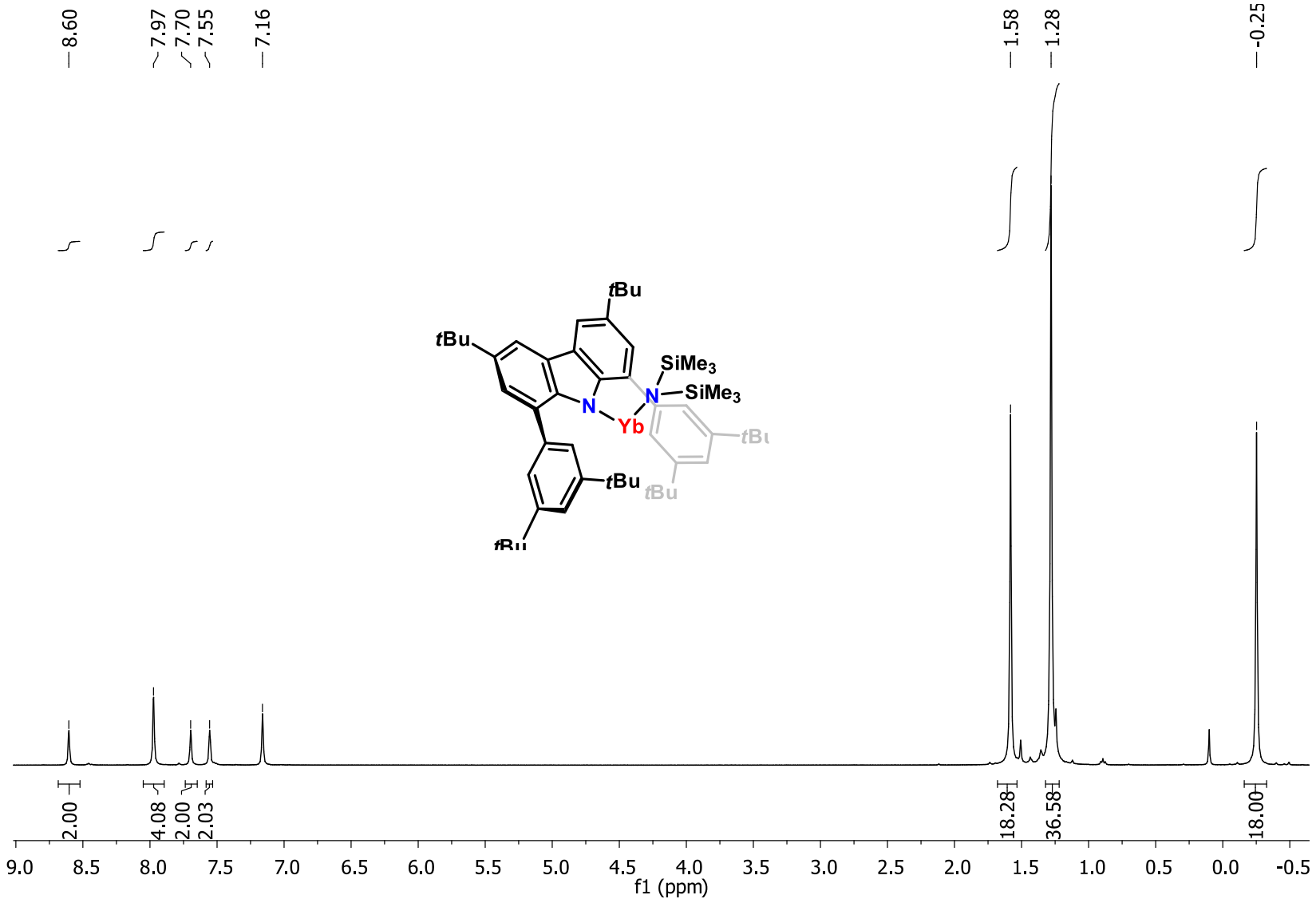

Figure S13. ^{1}H NMR spectrum of **8** (400 MHz, C_6D_6, 293 K).

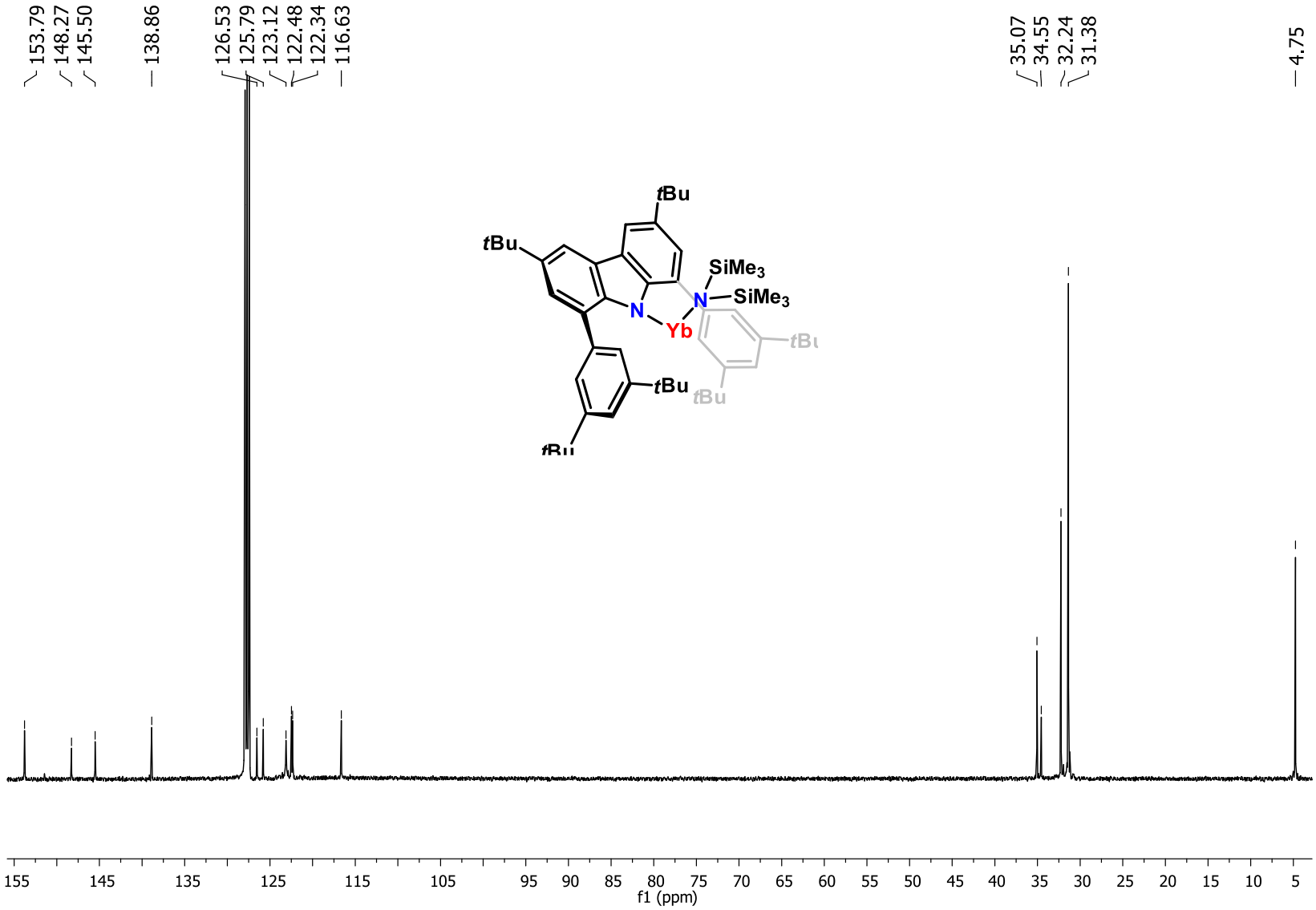

Figure S14. $^{13}C\{^{1}H\}$ NMR spectrum of **8** (100 MHz, C_6D_6, 293 K).

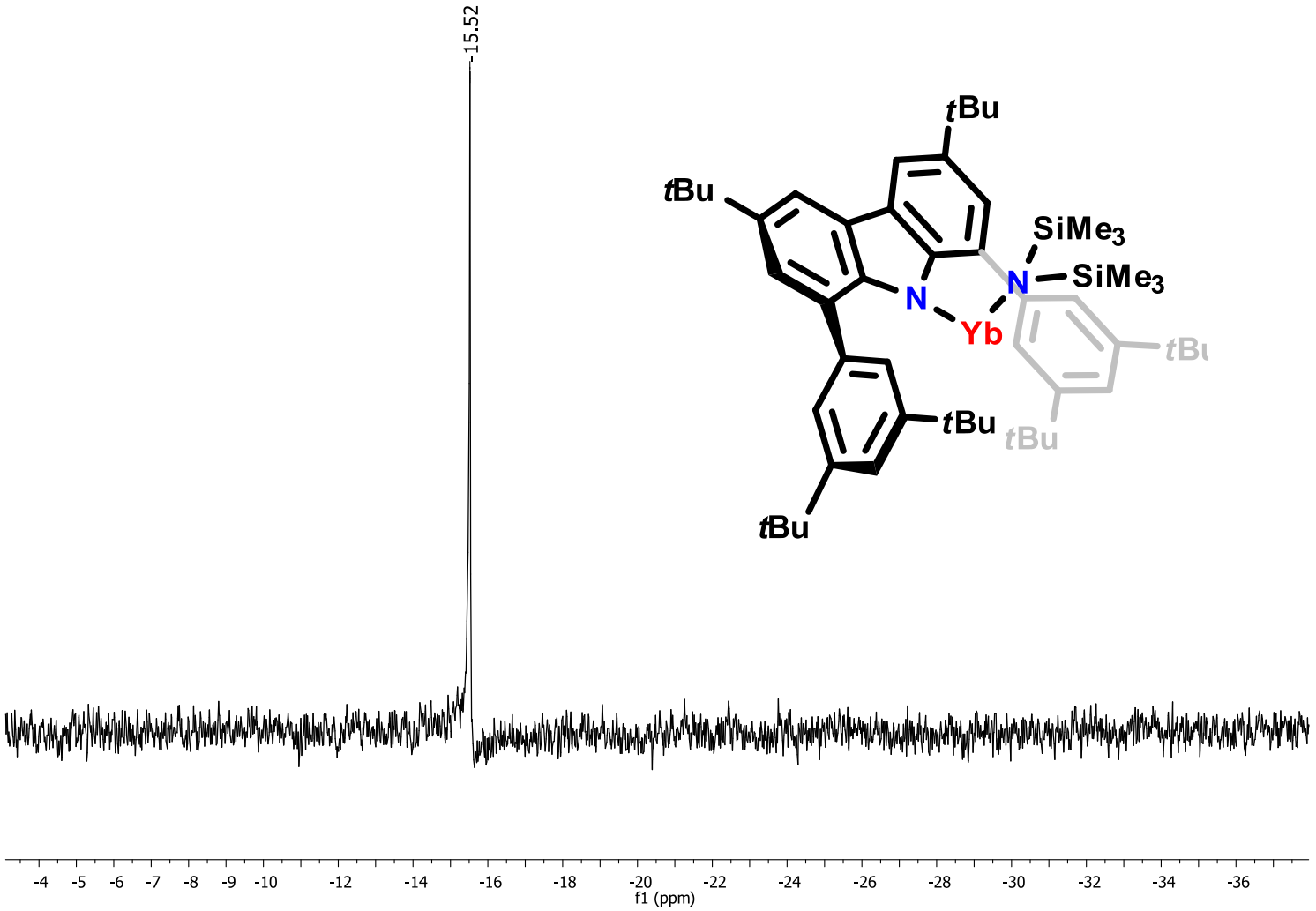

Figure S15. ^{29}Si NMR spectrum of **8** (79.5 MHz, C_6D_6, 293 K).

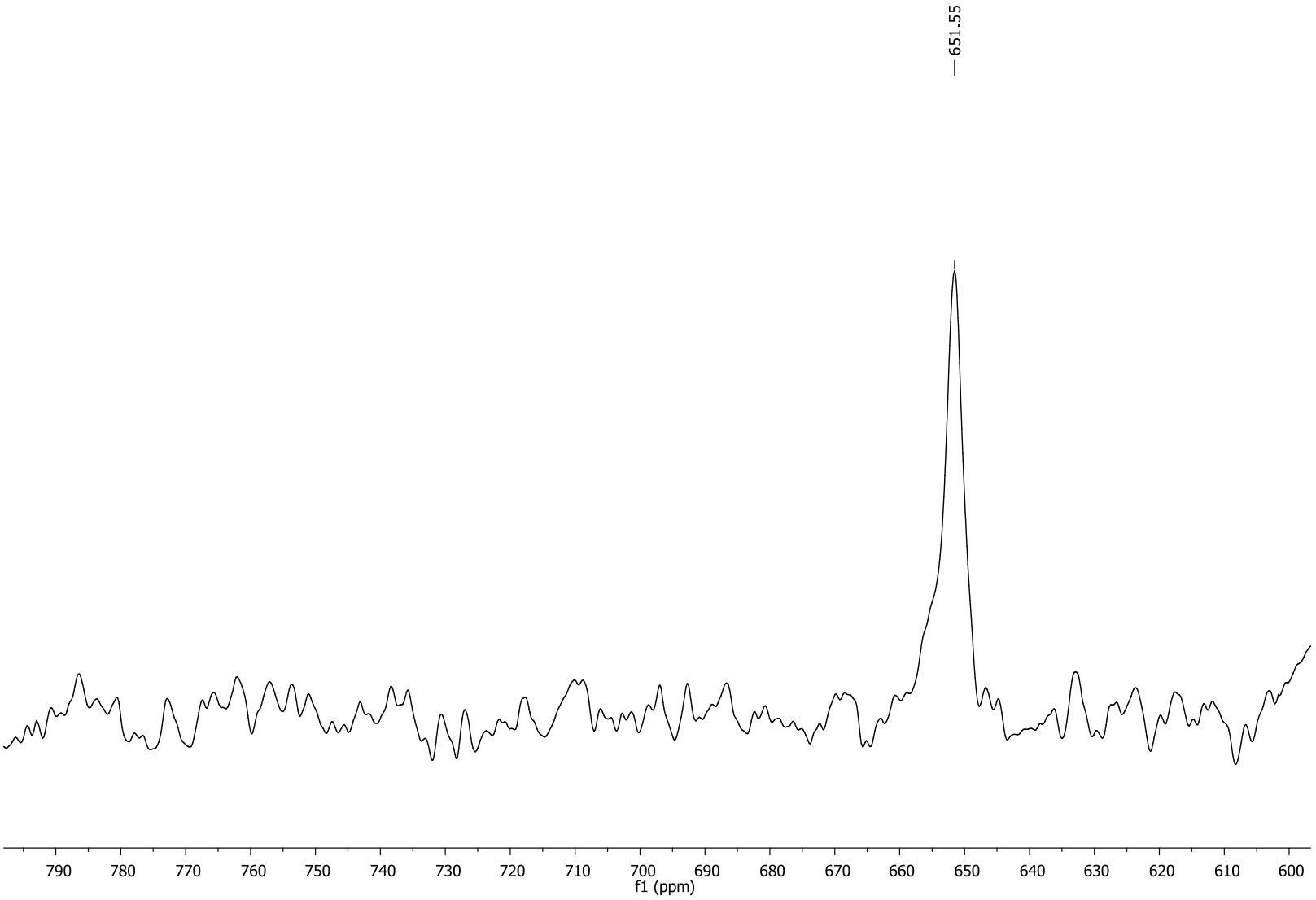

Figure S16. ^{171}Yb NMR spectrum of **8** (70 MHz, C_6D_6, 293 K).

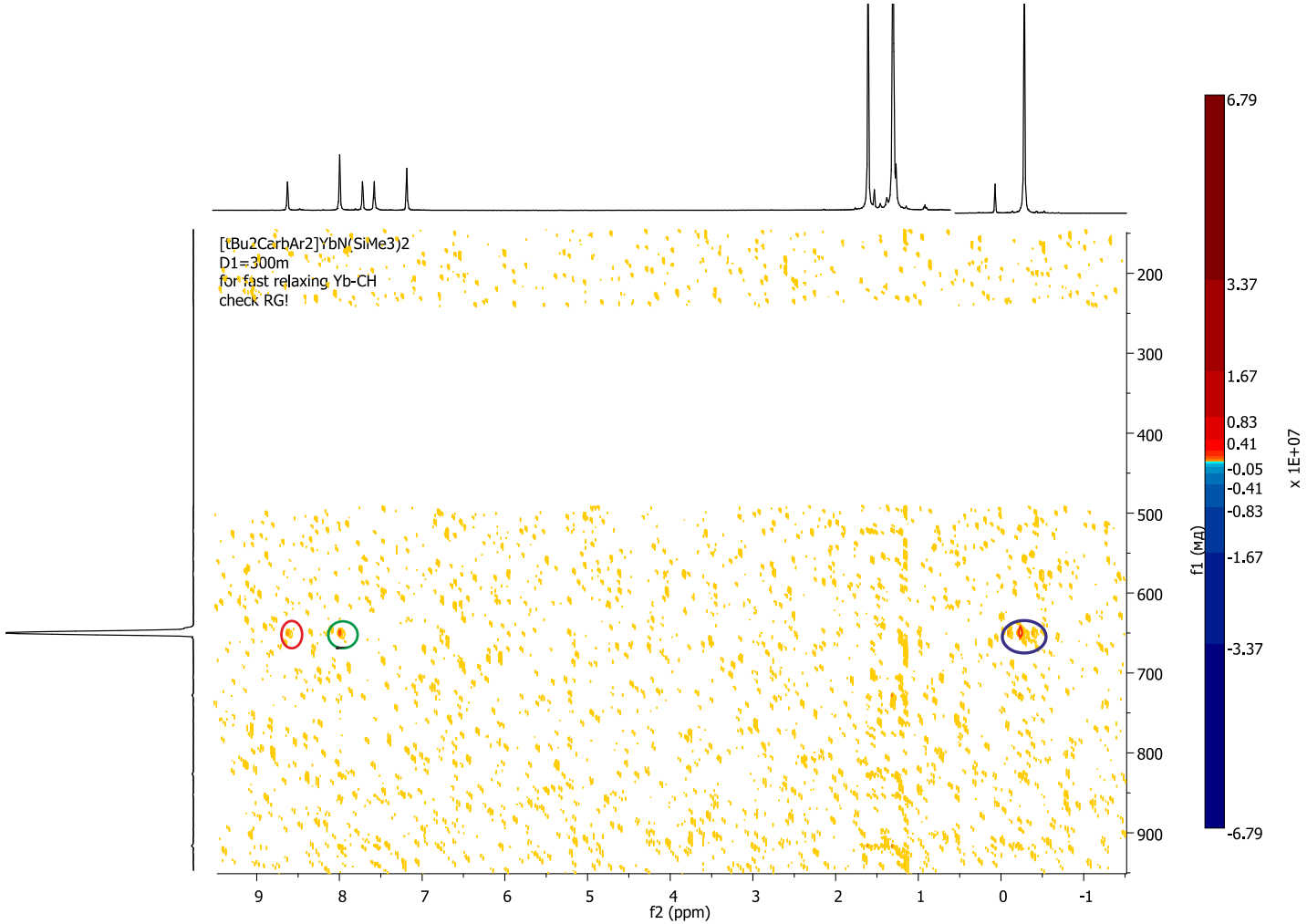

Figure S17. ^{171}Yb-^{1}H 2D *ge*-HMBC NMR spectrum of **8** (70 MHz, C_6D_6, 293 K).

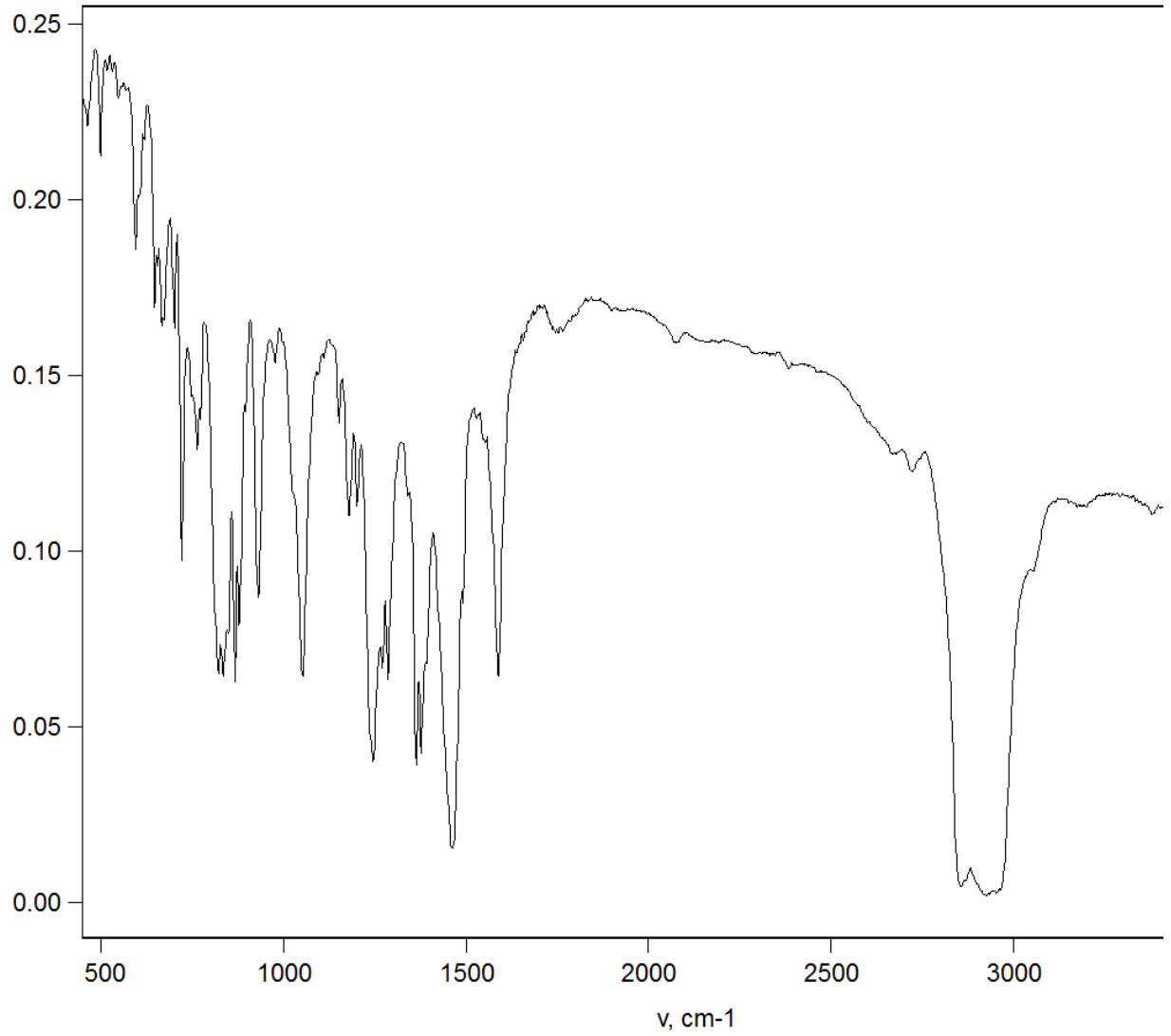

Figure S18. IR (KBr, Nujol) spectrum of complex **8**.

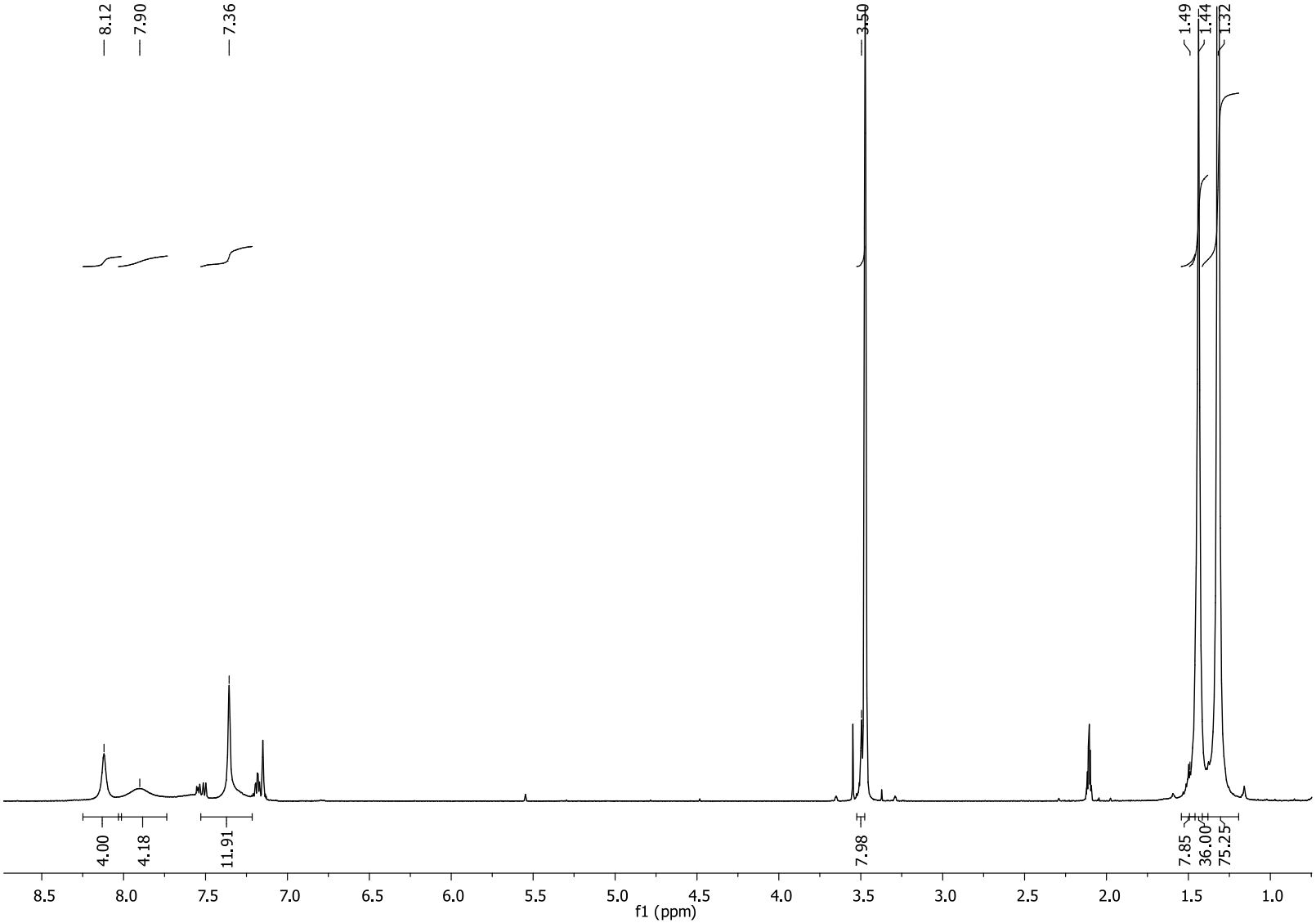

Figure S19. ^{1}H NMR spectrum of **9** (400 MHz, $C_5D_5CD_3$-THF-d_8 (1:1), 293 K).

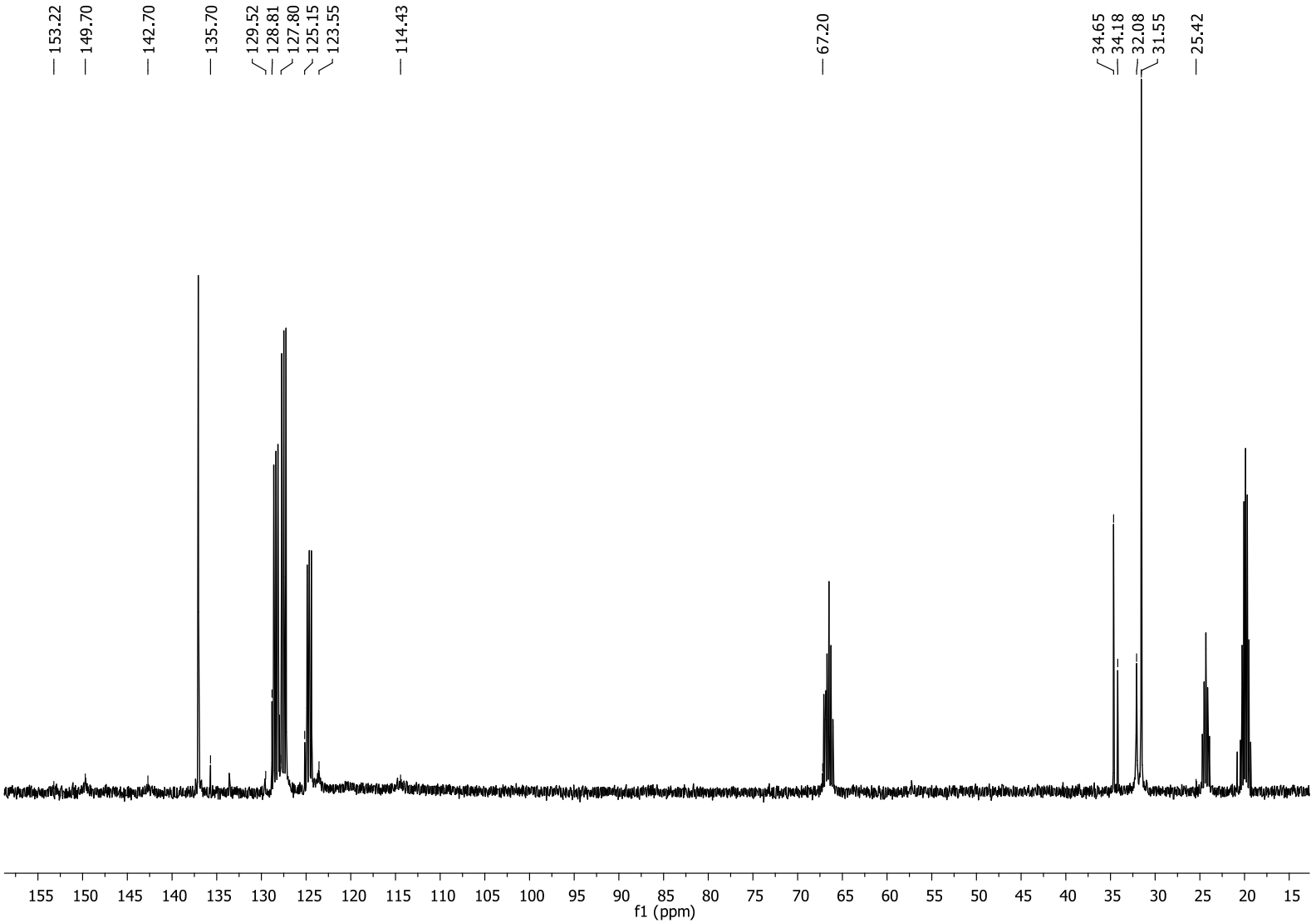

Figure S20. $^{13}C\{^{1}H\}$ NMR spectrum of **9** (100 MHz, $C_5D_5CD_3$-THF-d_8 (1:1), 293 K).

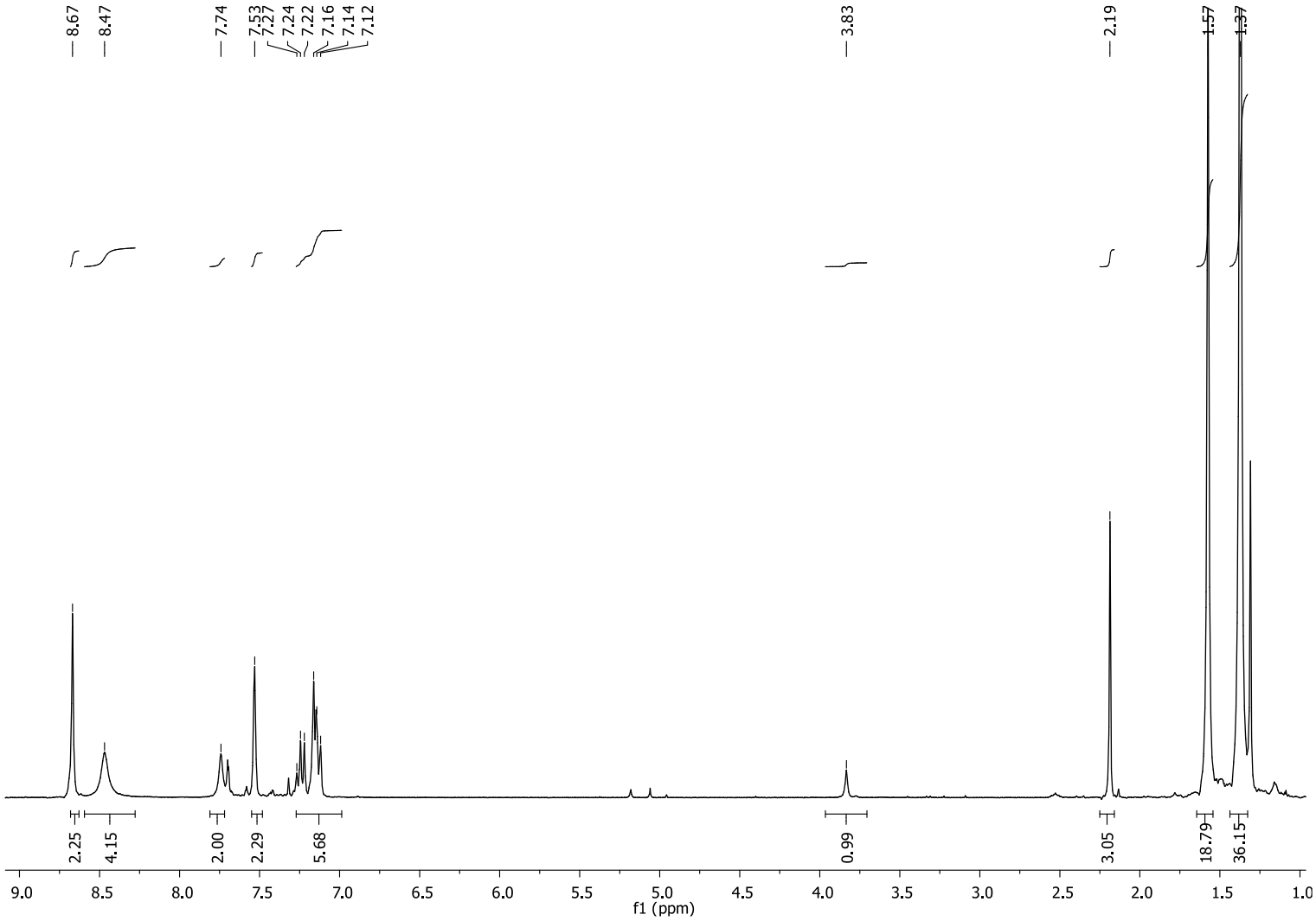

Figure S21. ^{1}H NMR spectrum of **11** (400 MHz, C_5D_5N, 293 K).

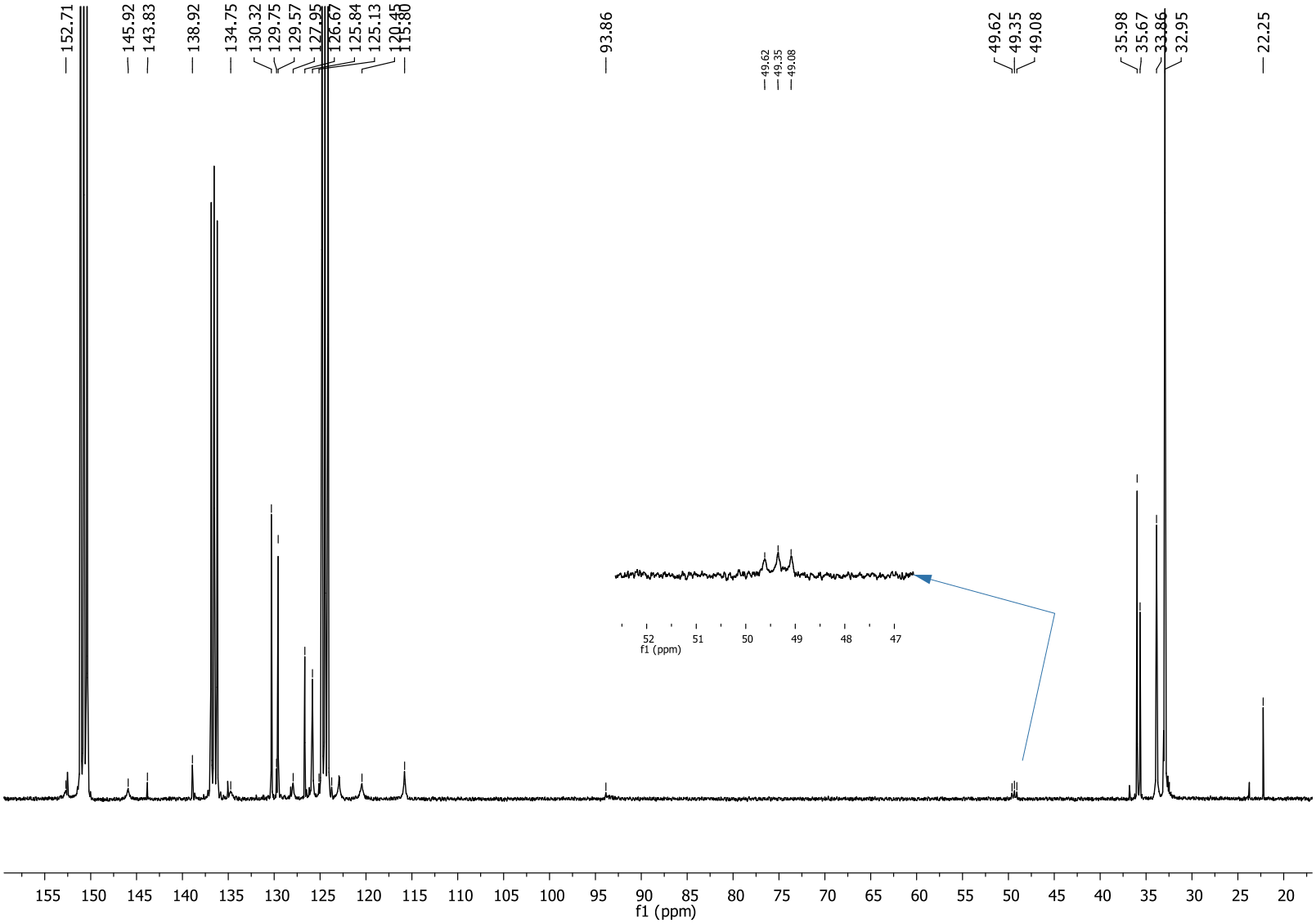

Figure S22. ^{13}C {^{1}H} NMR spectrum of **11** (100 MHz, C_5D_5N, 293 K).

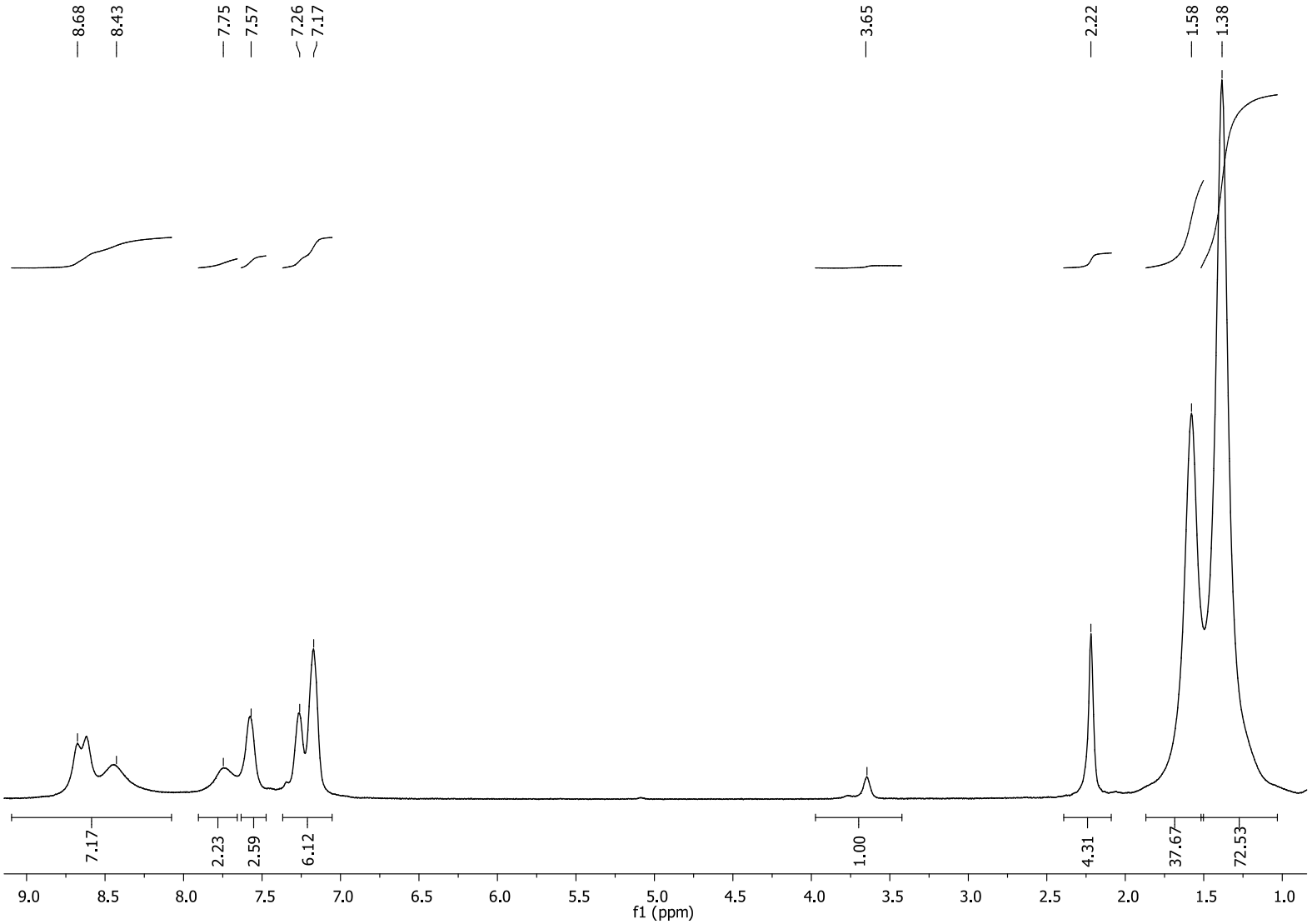

Figure S23. ^{1}H NMR spectrum of **12** (400 MHz, C_5D_5N, 293 K).

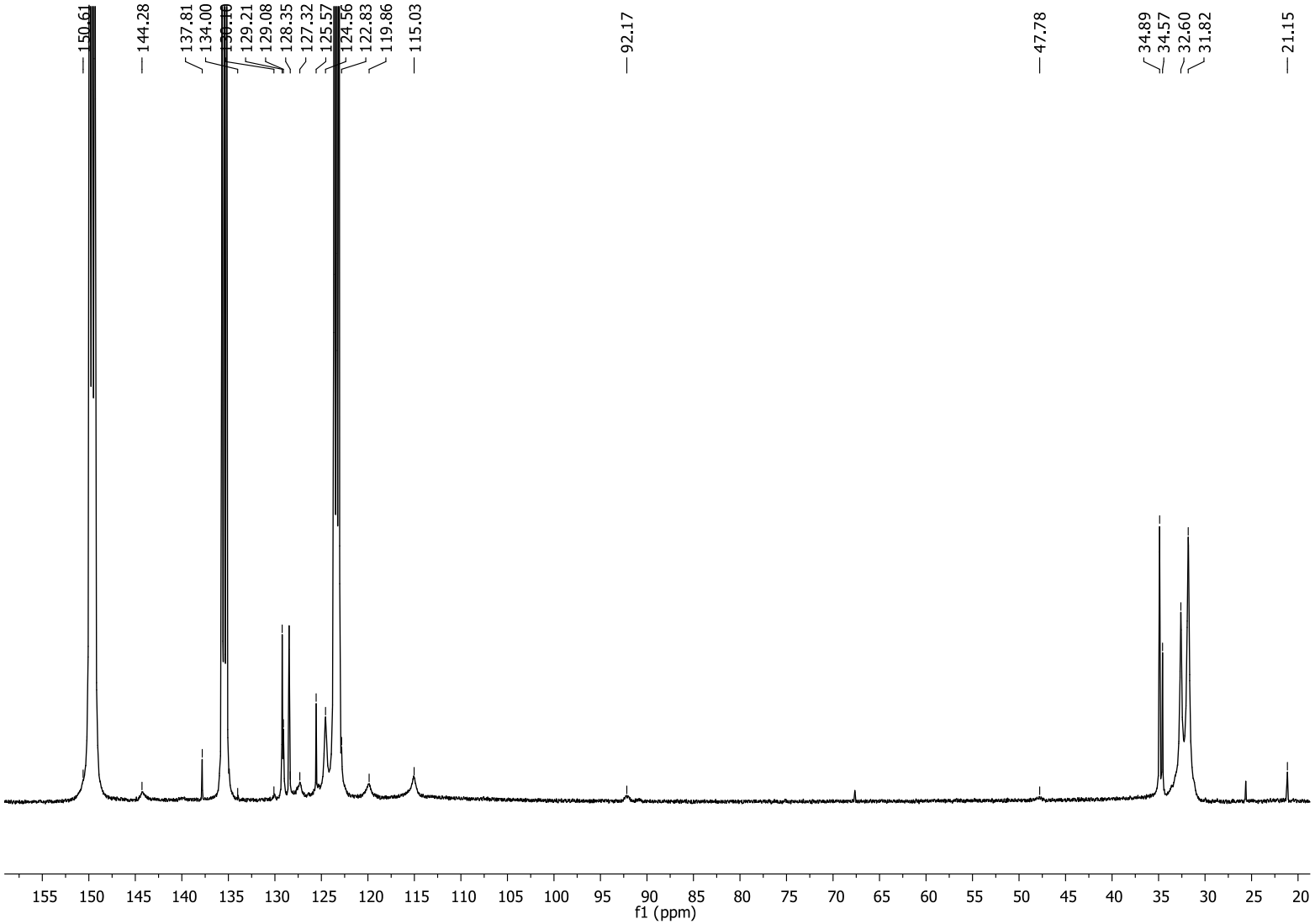

Figure S24. ^{13}C {^{1}H} NMR spectrum of **12** (100 MHz, C_5D_5N, 293 K).

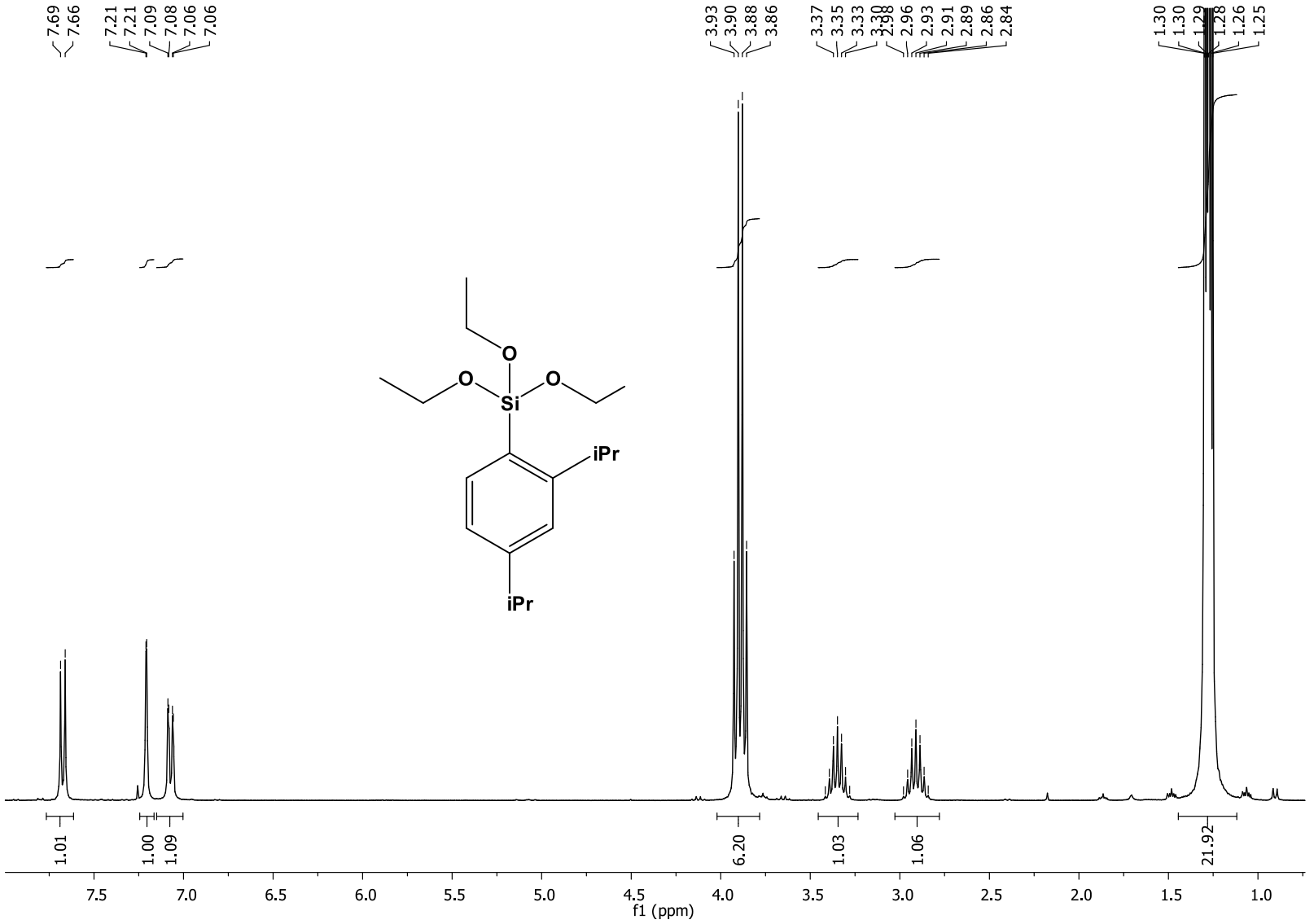

Figure S25. ^{1}H NMR spectrum of 2,4-diisopropylphenyl-triethoxysilane (300 MHz, $CDCl_3$, 293 K).

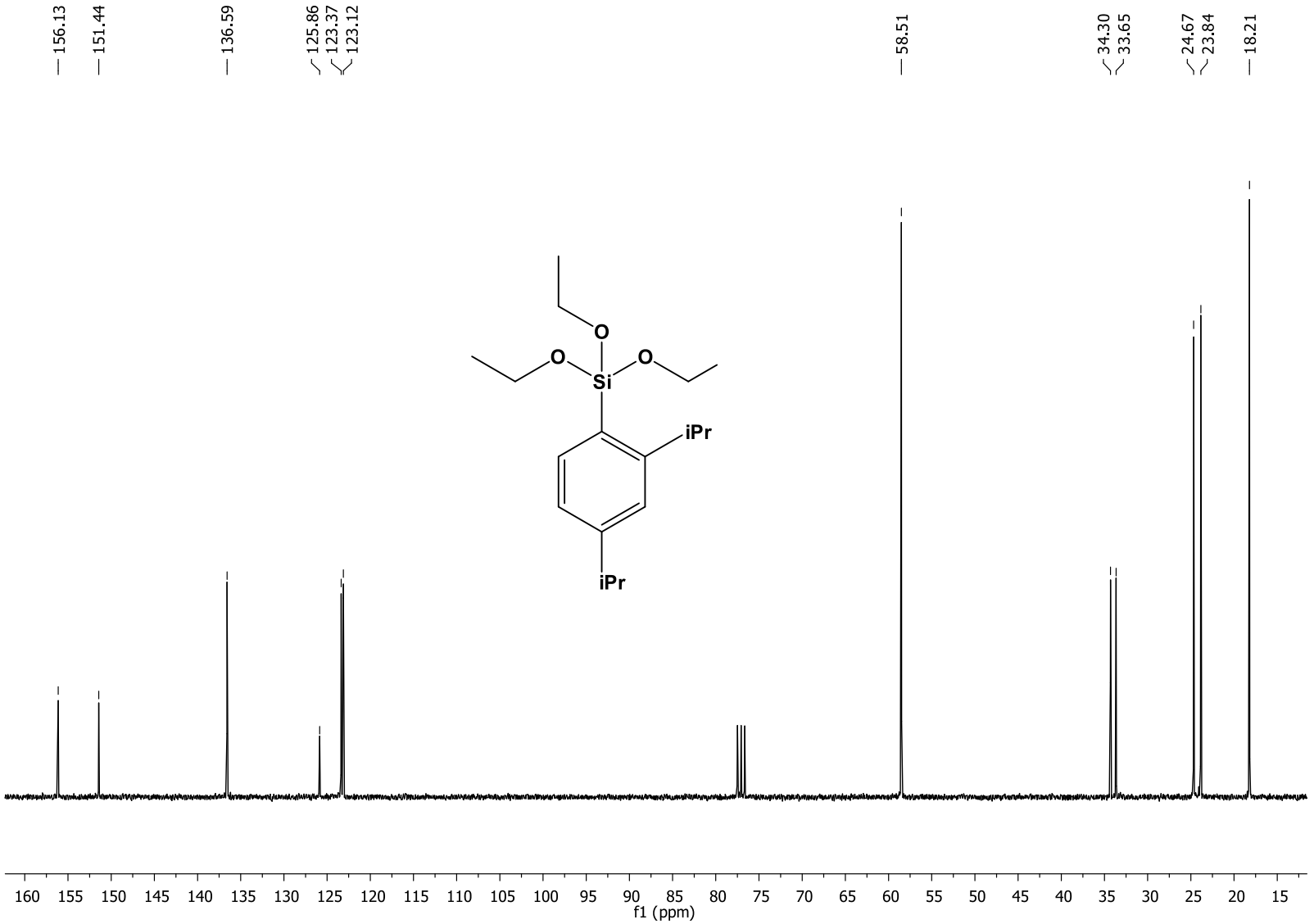

Figure S26. ^{13}C {^{1}H} NMR spectrum of 2,4-diisopropylphenyl-triethoxysilane (75 MHz, $CDCl_3$, 293 K).

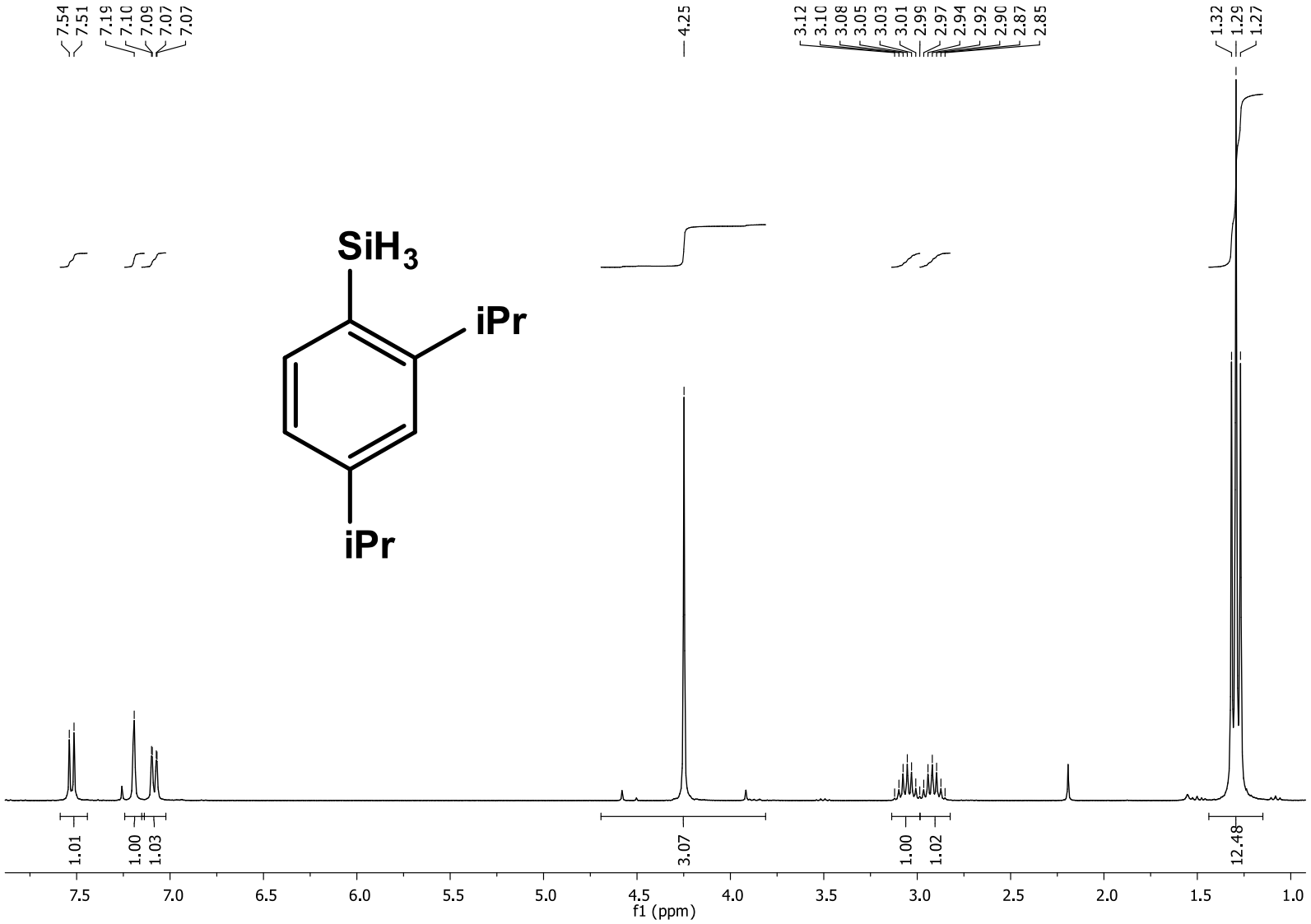

Figure S27. ^{1}H NMR spectrum of 2,4-diisopropylphenylsilane (300 MHz, $CDCl_3$, 293 K).

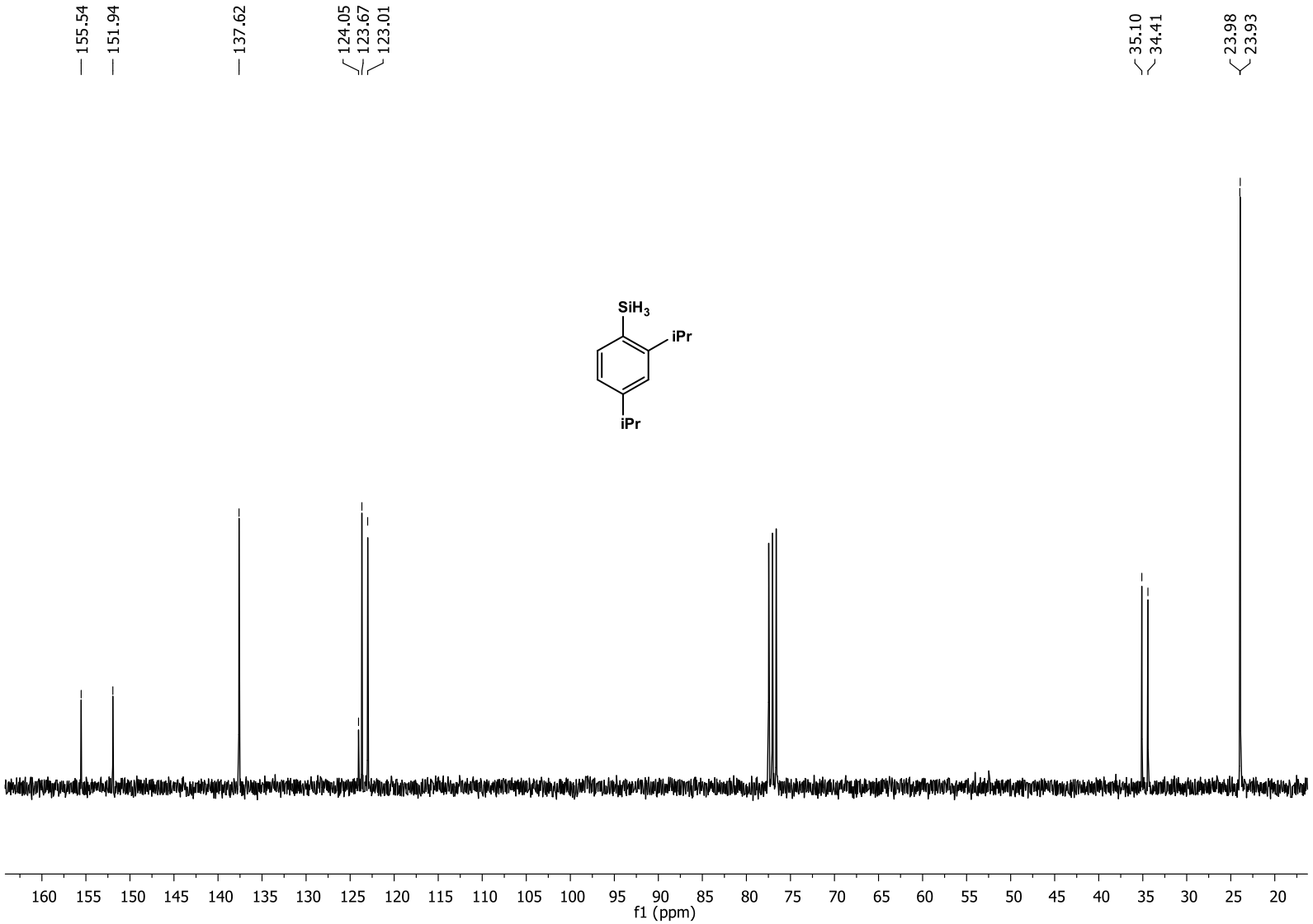

Figure S28. ^{13}C {^{1}H} NMR spectrum of 2,4-diisopropylphenylsilane (75 MHz, $CDCl_3$, 293 K).

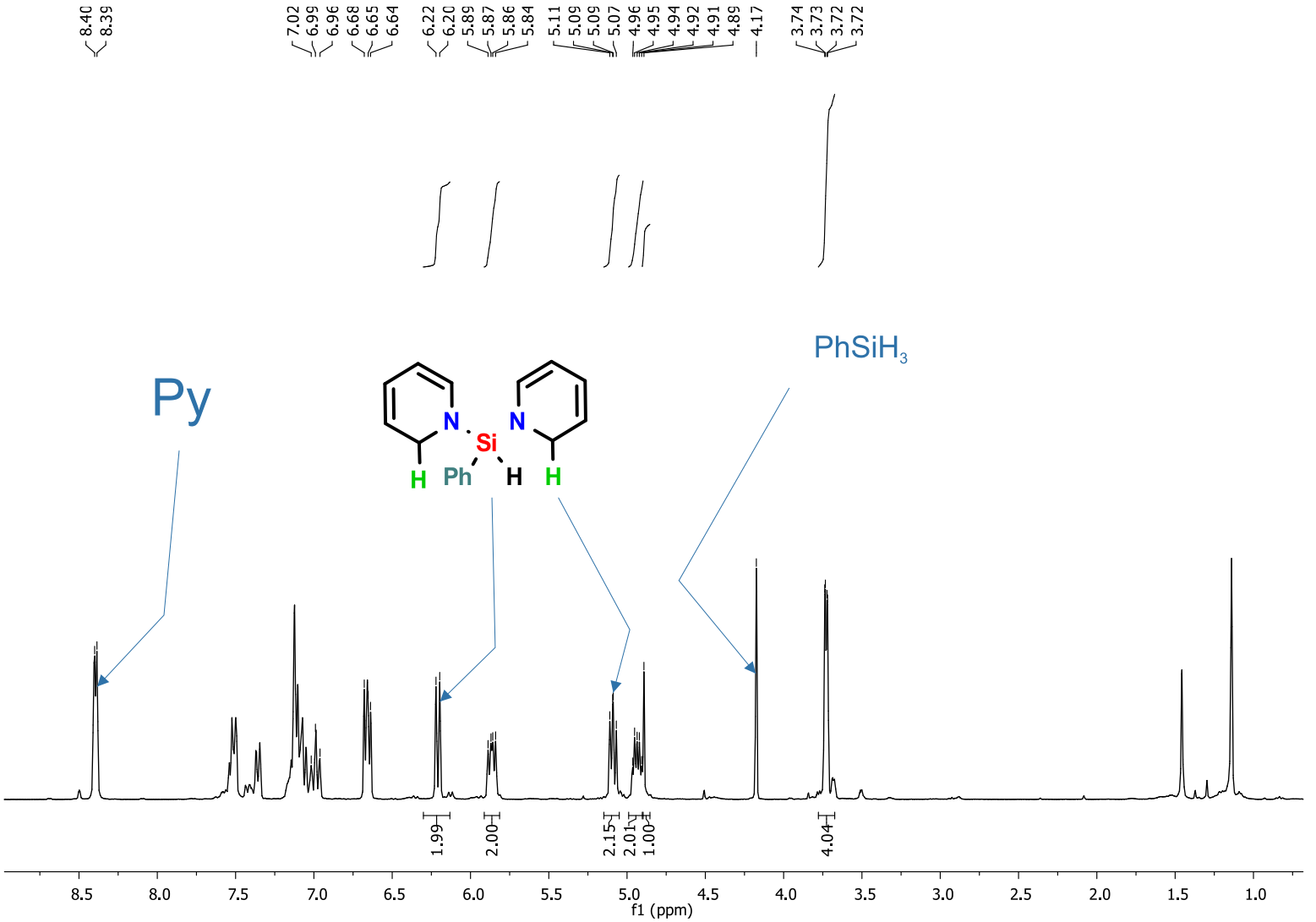

Figure S29. ^{1}H NMR spectrum of the pyridine dearomatization reaction mixture (complex **11** 2 mol %, 78h, 300 MHz, C_6D_6, 293 K).

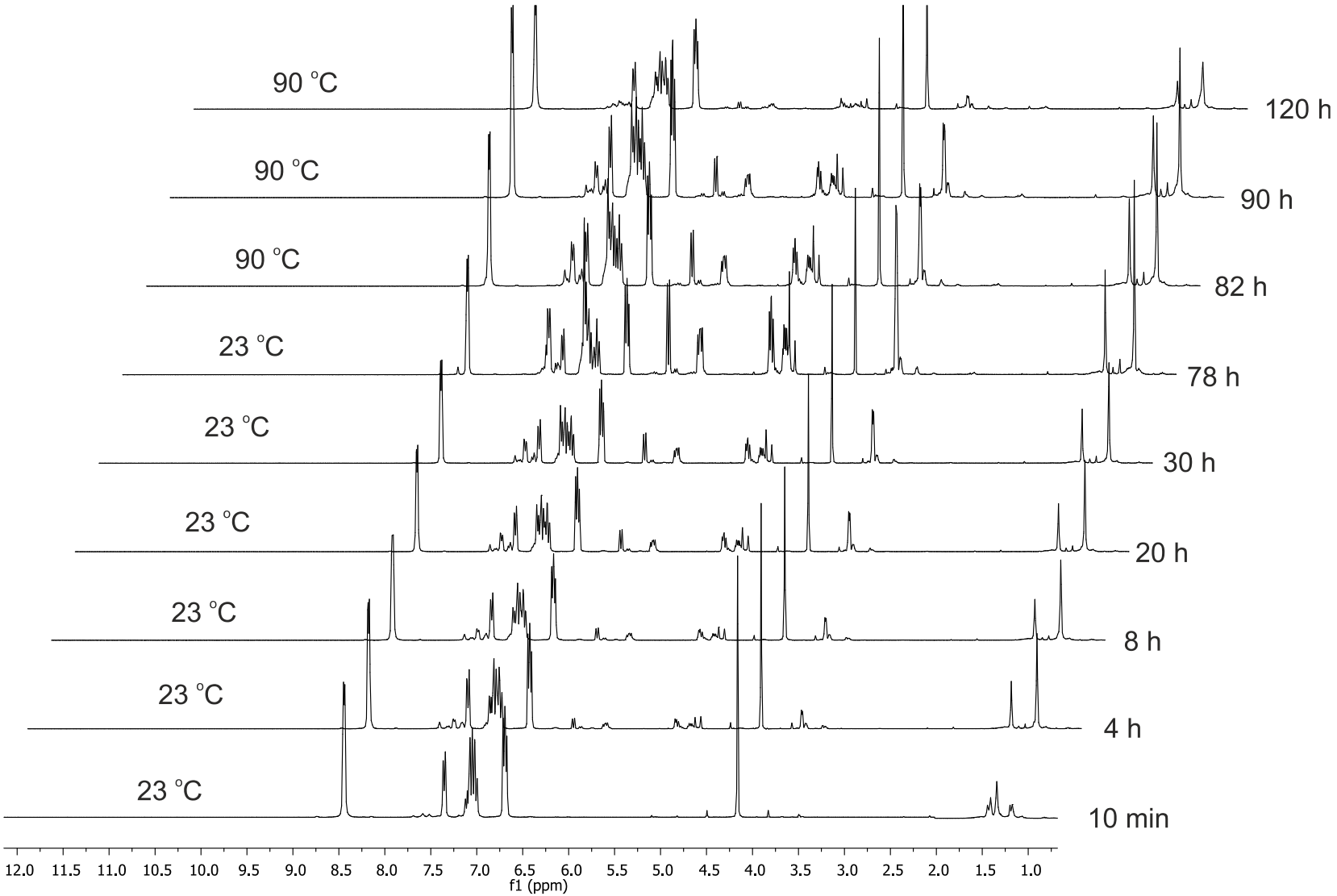

Figure S30. ^{1}H NMR monitoring of the pyridine dearomatization reaction at 23 and 90°C (complex **11** 2 mol %, 300 MHz, C_6D_6, 293 K).

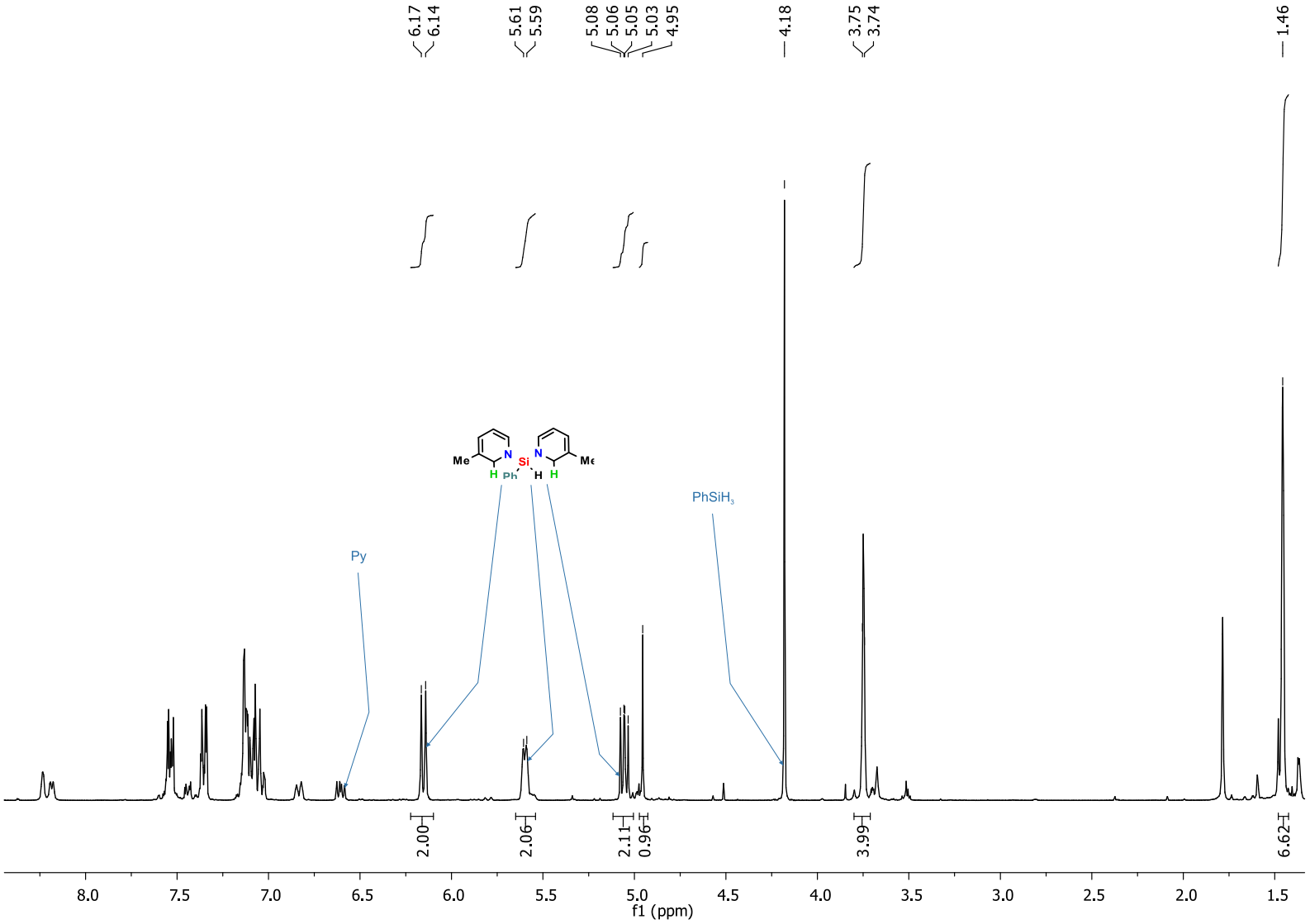

Figure S31. ^{1}H NMR spectrum of the 3-methylpyridine dearomatization reaction mixture (complex **11** 2 mol %, 78h, 300 MHz, C_6D_6, 293 K).

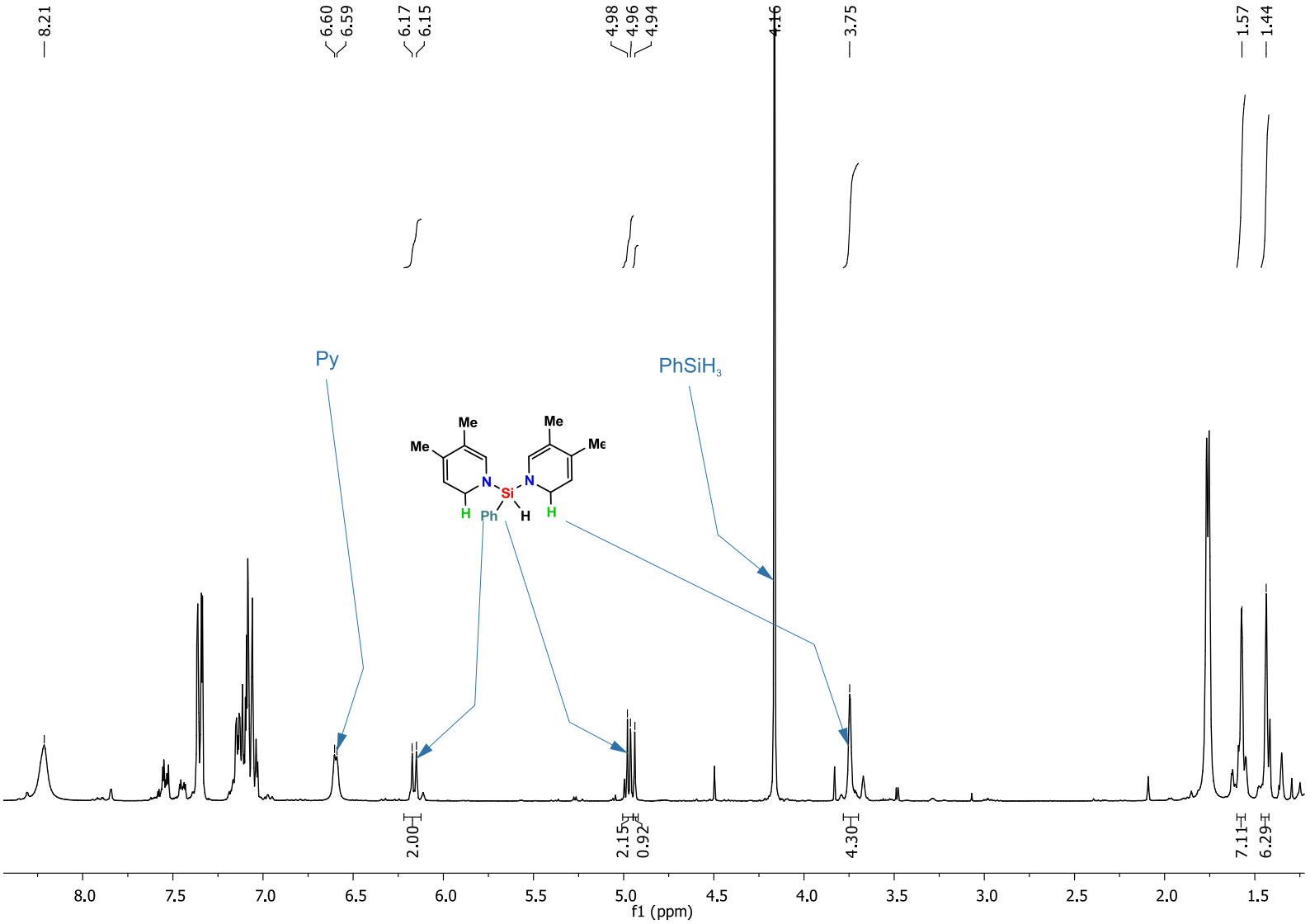

Figure S32. ^{1}H NMR spectrum of the 3,4-dimethylpyridine dearomatization reaction mixture (complex **11** 2 mol %, 78h, 300 MHz, C_6D_6, 293 K).

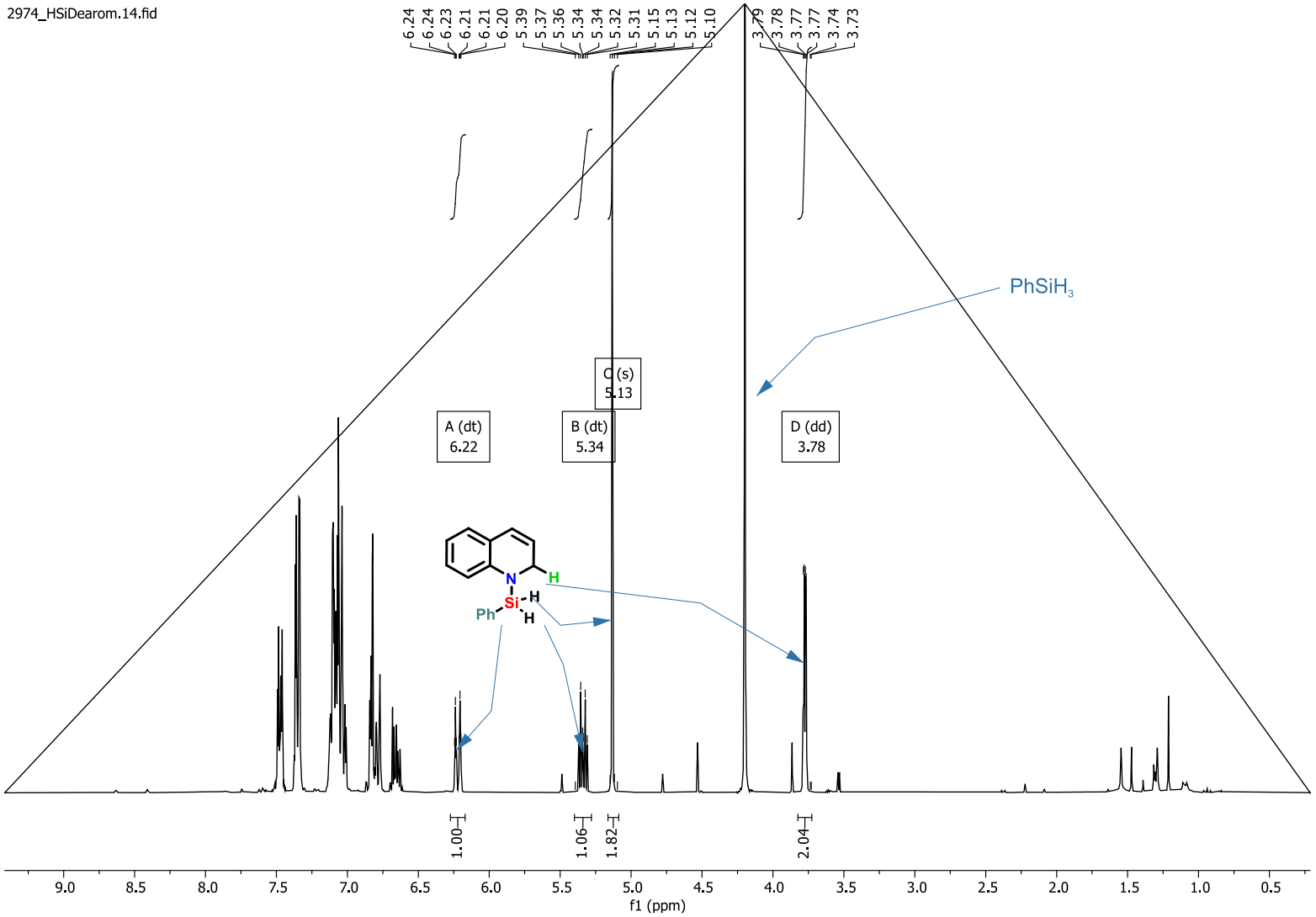

Figure S33. ^{1}H NMR spectrum of the quinoline dearomatization reaction mixture (complex **11** 2 mol %, 48h, 300 MHz, C_6D_6, 293 K).

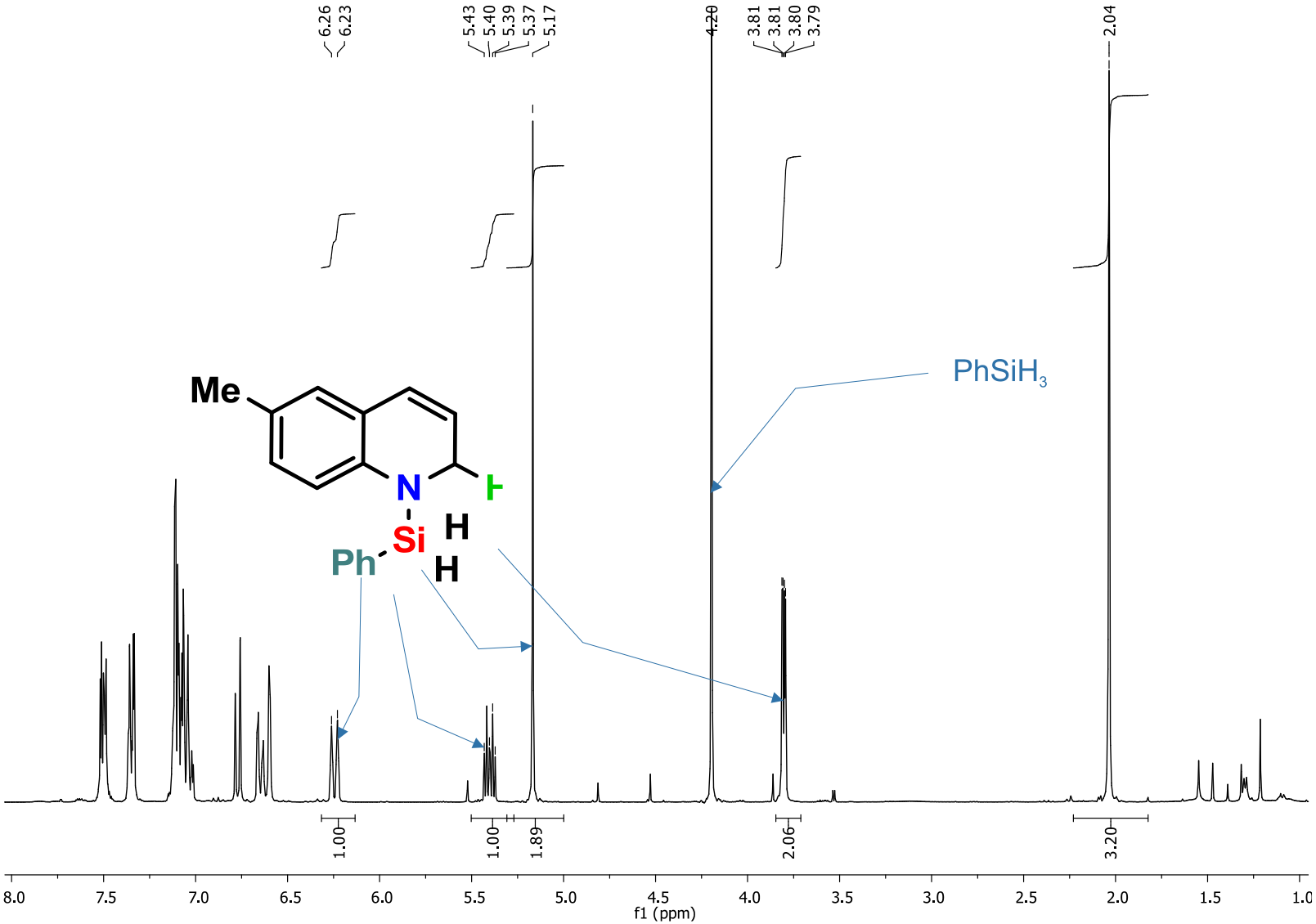

Figure S34. ^{1}H NMR spectrum of the 6-Methylquinoline dearomatization reaction mixture (complex **11** 2 mol %, 80h, 300 MHz, C_6D_6, 293 K).

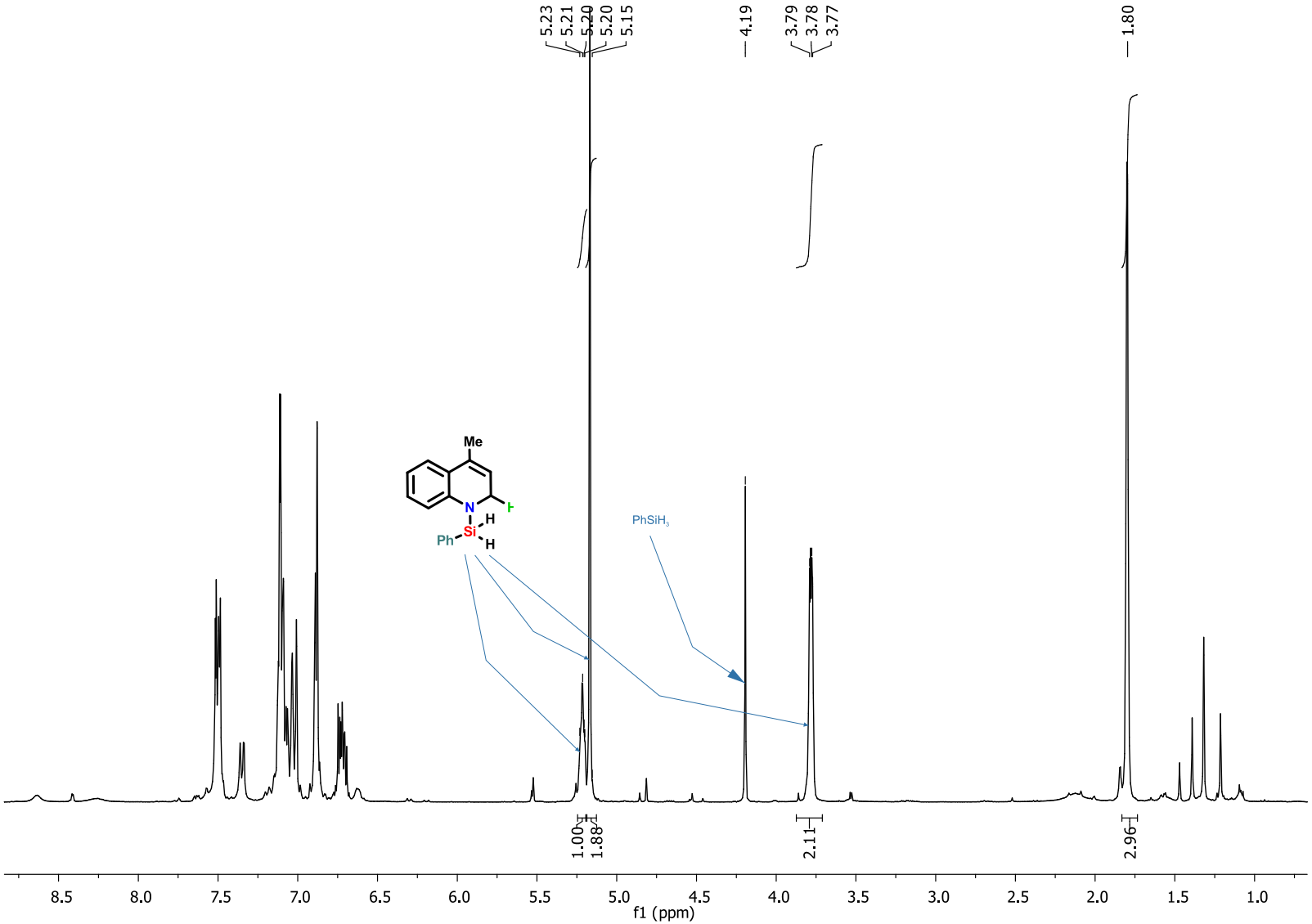

Figure S35. ^{1}H NMR spectrum of the 4-Methylquinoline dearomatization reaction mixture (complex **11** 2 mol %, 80h, 300 MHz, C_6D_6, 293 K).

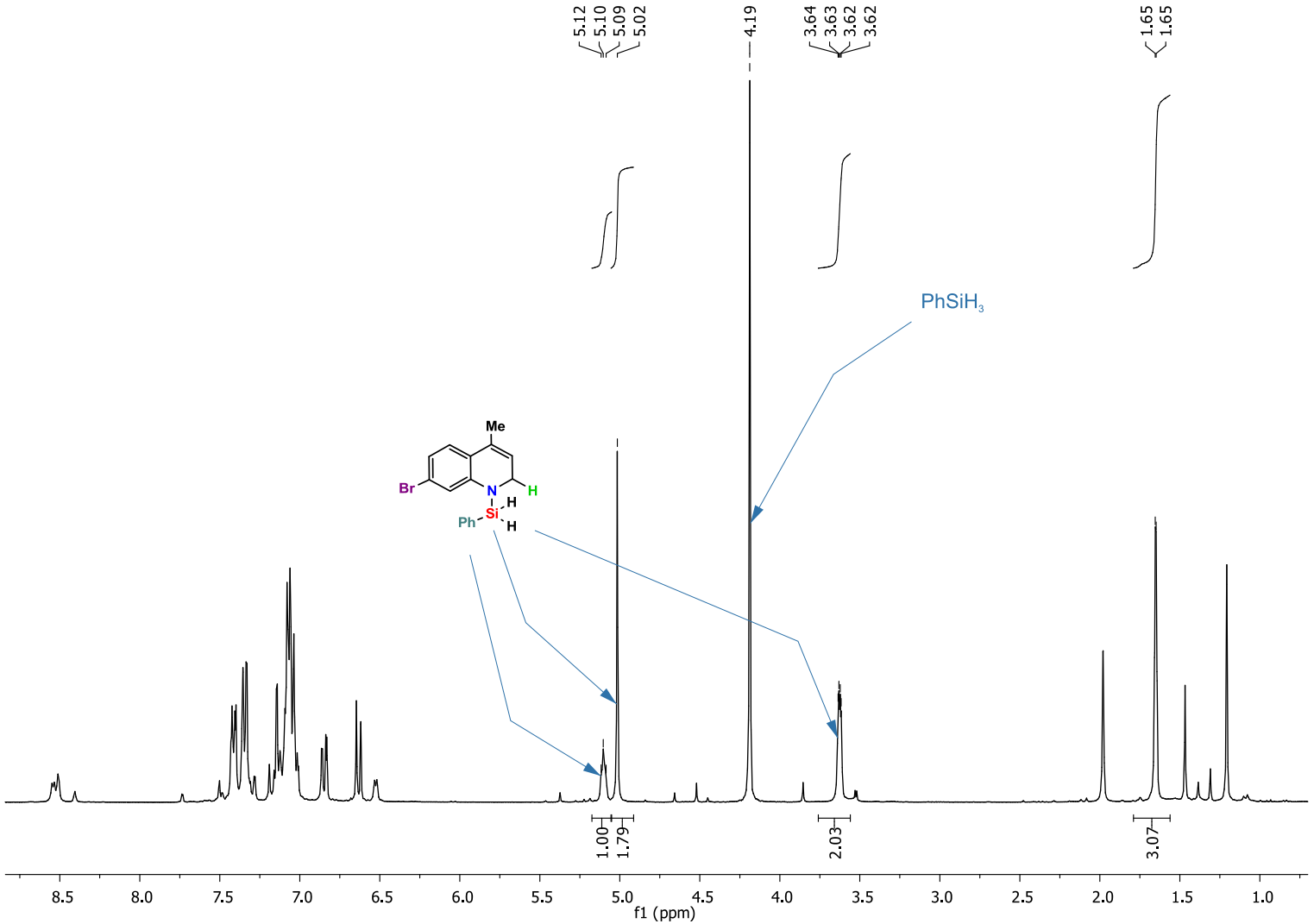

Figure S36. ^{1}H NMR spectrum of the 4-Methyl-7-bromoquinoline dearomatization reaction mixture (complex **11** 2 mol %, 80h, 300 MHz, C_6D_6, 293 K).

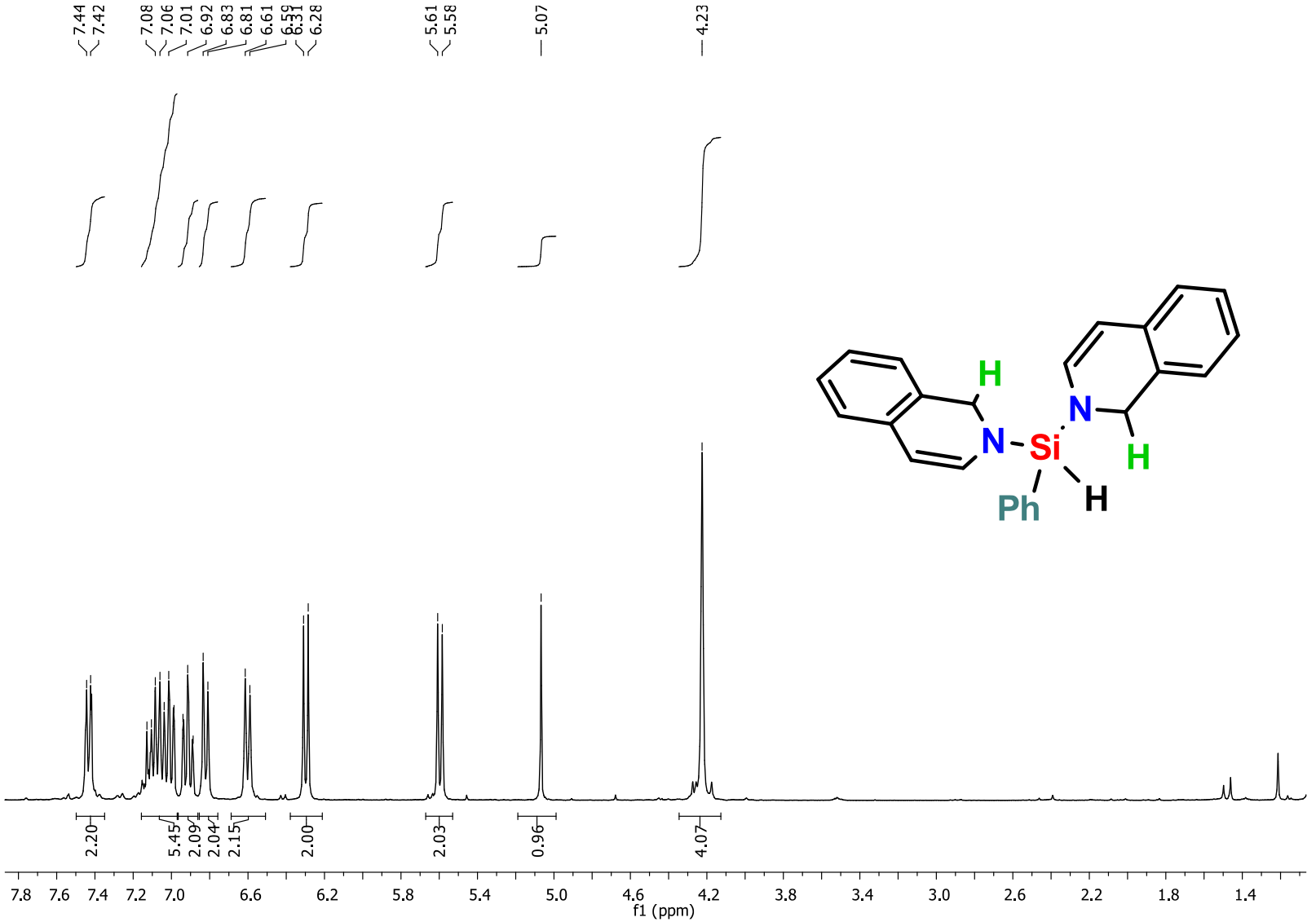

Figure S37. ^{1}H NMR spectrum of the isoquinoline dearomatization reaction mixture (complex **11** 2 mol %, 80h, 300 MHz, C_6D_6, 293 K).

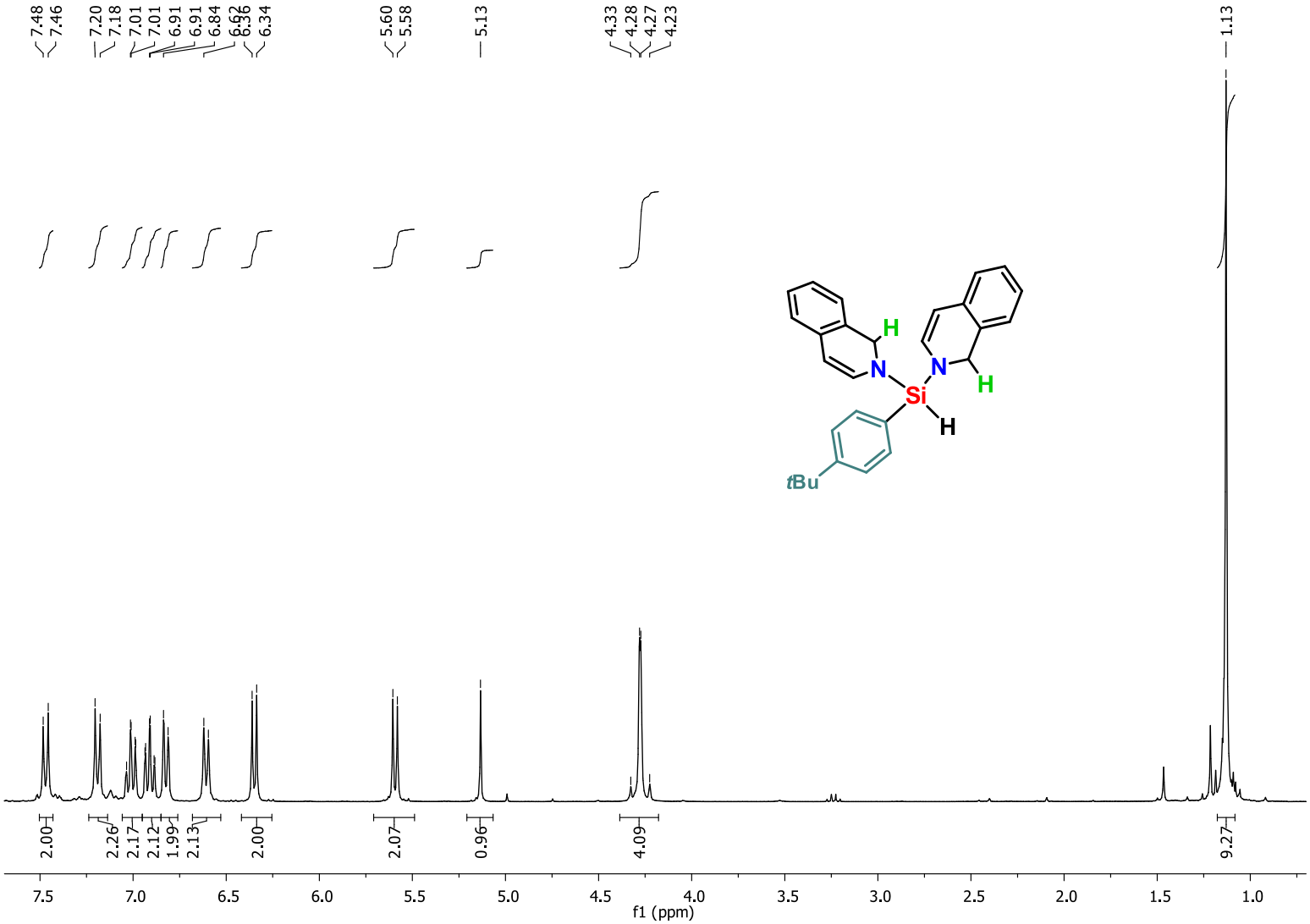

Figure S38. ^{1}H NMR spectrum of compound **15j** (300 MHz, C_6D_6, 293 K).

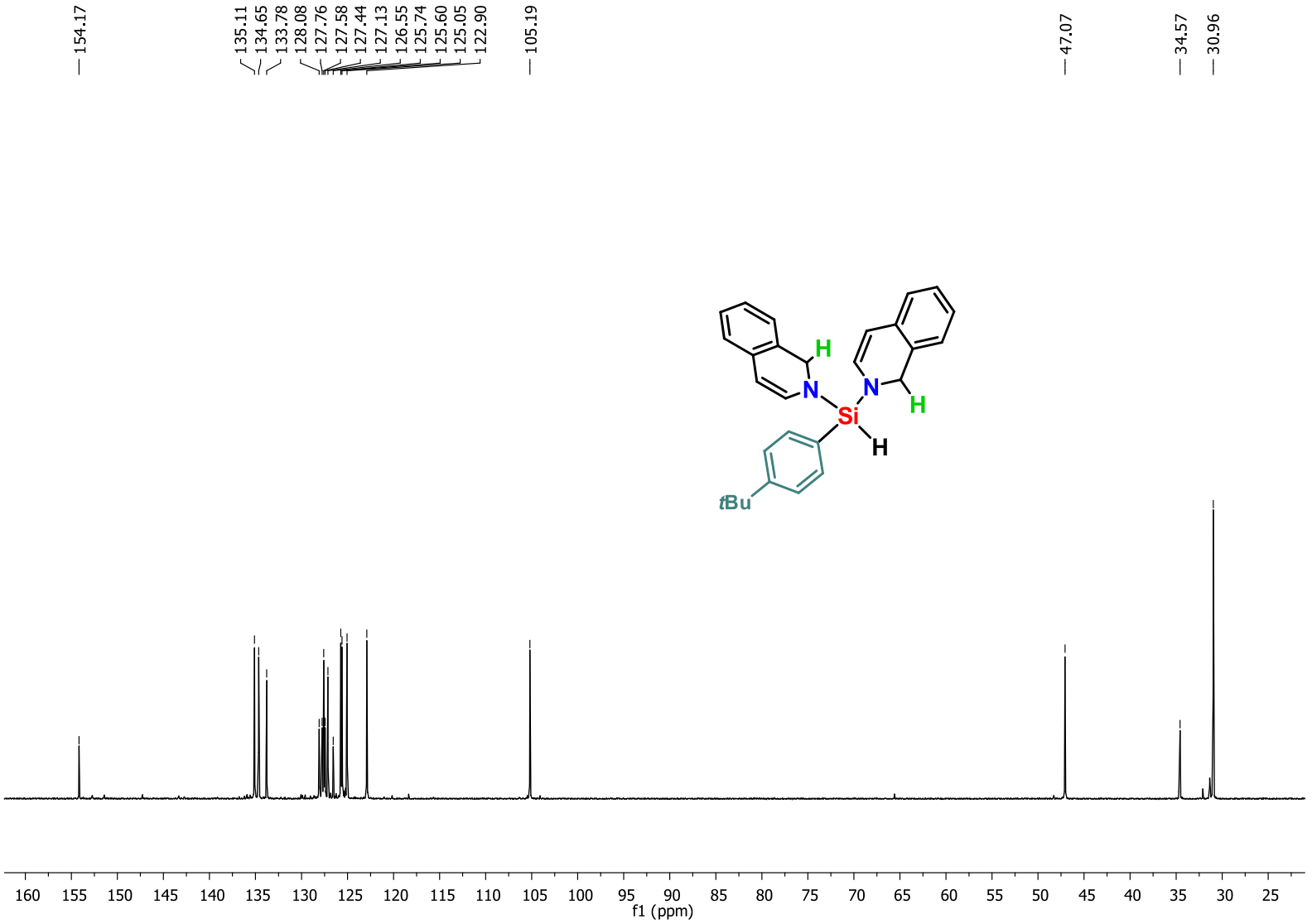

Figure S39. $^{13}C\{^{1}H\}$ NMR spectrum of compound **15j** (300 MHz, C_6D_6, 293 K).

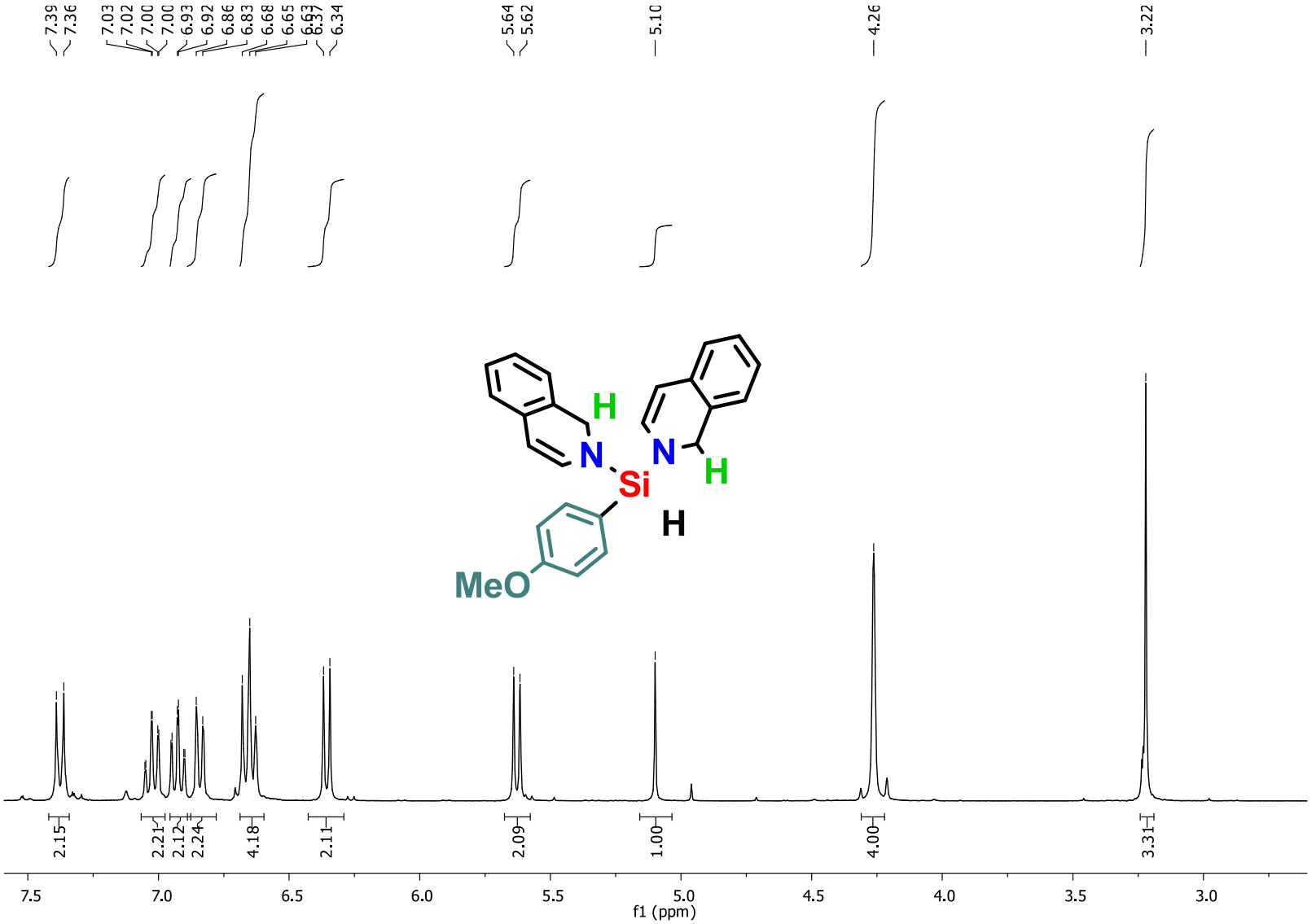

Figure S40. ^{1}H NMR spectrum of compound **15k** (300 MHz, C_6D_6, 293 K).

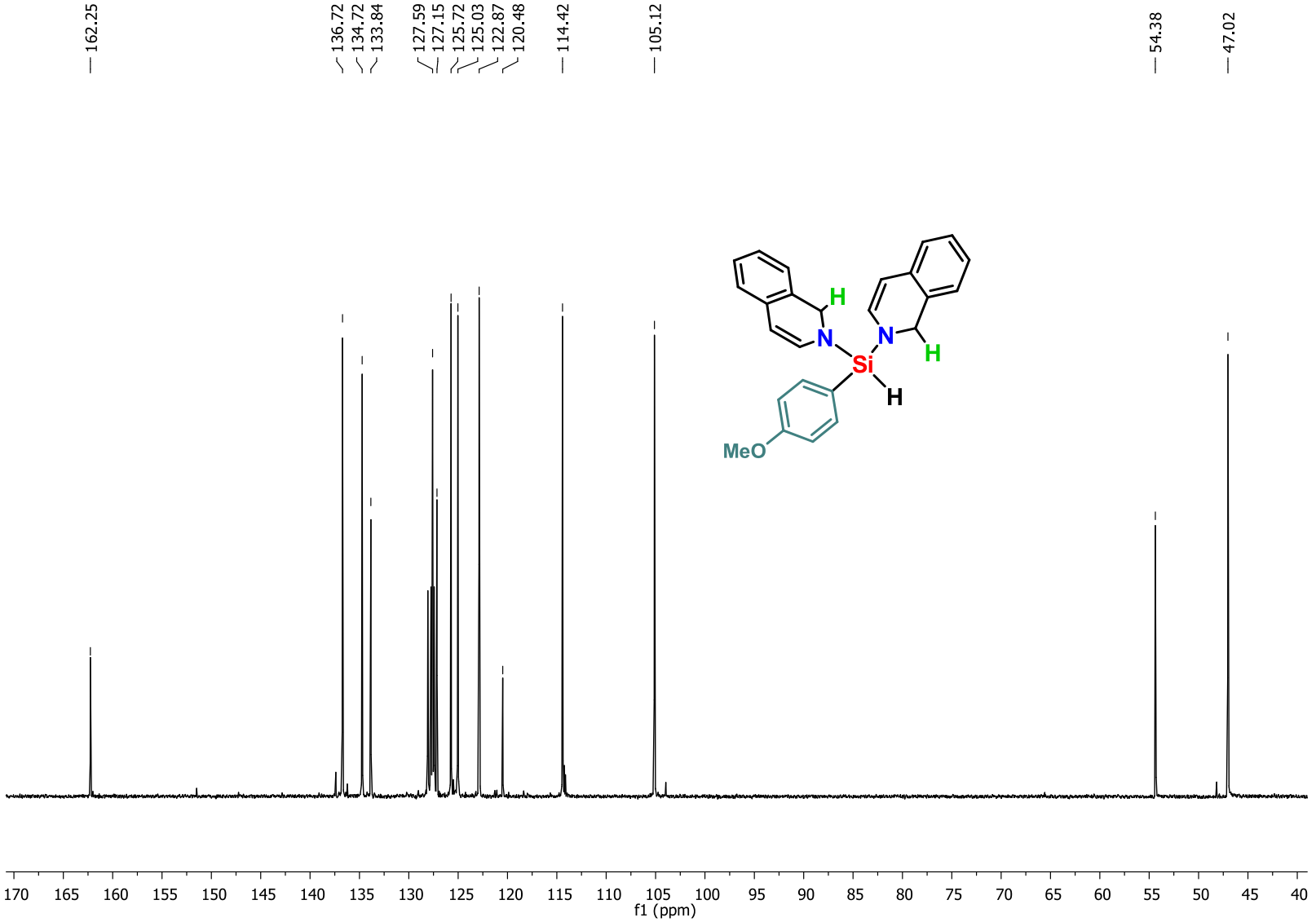

Figure S41. $^{13}C\{^{1}H\}$ NMR spectrum of compound **15j** (300 MHz, C_6D_6, 293 K).

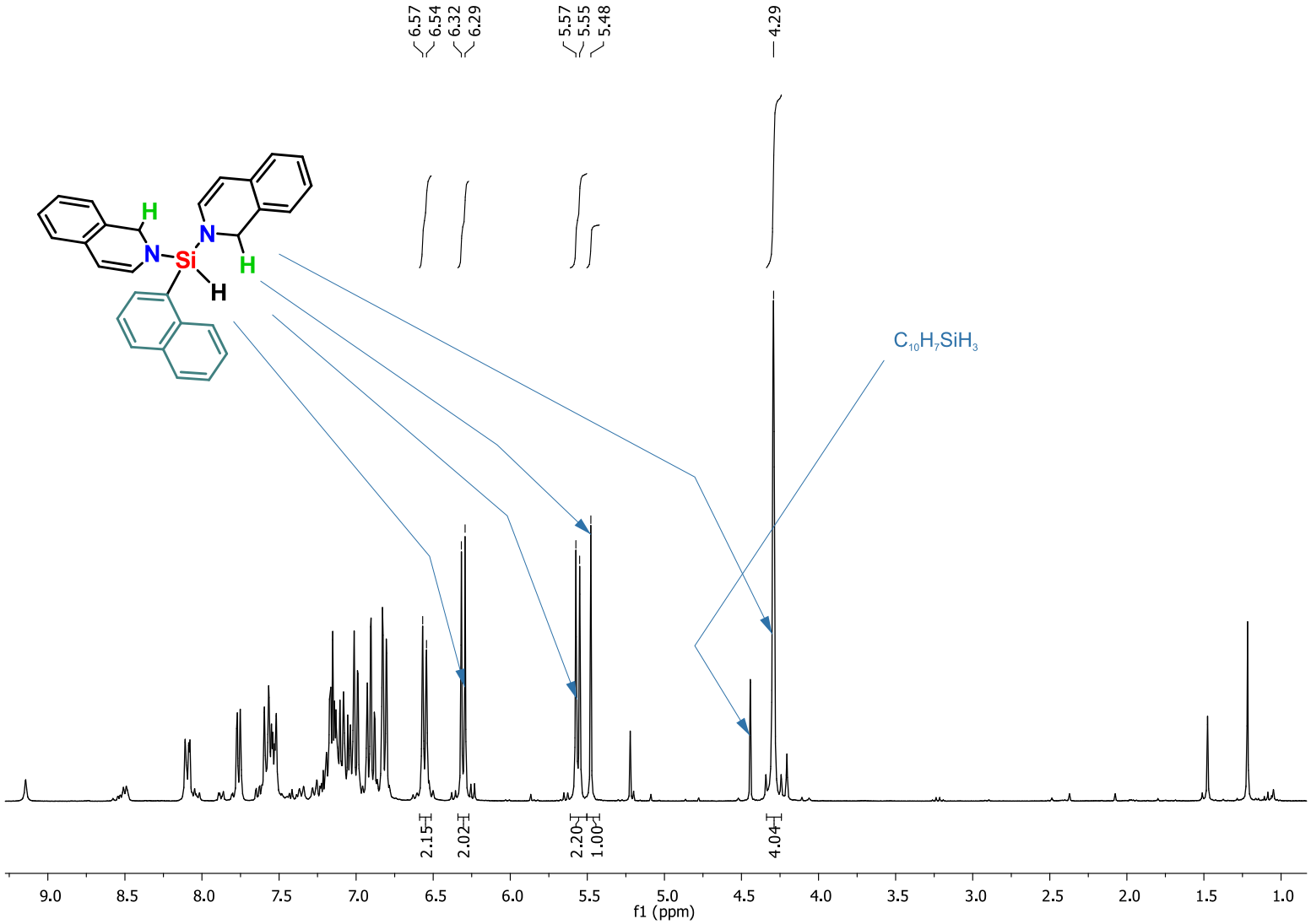

Figure S42. ^{1}H NMR spectrum of the dearomatization reaction mixture (isoquinoline + $C_{10}H_7SiH_3$) (complex **11** 2 mol %, 100h, 300 MHz, C_6D_6, 293 K).

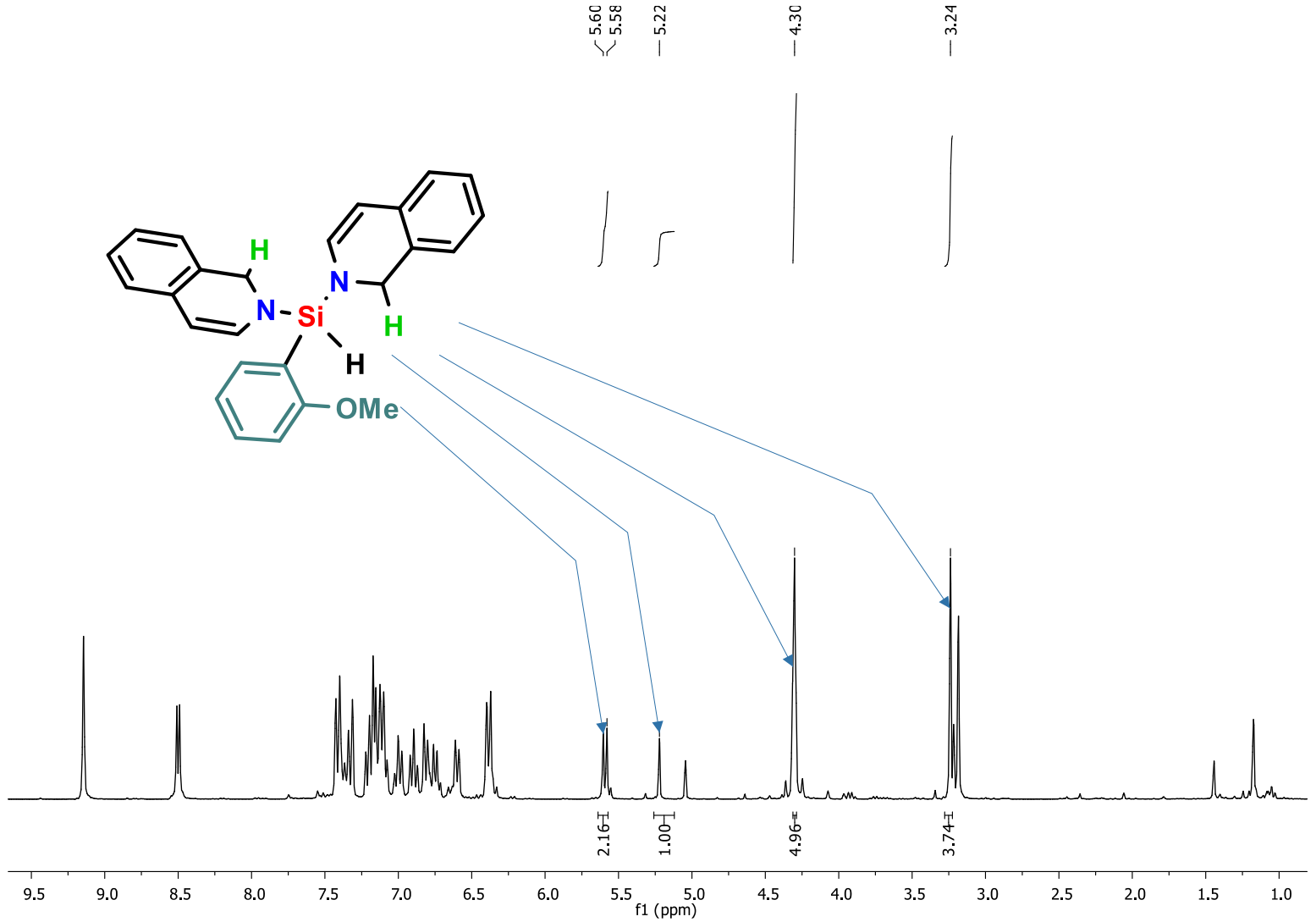

Figure S43. ^{1}H NMR spectrum of the dearomatization reaction mixture (isoquinoline + *o*-$MeOC_6H_4SiH_3$) (complex **11** 2 mol %, 100h, 300 MHz, C_6D_6, 293 K).

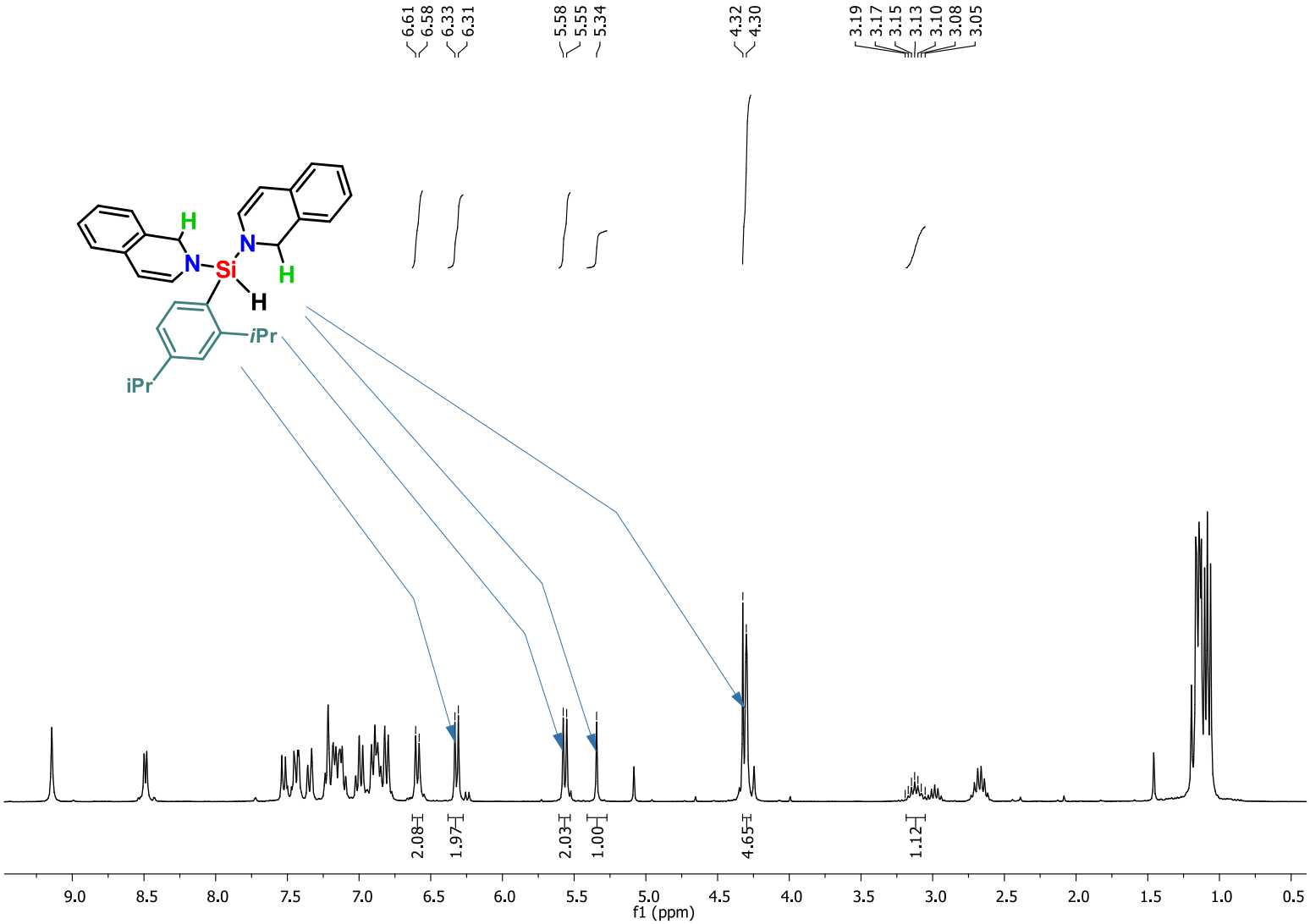

Figure S44. ^{1}H NMR spectrum of the dearomatization reaction mixture (isoquinoline + *o,p*-(*i*Pr$_2$)C$_6$H$_4$SiH$_3$) (complex **11** 2 mol %, 120h, 300 MHz, C$_6$D$_6$, 293 K).

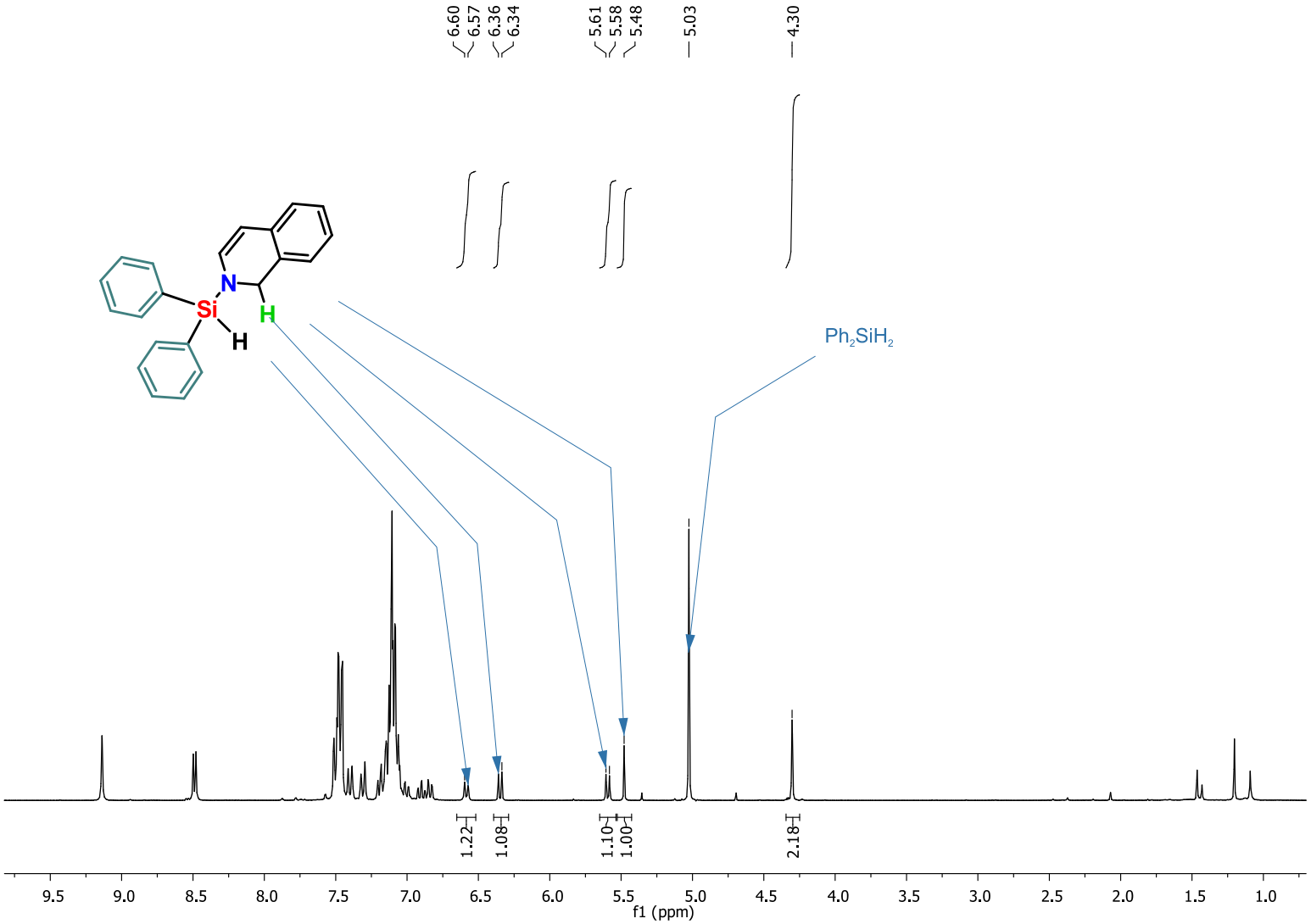

Figure S45. ^{1}H NMR spectrum of the dearomatization reaction mixture (isoquinoline + Ph_2SiH_2) (complex **11** 2 mol %, 120h, 300 MHz, C_6D_6, 293 K).

DFT-based description of the catalytic cycle

The reversible double hydrosilylation of pyridine catalyzed by **11** was investigated at the M062X/DGDZVP level of DFT taking into account the toluene medium by PCM. Preliminary, we studied bonding situation in the remarkable Ca_2H_2 cycle of the dimeric complex **11**, and then, to find out possible route of catalytic species formation, various modes of the dimeric hydride dissociation were considered (*vide infra*). DFT calculations suggest a catalytic model derived from the four-coordinated monohydride complex $CaH(L)(Py)_2$ (**A**, Figures S46, S47), where L = tBu$_2$CarbAr$_2$. At the initial stage of the catalytic cycle one of the pyridine rings in **A** undergoes dearomatization due to hydride transfer toward the α-carbon atom. As a result, a distorted 1,2-dihydropyridine anion $(HPy)^-$ is formed. In terms of thermodynamics, the conversion of **A** into **B** is an exergonic process ($\Delta G°_{sol}$ = –4.8 kcal mol^{-1}). A QST3 search procedure resulted in a four-membered transition state structure (**TS1**, Figure S48) with an activation barrier of $\Delta G^{\neq}_{sol}$ = 12.0 kcal mol^{-1}.

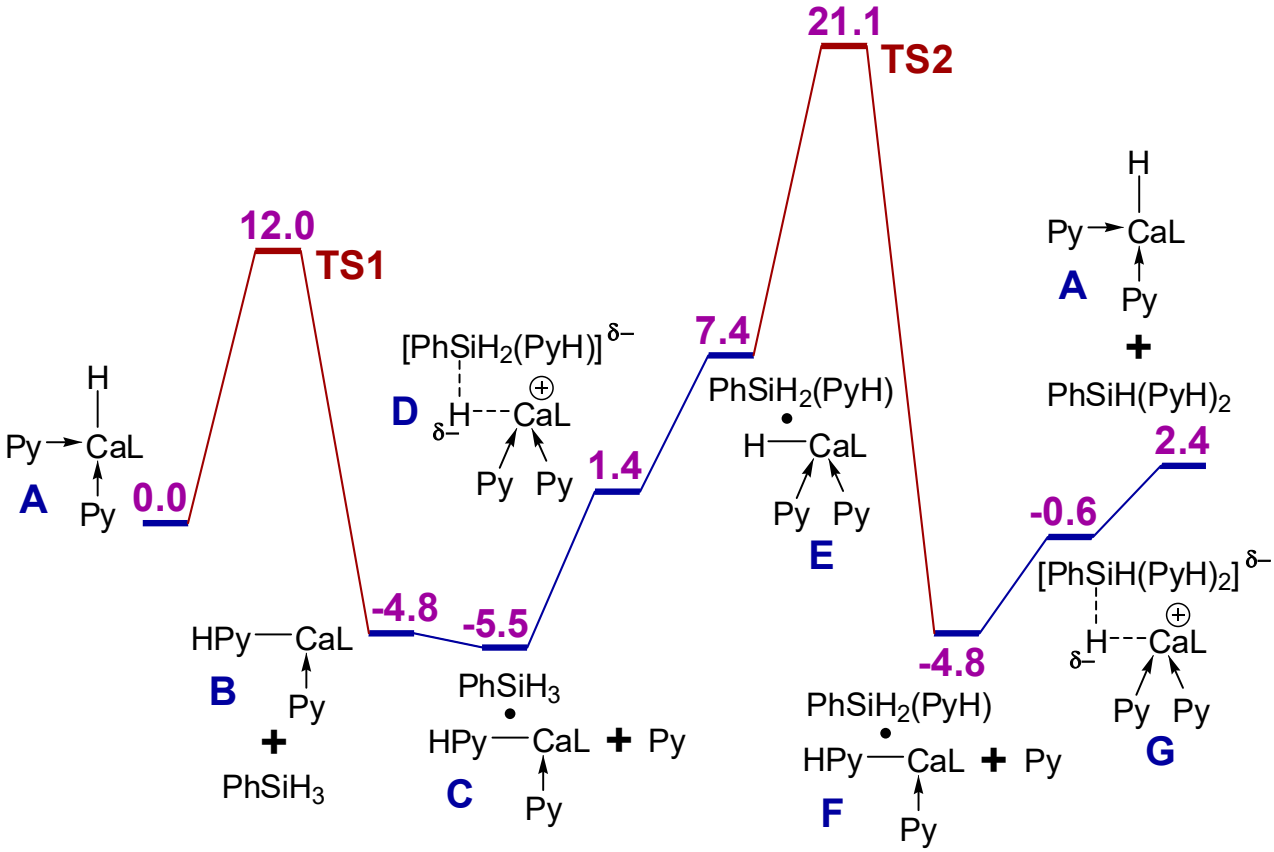

Figure S46. Profile of the Gibbs free energy ($G°_{sol}$) change at 25 °C for the double hydrosilylation of pyridine catalyzed by the complex **A**. The level of DFT calculations is PCM(PhMe)-M062X/DGDZVP.

Further binding between the intermediate **B** and phenylsilane is due to intermolecular interactions. This reaction forms complex **C** where the shortest distance Ca···H(Si) is 2.783 Å. A direct Si–H/Ca–N σ-bond metathesis leading to the *N*-silylated 1,2-dihydropyridine and calcium-hydride bond restoration in complex **E'** (Figure S48) occurred to be highly endergonic ($\Delta G°_{sol}$ = 19.4 kcal mol^{-1}, Scheme S1). Therefore, we assumed that additional coordination of Py molecule the Ca^{2+} ion could reduce the energy change accompanying the metathesis. The corresponding intermediate **E** was successfully optimized (Figure S47) which demonstrates remarkable flexibility

of the ligand environment. Moreover, for the reaction **C** + Py → **E** the change in the Gibbs free energy decreases to 12.9 kcal mol^{-1}.

Thus, coordination of additional pyridine molecule promotes the Si–H/Ca–N σ-bond metathesis. Our efforts to localize transition state for this reaction by QST3 led to a structure with bridging hydride anion located between Si and Ca. Further standard optimization converged the Si···(μ-H) and Ca···(μ-H) distances to 1.729 and 2.189 Å, respectively, and frequency analysis revealed a local minimum on the potential energy surface (PES). Corresponding intermediate **D** (Figure S47) lies (by the Gibbs free energy) 6.0 kcal mol^{-1} lower than **E**. Coordination environment of silicon in **D** represents a trigonal bipyramid, the atoms of C, N, and terminal H being located at the equatorial positions. It should be noted that an intermediate resembling complex **D** with activated Si–H bond elongated over 1.7 Å was confirmed to be a local minimum on PES for the Ni-catalyzed hydrosilylation reaction of quinoline with $PhSiH_3$. Search for a transition state of the reaction **C** + Py → **D** by QST3 resulted in a structure of unfavorable $[Ca(L)(Py)_2]^+[PhSiH_3(PyH)]^-$ ion pair which further was optimized by the standard procedure (intermediate **D'**, Scheme S1, Fugure S49).

The additional local minima found for the reaction **C** + Py → **E** instead of desired single transition state indicate complexity of PES. In our case, the situation is additionally complicated by high conformation flexibility of the carbazolyl ligand. The next stage of the catalytic cycle is another exergonic dearomatization leading to formation of **F** from **E**. In principle, the bridging hydride in the intermediate **D** can directly be added to pyridine (**D** → **F**). However, the QST3 procedure is not able to localize corresponding transition state at the complex PES suggesting the **D** → **E** → **F** route. Additional energy release on going from **E** to **F** (as compared with **A** → **B**) arises from spatial reorientation of the $PhSiH_2(PyH)$ fragment accompanying the hydride transfer. The $PhSiH_2(PyH)$ reorientation not only decreases energy of complex **F** but also promotes further formation of the final $PhSiH(PyH)_2$ molecule in the coordination sphere of the sterically hindered catalyst (Figures S47, S48). The corresponding intermediate **G** is another complex where the H^- anion is bridging. Notably, formation of **G** by addition of Py to **F** is less endergonic process (ΔG_{sol} = 4.2 kcal/mol) than the formation of **D** ($\Delta G°_{sol}$ = 6.9 kcal/mol). The release of the $PhSiH(PyH)_2$ molecule at the final stage of the catalytic cycle appears to be driven by the entropic effect ($T\Delta S°_{sol}$ = 18.0 kcal mol^{-1} at 298 K). The selected structural parameters of the **11, TS1, TS2, A - G** and **E', D'** optimized geometries are given in Table S2.

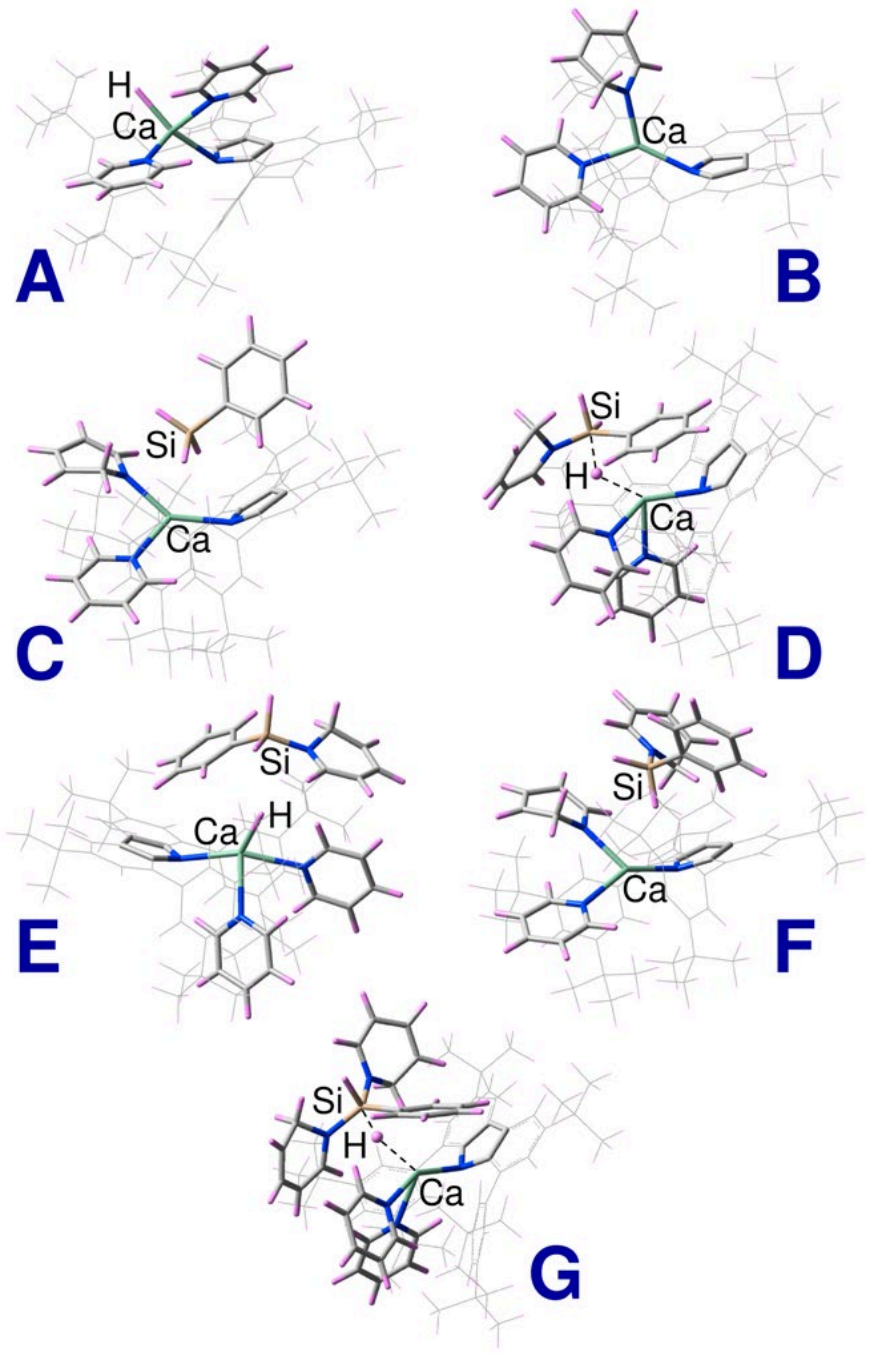

Figure S47. Structures of the catalytic intermediates **A**–**G** optimized at the PCM(PhMe)-M062X/DGDZVP level of DFT.

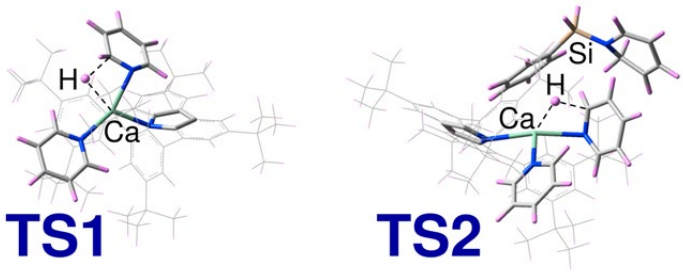

Figure S48. Structures of the transition states **TS1** and **TS2** optimized at the PCM(PhMe)-M062X/DGDZVP level of DFT.

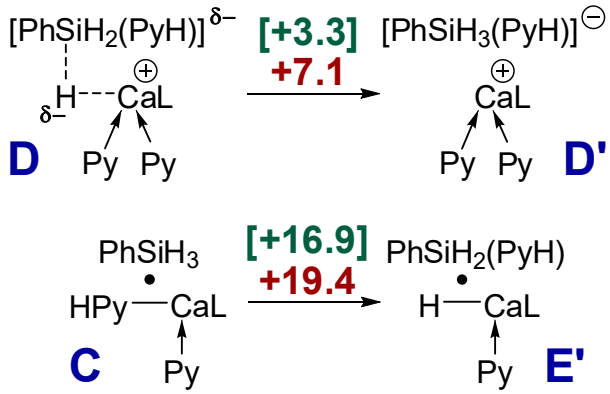

Scheme S1. Computed at 25 °C values (kcal mol^{-1}) of $\Delta H°_{sol}$ (in brackets) and $\Delta G°_{sol}$ for the conversions of **D** into **D'** and **C** into **E'**. The level of DFT calculations is PCM(PhMe)-M062X/DGDZVP.

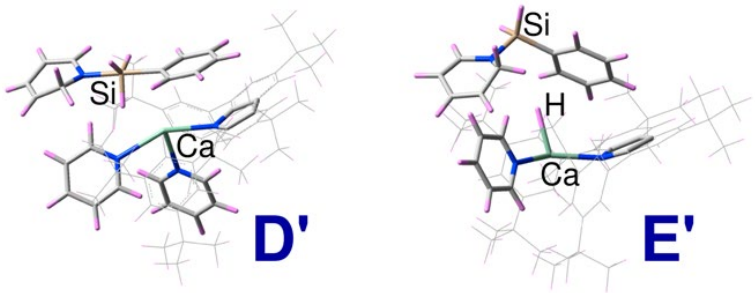

Figure S49. Structures of the possible intermediates **D'** and **E'** optimized at the PCM(PhMe)-M062X/DGDZVP level of DFT.

Table S2. Interatomic distances (Å) in the catalytic intermediates and transition states optimized at the PCM(PhMe)-M062X/DGDZVP level of DFT.

11	**A**	**TS1**
Ca–N(L) 2.392, 2.396 **Ca–H** 2.173, 2.176, 2.217, 2.224 **Ca–(π-C) (toluene)** 2.857–2.987 **Ca···Ca** 3.490 **H···H (hydrides)** 2.668	**Ca–N(L)** 2.413 **Ca–N(Py)** 2.465, 2.500 **Ca–H** 2.132	**Ca–N(L)** 2.368 **Ca–N(Py)** 2.481 **Ca–N(Py···H)** 2.430 **Ca···H** 2.178 **H···(α-C)** 1.756
B	**C**	**D**
Ca–N(L) 2.368 **Ca–N(Py)** 2.455 **Ca–N(PyH)** 2.301 **H–(α-C) (formed)** 1.095	**Ca–N(L)** 2.362 **Ca–N(Py)** 2.440 **Ca–N(PyH)** 2.319 **Ca···H(Si)** 2.783, 2.801 **Si–H** 1.474, 1.492, 1.497	**Ca–N(L)** 2.378 **Ca–N(Py)** 2.497, 2.512 **Ca···(μ-H)** 2.189 **Si···(μ-H)** 1.729 **Si–H** 1.503, 1.531 **Si–N** 1.807
E	**TS2**	**F**
Ca–N(L) 2.408 **Ca–N(Py)** 2.509, 2.556 **Ca–H** 2.116 **Si–H** 1.475, 1.491 **Si–N** 1.762 **Si···H(Ca)** 3.092	**Ca–N(L)** 2.394 **Ca–N(Py)** 2.455 **Ca–N(Py···H)** 2.455 **Ca···H** 2.132 **H···(α-C)** 1.843 **Si···H** 4.295 **Si–H** 1.477, 1.487 **Si–N** 1.751	**Ca–N(L)** 2.353 **Ca–N(Py)** 2.500 **Ca–N(PyH)** 2.318 **H–(α-C) (formed)** 1.110 **Ca···H(Si)** 2.719 **Si–H** 1.476, 1.490 **Si–N** 1.739
G	**D'**	**E'**
Ca–N(L) 2.394 **Ca–N(Py)** 2.499, 2.537 **Ca···(μ-H)** 2.233 **Si···(μ-H)** 1.636 **Si–H** 1.512 **Si–N** 1.791, 1.831	**Ca–N(L)** 2.358 **Ca–N(Py)** 2.557, 2.598 **Ca···H(Si)** 2.321 **Si–H** 1.501, 1.510, 1.541 **Si–N** 1.896	**Ca–N(L)** 2.376 **Ca–N(Py)** 2.508 **Ca–H** 2.087 **Si–H** 1.477, 1.486 **Si–N** 1.760 **Si···H(Ca)** 5.139

DFT analysis of the dimeric hydride dissociation pathways.

Among the analyzed reactions (1)–(4) (Scheme S2) the simple decomposition into two monomeric hydrides bearing toluene molecule (1) occurred to be less preferable with corresponding $\Delta G°_{sol}$ value of 35.5 kcal mol^{-1}. At the same time, replacement of the toluene molecules with pyridine in the coordination sphere of the dimer (2) is accompanied by the $\Delta G°_{sol}$ value of –16.3 kcal mol^{-1}. Such a negative change of the Gibbs free energy can be explained by a stronger interaction between Ca and Py due to the formation of the donor-acceptor Ca–N bonds (2.463, 2.538 Å) while toluene coordinates toward the metal by the aromatic π-system. However, dissociation of the pyridine-substituted dimer (3) also requires a lot of energy ($\Delta G°_{sol}$ = 33.6 kcal mol^{-1}) similar to the reaction (1). Additional coordination of the pyridine molecules toward the metal centers appears to promote dissociation of the pyridine-substituted dimer: the $\Delta G°_{sol}$ value decreases substantially from 33.6 to 19.2 kcal mol^{-1} for the reaction (4). Thus, the four-coordinated calcium monohydride complex CaH(L)(Py)$_2$ (L = *t*Bu$_2$CarbAr$_2$) can be considered as the catalytic species.

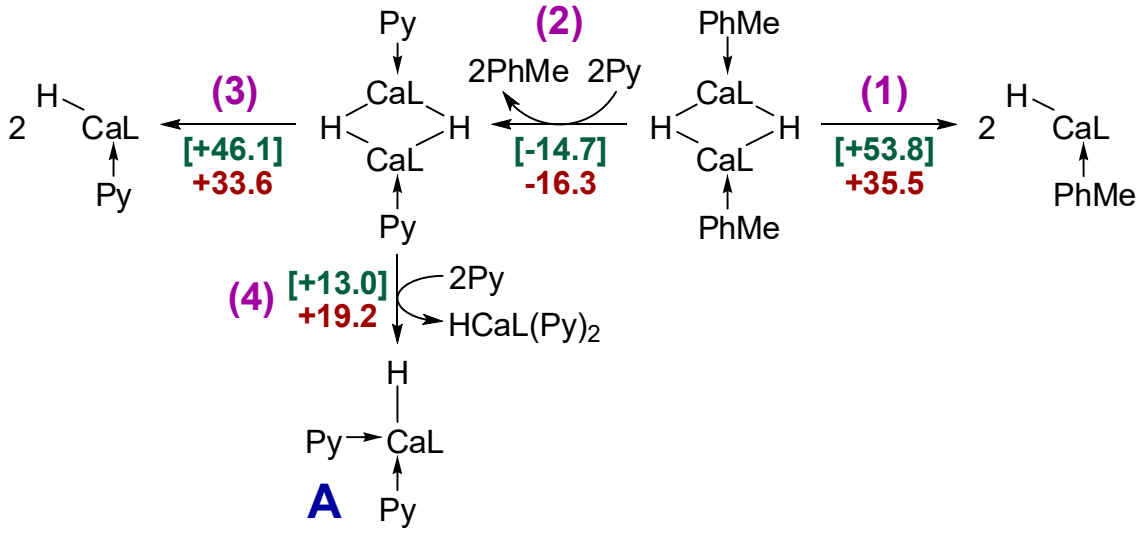

Scheme S2. Computed at 25 °C values (kcal mol^{-1}) of $\Delta H°_{sol}$ (in brackets) and $\Delta G°_{sol}$ for the dissociation reactions. The level of DFT calculations is PCM(PhMe)-M062X/DGDZVP.

References

1. A. Hinz, *Chem. Eur. J*. **2019**, *25*, 3267 – 3271.
2. M. Westerhausen, *Inorg. Chem*. **1991**, *30*, 96-101.
3. T. D. Tilley, R. A. Andersen, A. Zalkin, *Inorg. Chem*. **1984**, *23*, 2271-2276.
4. P. S. Tanner, D. J. Burkey, T. P. Hanusa, *Polyhedron* **1995**, *14*, 331-333.
5. M. M. Katzenmayer, B. M. Wolf, A. Mortis, C. Maichle-Mössmer, R. Anwander, *Chem. Commun*., **2021**, *57*, 243-246.
6. Y. Tokoro, N. Ohtsuka, S. Fukuzawa, T. Oyama, *RSC Adv*., **2018**, *8*, 25177-25180.
7. M. D. Visco, J. M. Wieting, A. E. Mattson, *Org.Lett*., **2016**, *18*, 2883−2885.
8. A. N. Selikhov, A. V. Cherkasov, Y. V. Nelyubina, A. A. Trifonov, *ACS Catal*., **2023**, *13*, 12582−12590
9. S. J. Lyle, M. M. Rahman, *Talanta* **1963**, *10*, 1177−1182.
10. G. M. Sheldrick. *Acta Cryst.* **2015**, *A71*, pp. 3-8.
11. O. V. Dolomanov, L. J. Bourhis, R. J. Gildea, J. A. K. Howard, H. Puschmann. *J. Appl. Cryst.* **2009**, *42*, pp. 339-341.
12. G. M. Sheldrick. *Acta Cryst.* **2008**, *A64*, pp. 112-122.
13. Frisch, M. J.; Trucks, G. W.; Schlegel, H. B.; Scuseria, G. E.; Robb, M. A.; Cheeseman, J. R.; Scalmani, G.; Barone, V.; Mennucci, B.; Petersson, G. A.; Nakatsuji, H.; Caricato, M.; Li, X.; Hratchian, H. P.; Izmaylov, A. F.; Bloino, J.; Zheng, G.; Sonnenberg, J. L.; Hada, M.; Ehara, M.; Toyota, K.; Fukuda, R.; Hasegawa, J.; Ishida, M.; Nakajima, T.; Honda, Y.; Kitao, O.; Nakai, H.; Vreven, T.; Montgomery, J. A., Jr.; Peralta, J. E.; Ogliaro, F.; Bearpark, M.; Heyd, J. J.; Brothers, E.; Kudin, K. N.; Staroverov, V. N.; Keith, T.; Kobayashi, R.; Normand, J.; Raghavachari, K.; Rendell, A.; Burant, J. C.; Iyengar, S. S.; Tomasi, J.; Cossi, M.; Rega, N.; Millam, J. M.; Klene, M.; Knox, J. E.; Cross, J. B.; Bakken, V.; Adamo, C.; Jaramillo, J.; Gomperts, R.; Stratmann, R. E.; Yazyev, O.; Austin, A. J.; Cammi, R.; Pomelli, C.; Ochterski, J. W.; Martin, R. L.; Morokuma, K.; Zakrzewski, V. G.; Voth, G. A.; Salvador, P.; Dannenberg, J. J.; Dapprich, S.; Daniels, A. D.; Farkas, O.; Foresman, J. B.; Ortiz, J. V.; Cioslowski, J.; Fox, D. J. *Gaussian 09*, Revision E.01; Gaussian, Inc.: Wallingford, CT, **2013**.
14. Y. Zhao, D. G. Truhlar, *Theor. Chem. Acc.* **2008**, *120*, 215–241.
15. N. Godbout, D. R. Salahub, J. Andzel, E. Wimmer, *Can. J. Chem.* **1992**, *70*, 560–571.
16. C. Sosa, J. Andzelm, B. C. Elkin, E. Wimmer, K. D. Dobbs, D. A. Dixon, *J. Phys. Chem.* **1992**, *96*, 6630–6636.
17. J. Tomasi, B. Mennucci, R. Cammi, *Chem. Rev.* **2005**, *105*, 2999–3093.
18. Ch. Peng, H. B. Schlegel, *Isr. J. Chem.* **1993**, *33*, 449–454.
19. Ch. Peng, P. Y. Ayala, H. B. Schlegel, M. J. Frisch, *J. Comp. Chem.* **1996**, *17*, 49–56.
20. F. Weigend, R. Ahlrichs, *Phys. Chem. Chem. Phys.* **2005**, *7*, 3297–3305.